ADAPTIVE LABORATORY EVOLUTION TO INDUCE ANTIBIOTIC PRODUCTION OF *STREPTOMYCES* SP. SSUT88A AGAINST DRUG-RESISTANT BACTERIA

WISSARUT SRISAKVARANGKOOL

A Thesis Submitted in Partial Fulfillment of the Requirements for the Degree of Master of Science in Microbiology

Suranaree University of Technology

Academic Year 2024

การปรับตัวทางวิวัฒนาการในห้องปฏิบัติการเพื่อกระตุ้นการผลิตยาปฏิชีวนะของเชื้อ *Streptomyces* sp. SSUT88A ต่อแบคทีเรียดื้อยา

นายวิศรุต ศรีศักดิ์วรางกูร

วิทยานิพนธ์นี้เป็นส่วนหนึ่งของการศึกษาตามหลักสูตรปริญญาวิทยาศาสตรมหาบัณฑิต

สาขาวิชาจุลชีววิทยา

มหาวิทยาลัยเทคโนโลยีสุรนารี

ปีการศึกษา 2567

ADAPTIVE LABORATORY EVOLUTION TO INDUCE ANTIBIOTIC PRODUCTION OF *STREPTOMYCES* SP. SSUT88A AGAINST DRUG-RESISTANT BACTERIA

Suranaree University of Technology has approved this thesis submitted in partial fulfillment of the requirements for the Degree of Master of Science.

Thesis Examining Committee

(Asst. Prof. Dr. Montri Yasawong)
Chairperson

(Asst. Prof. Dr. Nawarat Nantapong)
Member (Thesis Advisor)

(Asst. Prof. Dr. Watsana Penkhrue)
Member

(Asst. Prof. Dr. Duangkamol Maensiri)
Member

(Assoc. Prof. Dr. Yupaporn Ruksakulpiwat)
Vice Rector for Academic Affairs
and Quality Assurance

(Prof. Dr. Santi Maensiri)
Dean of Institute of Science

วิศรุต ศรีศักดิ์วรางกูร : การปรับตัวทางวิวัฒนาการในห้องปฏิบัติการเพื่อกระตุ้นการผลิตยาปฏิชีวนะของเชื้อ *Streptomyces* sp. SSUT88A ต่อแบคทีเรียดื้อยา (Adaptive Laboratory Evolution to Induce Antibiotic Production of *Streptomyces* sp. SSUT88A against Drug-resistant Bacteria) อาจารย์ที่ปรึกษา : ผู้ช่วยศาสตราจารย์ ดร. นวรัตน์ นันทพงษ์, 93 หน้า

คำสำคัญ: การปรับตัวทางวิวัฒนาการในห้องปฏิบัติการ, การเลี้ยงร่วม, *Streptomyces*, การผลิตยาปฏิชีวนะ, การศึกษาจีโนมแบบเปรียบเทียบ

ภัยคุกคามจากเชื้อก่อโรคที่ดื้อต่อยาหลายขนาน (multidrug-resistant; MDR) ที่เพิ่มขึ้นอย่างต่อเนื่อง ได้เร่งให้เกิดความพยายามในการเพิ่มประสิทธิภาพการผลิตยาปฏิชีวนะและพัฒนากลยุทธ์ในการค้นพบสารต้านจุลชีพรูปแบบใหม่ โดยเชื้อ *Streptomyces* ถือเป็นแหล่งสำคัญของสารชีวภาพใหม่ที่มีศักยภาพสูง ในการศึกษานี้ *Streptomyces* sp. SSUT88A ได้ถูกนำมาผ่านกระบวนการปรับตัวในห้องปฏิบัติการ (Adaptive Laboratory Evolution; ALE) ผ่านการเพาะร่วมแบบต่อเนื่องกับเชื้อดื้อยา ได้แก่ *Staphylococcus aureus* (MRSA), *Acinetobacter baumannii*, *Pseudomonas aeruginosa* หรือเชื้อผสมของทั้งสามชนิด หลังผ่านการคัดเลือกนานสูงสุด 9 ครั้ง เชื้อที่ผ่านการปรับตัวแสดงการเปลี่ยนแปลงทางฟีโนไทป์อย่างชัดเจน ทั้งในด้านฤทธิ์ต้านจุลชีพและการสร้างรงควัตถุ โดยสายพันธุ์ SSUT88A^{MR9-16} และ SSUT88A^{Ab9-5} แสดงผลผลิตสารสกัดหยาบเพิ่มขึ้นอย่างมีนัยสำคัญที่ 40% และ 43% ตามลำดับ ขณะที่สายพันธุ์ SSUT88A^{3P6-7} ซึ่งได้จากการเพาะร่วมกับเชื้อทั้งสามชนิด สูญเสียรงควัตถุสีเหลืองที่เป็นลักษณะเฉพาะ เกิดเป็นโคโลนีสีแดง และสูญเสียฤทธิ์ต้านจุลชีพโดยสมบูรณ์ นอกจากนี้ SSUT88A^{Ab9-5} ยังสามารถผลิตสารออกฤทธิ์ได้เร็วที่สุดเมื่อเทียบกับสายพันธุ์อื่น การทดสอบฤทธิ์ต้านจุลชีพยืนยันถึงความแรงที่เพิ่มขึ้นในสายพันธุ์ที่ได้รับการปรับตัว (โดย MIC/MBC ต่อ MRSA และ MRSE เพิ่มขึ้น 4–8 เท่า) ในขณะที่ SSUT88A^{3P6-7} ไม่มีฤทธิ์ที่สามารถตรวจพบได้ การประกอบจีโนมของทุกสายพันธุ์มีความสมบูรณ์เกิน 99.9% และยังคงความเหมือนทางอนุกรมวิธานกับสายพันธุ์ดั้งเดิม ไม่พบยีนดื้อยาที่ถูกถ่ายทอดมาหลังการปรับตัว การวิเคราะห์จีโนมเปรียบเทียบพบว่า สายพันธุ์ที่สามารถผลิตสารต้านจุลชีพได้ทุกสายพันธุ์มี Biosynthetic Gene Cluster (BGC) ร่วมกัน 6 กลุ่ม ซึ่งส่วนใหญ่เกี่ยวข้องกับสารออกฤทธิ์ที่รู้จักหรือคาดการณ์ว่ามีฤทธิ์ต้านจุลชีพ สายพันธุ์ที่ผลิตสารได้สูงเท่านั้นที่พบกลุ่ม NRPS และ T1PKS เฉพาะ ซึ่งอาจมีบทบาทในการเสริมฤทธิ์ดังกล่าว ตรงกันข้าม กลุ่ม BGC ที่พบเฉพาะในสายพันธุ์ดั้งเดิมและ

สายพันธุ์ที่ไม่ออกฤทธิ์มักไม่เกี่ยวข้องกับฤทธิ์ต้านจุลชีพและอาจไม่สำคัญต่อการสร้างสารปฏิชีวนะ นอกจากนี้สายพันธุ์ SSUT88A^{3P6-7} ยังขาดกลุ่ม aryl polyene ที่มีรายงานว่าเกี่ยวข้องกับรงควัตถุสีเหลืองสอดคล้องกับฟีโนไทป์ที่เปลี่ยนไป การวิเคราะห์กลุ่มยีนด้วยลำดับโปรตีนแบบ ortholog โดยใช้ OrthoVenn3 พบว่ามีความอนุรักษ์ของจีโนมในภาพรวม แต่ยังพบกลุ่มเฉพาะ 16 กลุ่มที่มีเฉพาะในสายพันธุ์ที่ผลิตสารได้สูง ซึ่งเกี่ยวข้องกับกระบวนการคลายโครงสร้าง RNA และเมแทบอลิซึมของ trehalose ในทางตรงกันข้าม มีกว่า 600 กลุ่มที่พบเฉพาะในสายพันธุ์ดั้งเดิมและสายพันธุ์ที่ไม่ผลิตสาร ซึ่งอาจสะท้อนยีนที่ไม่เกี่ยวข้องกับฤทธิ์ต้านจุลชีพ การสร้างแผนภูมิสายวิวัฒนาการจากกลุ่มยีนร่วมสนับสนุนความแตกต่างทางฟีโนไทป์ โดยสายพันธุ์ที่มีฤทธิ์เพิ่มขึ้นจัดกลุ่มใกล้กัน การวิเคราะห์โครงสร้างจีโนมโดย Breseq ร่วมกับข้อมูลจาก antiSMASH และ OrthoVenn แสดงให้เห็นว่าหลายบริเวณที่หายไปในสายพันธุ์ SSUT88A^{3P6-7} สัมพันธ์กับ BGCs และกลุ่มยีน ortholog ที่ขาดหายไป บ่งชี้ว่า “การสูญเสียยีน” มีส่วนต่อการสูญเสียฟีโนไทป์ Breseq ในโหมด consensus ยังตรวจพบ SNPs ที่มีความน่าเชื่อถือสูงเพียง 3 ตำแหน่ง โดยสองตำแหน่งอยู่ใกล้บริเวณ promoter σ^{70} ที่คาดการณ์ไว้ในสายพันธุ์ที่ผลิตสารได้สูง (ด้านหน้าของยีนที่เกี่ยวข้องกับการสังเคราะห์ผนังเซลล์หรือการควบคุมการถอดรหัส) ขณะที่อีกตำแหน่งเป็น SNP แบบ silent ในสายพันธุ์ที่ไม่ผลิตสาร ซึ่งอาจมีผลทางอ้อมต่อการแปลโปรตีนผ่าน codon usage bias หรือโครงสร้าง mRNA ข้อมูลทั้งหมดนี้สนับสนุนโมเดลที่ฟีโนไทป์ที่สังเกตได้มีที่มาจากการสูญเสียยีนโครงสร้างร่วมกับการปรับระดับการควบคุมทางพันธุกรรม การลบยีนสำคัญอาจทำให้เกิดการสูญเสียฟังก์ชัน ขณะที่การลบยีนที่ไม่จำเป็นอาจลดภาระเมแทบอลิซึมของเซลล์และหันทรัพยากรไปยังการผลิตสารทุติยภูมิ ผลการศึกษานี้แสดงให้เห็นว่า ALE ผ่านการเพาะร่วมสามารถปรับระดับการแสดงออกของเมแทบอลิซึมทุติยภูมิ และเพิ่มประสิทธิภาพการผลิตยาปฏิชีวนะได้อย่างมีนัยสำคัญ ซึ่งถือเป็นแนวทางที่มีศักยภาพสูงสำหรับการพัฒนาสายพันธุ์เชิงอุตสาหกรรมและการค้นพบสารชีวภาพใหม่ในอนาคต

สาขาวิชาปรีคลินิก ลายมือชื่อนักศึกษา ________

ปีการศึกษา 2567 ลายมือชื่ออาจารย์ที่ปรึกษา ________

WISSRUT SRIAKVARANGKOOL : ADAPTIVE LABORATORY EVOLUTION TO INDUCE ANTIBIOTIC PRODUCTION OF *STREPTOMYCES* SP. SSUT88A AGAINST DRUG-RESISTANT BACTERIA. THESIS ADVISER : ASST. PROF. NAWARAT NANTAPONG, Ph.D. 93 PP.

Keywords: Adaptive Laboratory Evolution, Co-culture, *Streptomyces*, Antibiotic Production, Comparative Genome Analysis

The growing threat of multidrug-resistant (MDR) pathogens has intensified efforts to enhance antibiotic production and improve antibiotic discovery strategies. *Streptomyces* spp. is a major promising source of novel antibiotics. In this study, *Streptomyces* sp. SSUT88A was subjected to adaptive laboratory evolution (ALE) via serial co-cultivation with drug-resistant pathogens, *Staphylococcus aureus* (MRSA), *Acinetobacter baumannii*, *Pseudomonas aeruginosa*, or a mixture of all three. After up to nine cycles of adaptation selection, evolved strains exhibited distinct phenotypic shifts in antimicrobial activity and pigment production. Strains SSUT88A^{MR9-16} and SSUT88A^{Ab9-5} exhibited significantly increased with crude extract yields increasing by 40% and 43%, respectively. While strain SSUT88A^{3P6-7}, isolated from the three-pathogen condition, lost its characteristic yellow diffusible pigment, formed red colonies, and exhibited a complete loss of antimicrobial activity. SSUT88A^{Ab9-5} also demonstrated the earliest onset of bioactive compound production. Bioactivity assays confirmed enhanced potency in adapted strains (4–8-fold stronger MIC/MBC against MRSA and MRSE) while strain SSUT88A^{3P6-7} exhibited no detectable activity. All genome assemblies were >99.9% complete and remained taxonomically identical to the wild-type. No acquired resistance genes were detected in any strain after ALE. Comparative genomic analysis identified six biosynthetic gene clusters (BGCs) shared among all antibiotic producers comprising primarily of classes with known or predicted antimicrobial activity. Only the High-antibiotic-producing strains possessed unique NRPS and T1PKS clusters potentially contribute to enhanced bioactivity. In contrast, clusters present only in the wild-type and non-producing strain were not commonly linked to antibacterial activity and may represent less relevant pathways. The SSUT88A^{3P6-7} strain lacked a yellow colored-associated aryl polyene cluster, consistent

with its phenotype. Orthologous clustering using OrthoVenn3 supported broad genomic conservation across strains but identified 16 unique clusters shared only by high-antibiotic-producing strains, including functions in RNA unwinding and trehalose metabolism. Conversely, over 600 clusters were shared only between the wild-type and non-producer, likely representing traits unrelated to antibiotic production. Phylogenomic analysis based on orthologs reflected phenotypic divergence, with enhanced strains clustering together. To link these patterns to structural variation, BGC predictions were cross-referenced with orthologous clusters and Breseq analysis. Multiple deletions in the non-producing strain overlapped with missing BGCs and ortholog clusters, suggesting that gene loss contributed to phenotypic loss. Breseq consensus mode also identified three high-confidence SNPs: two located near predicted σ^{70} promoter regions in the high-producing strains (upstream of genes involved in cell wall biosynthesis or transcriptional regulation), and one synonymous SNP in the non-producing strain that may subtly affect translation via codon usage bias or translational efficiency. Taken together, these findings support a model in which observable phenotypes arise from a combination of structural gene loss and regulatory fine-tuning. While deletion of functionally important regions can lead to phenotypic loss, gene loss in non-essential regions may reduce metabolic burden and shift cellular resources toward secondary metabolite production. These results demonstrate how ALE via co-cultivation can fine-tune secondary metabolism and enhance antibiotic production, offering a promising strategy for future industrial strain improvement and bioactive compound discovery.

School of Preclinical Sciences
Academic Year 2024

Student's Signature Wissanut Srisakvarangkool
Advisor's Signature

ACKNOWLEDGEMENTS

This project was able to commence and succeed due to the invaluable assistance and excellent suggestions I received from professional researchers and highly skilled individuals with extensive experience. First, I would like to thank Asst. Prof. Dr. Nawarat Nantapong, my advisor, for drawing my attention to laboratory evolution and providing insightful ideas and suggestions throughout this project. Second, I am grateful to Asst. Prof. Dr. Montri Yasawong, from the Chulabhorn Graduate Institute, for advising on genomic analysis. Furthermore, I extend my thanks to the Nawarat research group and the Archaea Lab for their unwavering assistance and support. Lastly, I am sincerely thankful to Suranaree University of Technology for providing laboratory space, chemicals, and tools for my research.

Wissarut Srisakvarangkool

CONTENTS

CONTENTS (Continued)

CONTENTS (Continued)

Page

LIST OF TABLES

LIST OF FIGURES

LIST OF FIGURES (Continued)

LIST OF ABBREVIATIONS

ALE	Adaptive Laboratory Evolution
MRSA	Methicillin-resistant *Staphylococcus aureus*
MDR	Multidrug Resistant
rpm	Round per minute
ISP-2	International *Streptomyces* Project-2 Medium
OD_{600}	Optical density at 600 nm
g	Gram(s)
h	Hour(s)
min	Minute(s)
°C	Degree Celcius
×g	G-force (relative centrifugal force; RCF)
mL	Milliliter(s)
mg	Milligram(s)
µg	Microgram(s)
µm	Micrometer(s)
bp	Base pair(s)

CHAPTER I

INTRODUCTION

1.1 Significance and Background

The discovery and utilization of one of the first the first antibiotic, Salvarsan, in 1910 extended our past human lifespan by 23 years (Adedeji, 2016; Hutchings et al., 2019). The golden age of antibiotic discovery initiated in 1928, when Alexander Fleming found Penicillin and revolutionized our medical treatment of microorganism infections (Demain and Elander, 1999; Fleming, 1929). Besides the decline in antibiotics discovery and development rate (Katz and Baltz, 2016), misuse of antibiotics lead to a rapid rise in multidrug resistance (MDR) making the treatment of various infections tougher (Prescott, 2014). Nowadays, we still seek new antibiotics to treat infections caused by diverse MDR pathogens e.g., *Acinetobacter baumannii*, *Staphylococcus aureus, Klebsiella pneumoniae*, *Pseudomonas aeruginosa*, *Mycobacterium tuberculosis*, etc. which happens to be one major threat to human life (Appelbaum, 2006). MDR has been a global health challenge as well as an expense that threatens our ability to control and treat life-threatening infections (Liu et al., 2021). Moreover, there have been reports that during the COVID-19 pandemic overall incident density (ID) of MDR infections increased by 23% mainly from methicillin-resistant *Staphylococcus aureus* (MRSA) and *Acinetobacter baumannii* (Polly et al., 2022). Failure of the primary antimicrobial treatment results from multidrug-resistant bacteria increases the risk of secondary complications and death. Treatment is then forced to switch to second- or third-line drugs, which are much more expensive and more toxic as well (World Health Organization. Regional Office for South-East, 2011).

Bacteria in the genus *Streptomyces* have been reported to have a fascinating complex secondary metabolite (Wu et al., 2005) which is a major promising source of novel antibiotics (Challis and Hopwood, 2003) as the matter of fact that two-thirds of our currently used natured-based antibiotics came from this genus (Papagianni, 2012).

In order to trigger/increase antibiotic production, mimicking natural conditions where more than one bacterial species habits together could be done in the laboratory via co-cultivation method which involves repeating exposure of *Streptomyces* spp. to MDR pathogens (De Roy et al., 2014).

1.2 Research Objectives

This research aimed to investigate the potential of adaptive laboratory evolution (ALE) through co-cultivation with drug-resistant pathogens to enhance antibiotic production in *Streptomyces* sp. SSUT88A and to explore the underlying genetic changes associated with this adaptation.

1.2.1 Study the effect of adaptive laboratory evolution using co-cultivation method to trigger the production of antibiotics of *Streptomyces* sp. SSUT88A against drug-resistant bacteria.

1.2.2 Evaluate antimicrobial activities of crude compounds of wild-type and adapted strains of SSUT88A.

1.2.3 Investigate genetic background of adapted strains of SSUT88A compares to wild-type using whole genome sequencing and bioinformatics analysis.

1.3 Research Scope

This research will be using *Streptomyces* strain SSUT88A co-cultivate (both bi-culture and quadri-culture) with clinical isolate drug-resistant pathogens *Acinetobacter baumannii* SUTH-Isolate, methicillin-resistant *Staphylococcus aureus* (MRSA) DMST20651 and *Pseudomonas aeruginosa* SUTH-Isolate N90PS for 9 cycles, 10 days/cycle. Determination of adaptive laboratory evolution will be indicated via antimicrobial activities compared to wild-type strain (monoculture). The antimicrobial activity of crude extract will be tested with 16 human pathogens, listed in the material section, using agar well diffusion method. The genetic background of the most adapted strains based on antimicrobial activity improvement against MDR pathogens were analyzed compares to the wild-type strain using whole genome sequencing.

1.4 Research Hypothesis

Adaptive laboratory evolution using co-cultivation with drug-resistant bacteria can stimulate *Streptomyces* sp. SSUT88A to produce antibiotics with enhanced activity. This adaptation would be associated with genetic variations that contribute to increased antimicrobial production or stress response mechanisms.

CHAPTER II

LITERATURE REVIEW

2.1 Antibiotics

2.1.1 Definition and Classification

The term antibiotics was first used in 1942 by Selman Waksman and his collaborators to describe any substance produced by a microorganism that opposes/inhibits the growth of other microorganisms in high dilution (Waksman, 1947).

This definition is then redefined as - any medications which kill or inhibit growth of microorganisms - to include synthetic antibiotics.

Three types of antibiotics were classified based on production: (1) natural products which are the antibiotics produced solely from microorganisms themselves, for instance, penicillin, cephalosporins; (2) semi-synthetic products which are modified natural substances, like carbapenems; and (3) fully synthetic products which are medications that are 100% synthesized from commercially available precursors e.g., the sulfonamides, the quinolones, and the oxazolidinones (von Nussbaum et al., 2006).

The other way to classify antibiotics is based on their mechanism of action which could categorize them into

- Cell wall synthesis inhibitors/disruptors: primarily prevent peptidoglycan synthesis consequently led to bacterium lysis e.g., Cycloserine, Vancomycin, Bacitracin, Penicillin, Cephalosporins, Monobactams, Carbapenems, etc. (Kapoor et al., 2017)
- Cell membrane disruption: binding or integrating into the lipid moiety of the plasma membrane e.g., Polymyxins, Daptomycins, etc. (Etebu and Arikekpar, 2016)

- Nucleic acid synthesis inhibition: suppress DNA or RNA synthesis e.g., Nalidixic acid, Ciprofloxacin, Novobiocin, Actinomycin, Rifampin, Streptovaricins, etc.
- Protein synthesis inhibitors: targeting small and large subunit of ribosome by various approach accordingly blocking protein synthesis e.g., Erythromycin, Chloramphinicol, Clindamycin, Lincomycin, Tetracyclines, Streptomycins, Gentamycin, Kanamycin, Puromycin, Amikacins, Nitrofurans, etc.
- Metabolic pathway inhibitors: by mimicking or bonding with substrate within metabolic pathway and ultimately suppress the production of essential molecules e.g., Sulfonamides, Trimethoprim, Izoniacid, etc.

(Etebu and Arikekpar, 2016)

2.1.2 Brief History of Antibiotics

In 1910 Paul Ehrlich developed the synthetic arsenic-based drugs salvarsan (salvation arsenic) and neo-salvarsan circa for treating syphilis caused by *Treponema pallidum* (Gelpi et al., 2015). Salvarsan had been widely used as a broad-spectrum antibiotic until the discovery of penicillin by Alexander Fleming who observed blue-green mold contaminated on *Staphylococcus aureus* petri dish in 1928 (Fleming, 1929). Since Gramicidin was discovered from soil bacterium, *Bacillus brevis*, soil bacteria have gained interest as a potential approach to finding novel antibiotics (Andersen, 1984).

The introduction of antibiotics into clinical use was conceivably the substantial medical improvement of the 20th century. From the 1930s to the 1960s, the discovery of antibiotics accelerated rapidly, leading to what is known as the “Golden Age of Antibiotics.” During this period, numerous groundbreaking compounds such as penicillin and streptomycin were introduced, transforming the treatment of bacterial infections. However, this era also marked the first observations of antibiotic-

resistant strains, signaling the beginning of the ongoing challenge posed by antimicrobial resistance (AMR) (Figure 2.1).

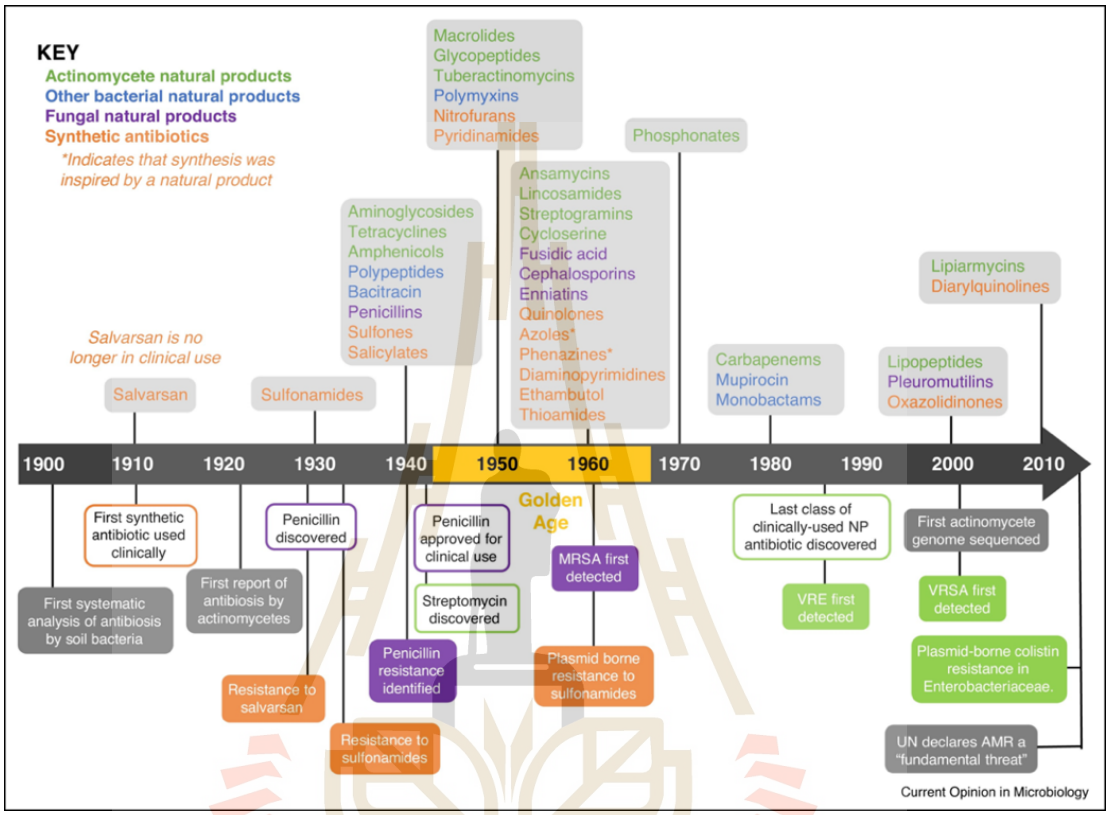

Figure 2.1 Timeline illustrates the decade of antibiotics development. Colors indicate source of each antibiotic – green = actinomycetes, blue = other bacteria, purple = fungi and orange = synthetic. With MDR pathogens reported including methicillin-resistant *S. aureus* (MRSA), vancomycin-resistant enterococci (VRE), vancomycin-resistant *S. aureus* (VRSA) and plasmid-borne colistin resistance in Enterobacteriaceae (Hutchings et al., 2019).

2.2 Antibiotics Producing Microorganisms

Following the discovery of penicillin, the first natural antibiotic, many antibiotic production techniques have been established. Scientists continued to seek further new antibiotics to combat infectious diseases. Nowadays most of clinically used antibiotics

are produced/derived from microorganisms including bacteria and fungi. Within the microorganism part, actinomycetes is considered as a major group of antibiotic producers, accounting for approximately 64 percent of all antibiotics producing industries (Figure 2.2). They are gram-positive filamentous bacteria that form a branching network of filaments and produce spores. They grow through both extension and branching of hyphal tip, hence giving them their name “Actinomycete” derived from the Greek words for "ray" (aktis or aktin) and "fungi" (mukēs). Actinomycetes are abundant in soil and marine sediments (Barka et al., 2016).

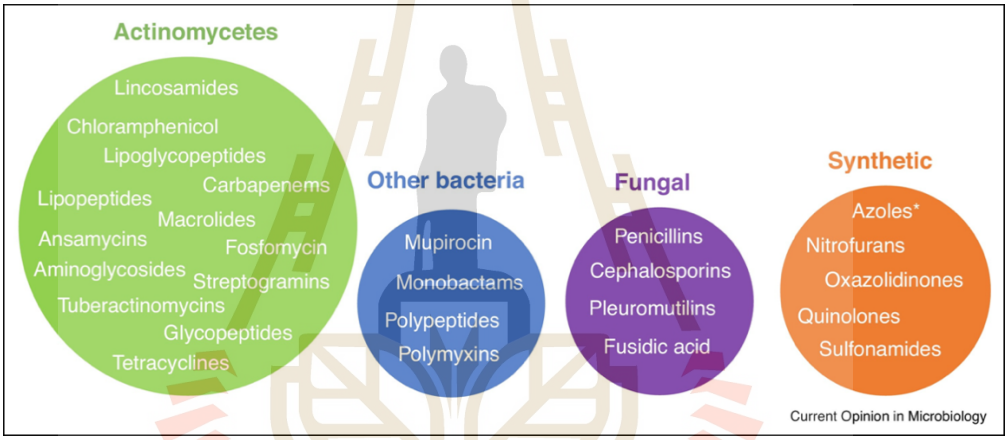

Figure 2.2 The majority of clinically used classes of antibiotics are derived from natural products mainly actinomycetes (Hutchings et al., 2019).

Within the phylum Actinobacteria, the genus *Streptomyces* exhibits a remarkable capacity to produce antibiotics. The attention to *Streptomyces* initially dated back to the discovery of actinomycin and streptomycin in the 1940s (de Lima Procópio et al., 2012) and was further intensified when Benjamin Minge Duggar identified tetracycline, a broad-spectrum antibiotic, from *Streptomyces aureofaciens* isolated from campus soil in the United States (Nelson and Levy, 2011).

Following then, *Streptomyces* remained a promising source of several currently therapeutic antibiotics (Table 2.1).

Table 2.1 List of currently used antibiotics derived from *Streptomyces* species and their mechanism of action (de Lima Procópio et al., 2012).

Antibiotics	*Streptomyces* sp.	Mechanism of Action
Cephalosporin	*S. clavuligerus*	Cell Wall Synthesis Inhibition
Neomycin	*S. fradiae*	
Vancomycin	*S. orientalis*	
Phosphomimic	*S. fradiae*	
Nystatin	*S. noursei*	Cell Membrane Disruption
Daptomycin	*S. rosesporus*	
Novobiocin	*S. niveus*	Inhibits Nucleic Acid Synthesis and Metabolism
Streptomycin	*S. griseus*	Inhibits Protein Synthesis
Chloramphenicol	*S. venezualae*	
Tetracyclin	*S. aurofaciens*	
Viomycin	*S. vinaceus* & *S. capreolus*	
Virginiamycin	*S. pristinaespirallis* & *S. virginae*	
Erythromycin	*S. erythreus*	
Lincomycin	*S. lincolnensis*	
Kanamycin	*S. kanamyceticus*	
Ribostamycin	*S. ribosidificus*	

2.2.1 The Genus *Streptomyces*

Streptomyces is the largest genus of phylum Actinobacteria. They are complex bacteria having various notable characteristics for instance aerobic respiration, gram-positive, high GC content, filamentous, spore-producing bacteria. Cell wall type I distinguished by the presence of *LL* form α, ε-diaminopimelic acid (*LL*-DAP) composition and the lack of characteristic sugars of the cell wall is exclusively found in *Streptomyces* which differ them form other genera of Actinobacteria (Ramasamy and Sudalaimuthu, 2022). They are prevalent in soil microbiomes and marine sediments (Khanna and Solanki, 2012). Another unique trait of streptomycetes is the production of substrate and aerial mycelia, which is comparable to that of fungi. Their aged aerial mycelia (hyphae) will form multinucleated mycelia which could undergo synchronous cell division and differentiate into spores (Law et al., 2019; Ohnishi et al., 2008). When the spores reached the favorable temperature, nutritional, and moisture conditions, the germ tube developed, and a new bacterium emerged (Figure 2.3). The color of the colony with diffusible pigments could be utilized to roughly differentiate the species as well (Figure 2.4). They are well-known for their remarkable bioactive secondary metabolites for instance antifungals, antivirals, antitumoral, anti-hypertensives, and greatly antibiotics and immunosuppressants as well (Khan et al., 2011; Ōmura et al., 2001).

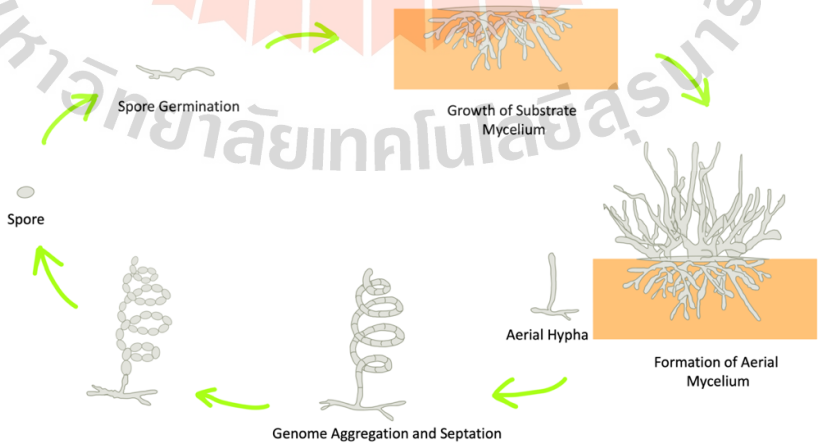

Figure 2.3 Illustration depicts the life cycle of Streptomycetes, adapted figure from Law et al., 2019 and Barka et al., 2016.

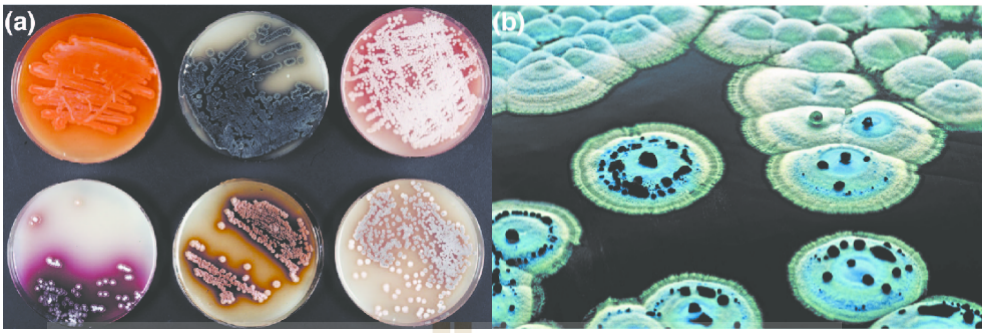

Figure 2.4 *Streptomyces* produce diversified pigments (Thompson et al., 2002).

2.3 Multidrug-Resistant (MDR) Pathogens

MDR bacteria are well-recognized to be one of the most important current public health problems. The Infectious Diseases Society of America (IDSA) identified antimicrobial resistance as "one of the greatest threats to human health worldwide" (Spellberg et al., 2011). For example, only methicillin-resistant *Staphylococcus aureus* (MRSA), ends more Americans' lives each year (~19,000) than emphysema, HIV/AIDS, Parkinson's disease, and homicide all combined (Klevens et al., 2007). In 2017, there are approximately 120,000 MRSA bloodstream infections and 20,000 MRSA-associated deaths in the United States (Kourtis et al., 2019). Failure of primary antimicrobial therapy results from multidrug-resistant bacteria increases the risk of complications and fatality. Second- or third-line drugs, which are far more expensive and toxic, are required to treat patients, yet they still raise treatment expenses (World Health Organization. Regional Office for South-East, 2011). It is estimated that failing to treat MDR infections would result in 10 million deaths per year by 2050, costing nearly 100 trillion US dollars (Neil, 2016). Shifting from non-MDR infection cases to MDR infection cases could raise the expenses for treatment by 42% per patient (Phodha et al., 2019). In Thailand, a study showed that in 2010 the annual cost of antibiotics used in the treatment of MDR infections ranged from 83 to 200 million US dollars and the additional cost due to the morbidity and mortality consequences from MDR infections were at least 1.3 billion US dollars (Phumart et al., 2012). Thus, MDR infection is an

important worldwide public health threat and should be approached abruptly and proactively (van Duin and Paterson, 2016).

2.4 Adaptive Laboratory Evolution: Co-Cultivation Method

Microorganisms can adapt to drastic alterations in their environment by mutation followed by natural selection, this phenomenon is known as “adaptive evolution” (Shi et al., 2021). Adaptive laboratory evolution is the term to describe protocol(s) of forcing the microorganisms to adapt to yield desired results (Boruta, 2021). Based on the fact that evolution and adaptation occur through generations which in higher organisms would take years, in microorganisms it could happen in days. They also have a significantly smaller genome than higher organisms thus one mutation delivers more observable results (Herron and Freeman, 2013). Therefore, the desirable traits can be chosen in the laboratory by manipulating microbial growth conditions. Any microorganisms lacking adaptability to the defined conditions will not be able to reproduce, leaving just the adaptive ones. For example, an experiment was conducted in which the carbon source of *E. coli* was altered by serially lowering the normal carbon supply and gradually increasing the new carbon source (glycerol or lactate) through time; as a result, *E. coli* was able to use glycerol or lactate as the sole carbon source (Conrad et al., 2009; Herring et al., 2006); Adaptive evolution has been applied to examine mechanisms of ethanol (Wang et al., 2011) and osmotic stress tolerance in *E. coli* as well (Stoebel et al., 2009). The competition between microbes for limiting natural resources such as oxygen, nutrients, space, in the microbiomes is believed to be the selective factor that promotes biosynthesis of secondary metabolites especially antimicrobial compounds (Slattery et al., 2001). In laboratory, the contamination from other strain tends to be avoided since pure cultivation is more common approach, to the extent that there are techniques developed by Robert Koch and colleagues to eliminate those contaminations. But interestingly, several studies have found that imitating the natural habitat of bacteria by 'co-cultivating' them with either natural co-

existing bacteria from the same isolated sample or pathogens might trigger/increase the synthesis of bioactive compounds (Harwani et al., 2018; Kurosawa et al., 2008; Oh et al., 2007; White Jr and Torres, 2009).

2.5 Bioinformatical Approach: Whole Genome Sequencing

Whole genome sequencing and adaptive laboratory evolution in combination is a robust technique in order to understand the underlying molecular mechanisms of the adapted strains (Dettman et al., 2012). Whole genome sequencing analysis was used to identify the polymorphism and further possible influence on adapted traits in various adaptive laboratory evolution experiment including the production of antibiotics by *Streptomyces* sp. (Harwani et al., 2022). For instance, the whole genome comparison between *Streptomyces clavuligerus* strain adapted by co-culture with methicillin-resistant *Staphylococcus aureus* N315 found to have 6 mutations different form wild-type. The mutations occur at various locations including loss of megaplasmid, malate dehydrogenase gene, glycosyl hydrolase gene, pyrroloquinoline quinone biosynthesis protein B gene, N-(5-carboxylpentanoyl)-L-cysteinyl-valine synthase gene (Charusanti et al., 2012).

2.6 Related Research

Previously, certain studies, especially from the early 2000s, reported the co-cultivation approach of *Streptomyces* spp. to promote the formation of bioactive metabolites (Harwani et al., 2018; Kurosawa et al., 2008; Oh et al., 2007; Ueda et al., 2000; White Jr and Torres, 2009). In this research, the co-cultivation method will be modified from Wu et al. (2015), and Harwani et al. (2022), both of which are related to co-culture adaptive laboratory evolution of *Streptomyces* spp. in liquid medium (Harwani et al., 2022; Wu et al., 2015). Since, the *Streptomyces* strain of interest, SSUT88A, was previously isolated and purified by a former graduated Ph.D. student in

Microbial Resources Laboratory, Suranaree University, Thailand. Based on 16s rRNA gene analysis, *Streptomyces* sp. SSUT88A had only 98.8% similarity to *Streptomyces chiangmaiensis* TA4-1^{T} and was only be used for single research purpose to mediate the green synthesis of silver nanoparticles (Rosyidah et al., 2022). Thus, neither SSUT88A nor *Streptomyces chiangmaiensis* TA4-1^{T} have been utilized in any adaptive laboratory evolution.

CHAPTER III

RESEARCH METHODOLOGY

3.1 Materials and Instruments

3.1.1 Microbial Isolates and Tested Pathogens

The bacterial of interest *Streptomyces* sp. strains, SSUT88A and SSUT88Red, were isolated from soil samples collected from Sakaerat Environmental Research Station (14°25′-14°33′ N 100°48′-100°56′ E), Wang Nam Khieo District, Nakhon Ratchasima, Thailand. The strains were kindly provided by A'liyatur Rosyidah, a former graduated Ph.D. student in the same research group (Rosyidah et al., 2021).

The pathogenic strains were obtained from, Thailand Institute of Scientific and Technological Research (TISTR), Department of Medical Sciences Thailand (DMST), and Suranaree University of Technology Hospital (SUTH). The list of pathogens are *Bacillus cereus* TISTR687, *Bacillus subtilis* TISTR008, *Enterobacter aerogenes* TISTR1540, *Escherichia coli* TISTR780, *Proteus mirabilis* TISTR100, *Pseudomonas aeruginosa* TISTR1287, *Salmonella typhimurium* TISTR292, *Staphylococcus aureus* TISTR1466, *Staphylococcus epidermidis* TISTR518, methicillin-resistant *Staphylococcus aureus* DMST20651 (MRSA), methicillin-resistant *Staphylococcus epidermidis* (MRSE) SUTH-isolate, *Acinetobacter baumannii* SUTH-isolate, *Escherichia coli* 2026 SUTH-isolate, *Klebsiella pneumoniae* 1617 SUTH-isolate, *Pseudomonas aeruginosa* N90PS SUTH-isolate, and *Serratia marcescens* SUTH-isolate.

3.1.2 Culture Media and Solutions

- International *Streptomyces* Project-2 Medium (ISP-2) contains 4.0 g of yeast extract, 10.0 g of malt extract, 4 g of dextrose (Glucose), 1 L of deionized water, pH was adjusted to 7.2. 20 g of agar is added to the mixture in case of making the agar medium.
- The liquid nutrient broth (NB) medium is prepared by dissolving 3 g of beef extract, 10 g of bacteriological tryptone, and 5 g of NaCl in

- 1 L of deionized water. The pH of the NB medium is adjusted to approximately 7.0.
- Starch Casein Medium (SC) per 1 liter contains 10.0 g of soluble starch, 0.30 g of casein hydrolysate, 2.0 g of KNO_3, 0.05 g of $MgSO_4 \cdot 7H_2O$, 2.0 g of K_2HPO_4, 2.0 g of NaCl, 0.02 g of $CaCO_3$, 0.01 g of $FeSO_4 \cdot 7H_2O$ in deionized water, pH = 7.0. 18 g of agar is added to the mixture in case of making the agar medium.
- The Luria-Bertaini (LB) medium is prepared with deionized water containing (per 1 L) 10 g of bacteriological tryptone, 5 g of yeast extract, and 10 g of NaCl, adjusting the pH to 7.2.
- Mueller-Hinton medium (MH) is purchased from Himedia, India. Suspend 21.0 g of MH in 1 L deionized water and add 15 of g agar if needed. pH = 7.3.
- Saline water (SW) is prepared by dissolving 8.5 g of NaCl (0.85%, w/v) with 1 L of deionized water, and the pH is adjusted to 7.2
- All media and solutions are sterilized by autoclaving at 121 °C, 15 psi for 15 min.

3.2 Adaptive Laboratory Evolution Experimental protocol

3.2.1 Preliminary Experiment: Strain of Interest Selection

Strain of *Streptomyces* used in this study was selected by their antimicrobial activity against test pathogens using perpendicular streak method (Bhat and Nayaka, 2023). Briefly, the *Streptomyces* strains were inoculated on one sector of Mueller-Hinton agar (MHA) plate and incubated at 30 °C for 7 days. Following incubation, 0.5 McFarland Standard concentrations of test pathogens are streaked in straight line starting 1 cm apart perpendicularly to the lined *Streptomyces* colony. The plates are incubated at 37 °C for 12 h. An antimicrobial activity is evaluated based on the distance of inhibition between the colony margin of *Streptomyces* and test pathogen.

The condition for co-culture method was chosen by optimizing *Streptomyces* growth condition that yields highest antibacterial activity. The *Streptomyces* strains were cultured in various media and incubated at 30 °C and 37 °C under 200 rpm shaking condition. After that, the cell-free supernatant(s) was then used to evaluate an antimicrobial activity by using agar well diffusion method.

Based on the preliminary results of antimicrobial activities, the following was used for co-culture ALE experiment.

- Bacterial strain: *Streptomyces* sp. SSUT88A.
- Co-culturing Pathogens: MDR-*Acinetobacter baumannii* SUTH-Isolate, methicillin-resistant *Staphylococcus aureus* DMST20651 (MRSA), and MDR-*Pseudomonas* aeruginosa SUTH-Isolate N90PS.
- Media: International *Streptomyces* Project-2 Medium (ISP-2).
- Temperature: 30 °C.

3.2.2 Co-Cultivation: Adaptive Laboratory Evolution

The co-cultivation method was be adapted form Dharmesh Harwani et al., 2022. *Streptomyces* sp. SSUT88A was inoculated into 5 different flasks (No.1, No.2, No.3, No.4, No.5) each containing sterilized 50 mL of ISP-2 broth to an initial OD_{600} of 0.01 and incubated at 30 °C, 180 rpm. After 72 hours of incubation and visible growth of SSUT88A, the flasks were inoculated with 100 µL of target pathogen(s) at OD_{600} = 0.50, following these conditions: Flask No.1 was not co-cultured with any pathogen and served as a negative control. While flask No.2, 3, and 4 were inoculated with MDR-*Acinetobacter baumannii* SUTH-Isolate, MRSA DMST20651, and MDR-*Pseudomonas* aeruginosa SUTH-Isolate N90PS, respectively. Flask No.5 was inoculated with all *A. baumannii*, MRSA, and *Pseudomonas aeruginosa* N90PS.

All the flasks were incubated at 30 °C, 200 rpm for 10 days to complete the first adaptation cycle (Cycle 1). Following co-culture incubation, cultures from each flask were serially diluted in normal saline and plated on Starch Casein agar (SCA) using spread plate technique. The plates were incubated at 30 °C for 5 days, or until the colonies of SSUT88A appear.

At least 40 colonies from each flask were randomly selected and streaked separately onto ISP-2 agar plates containing exactly 25 mL of medium per plate and incubated at 30 ℃ for 7 days. The colonies were tested for their antimicrobial activities via agar plug method (Rütten et al., 2022). In brief, a 6 mm cork borer was used to cut out the agar plugs from the grown cultures. To minimize variation due to biomass differences, the agar plugs were carefully selected from lawn with visually similar bacterial density, as different biomass may lead to inconsistent antibiotic production. The plugs were subsequently placed on MHA pre-seeded with MRSA DMST20651, used as representative pathogens to indicate antimicrobial activity. The strains of SSUT88A isolated from flask No.1, 2, 3, 4 and 5 exhibiting highest antimicrobial activity by zone of inhibition around agar plug were served as cycle 1 adapted strains. These strains were used to initiate cycle 2 of adaptation by following the same procedure as described for cycle 1 (Harwani et al., 2022). This experimental procedure was repeated for a total of 9 cycles (Figure 3.1). All strains were preserved in 25% glycerol (v/v) and kept at -80 ℃ until further experiment.

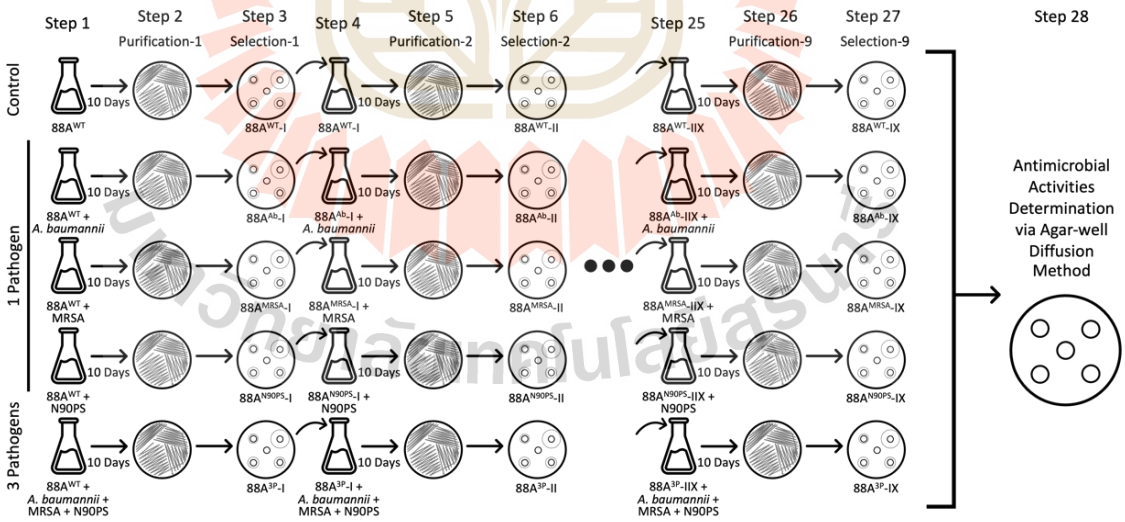

Figure 3.1 Flowchart depicting the Adaptive Laboratory Evolution process aiming to enhance antimicrobial compound production in co-cultured *Streptomyces* sp. SSUT88A and multidrug-resistant pathogens.

3.3 Crude Bioactive Compound Production

A dense spore suspension, pregerminated in ISP-2 media for 6-8 h at 30 °C, 200 rpm, was used to inoculate new ISP-2 media to the initial OD_{600} of 0.03, and incubated at 30 °C, 200 rpm for 10 days. The cell-free supernatant containing bioactive compounds of both wild-type and evolved strains were extracted using ethyl acetate-based liquid extraction method. Briefly, the cell-free supernatant obtained after centrifugation was mixed with an equal volume of ethyl acetate (1:1, v/v) in a separatory funnel and shaken vigorously for 10 minutes and left to allow phase separation, the extraction was performed twice (Ahsan et al., 2017). The combined ethyl acetate phases were collected, evaporated to dryness using a rotary evaporator, weighed and stored at -20 °C until further analysis.

3.4 Antimicrobial Activity Assessment

3.4.1 Primary Antimicrobial Activity Assay: Agar Well Diffusion

Agar well diffusion method was used to determine a primary antimicrobial activity of crude extract. A 0.5 McFarland standard concentration of test pathogen was evenly swabbed onto MHA plates. Wells were then punched aseptically with a sterile cork borer, and a 50 µL of the crude extract at desired concentration is pipetted into the well. The plates will be incubated at 37 °C for 12 h. After incubation, the zone of inhibition in diameter (mm) will be observed and recorded (Abirami and Kannabiran, 2016).

3.4.2 Antimicrobial Activity Monitoring of Selected Strains

To further monitor the onset and progression of bioactive compound production, a time-course study was performed on the adapted strains SSUT88A those exhibited the strongest antimicrobial activity in the primary agar well diffusion assay. Each strain was cultured in ISP-2 medium under the same conditions as described previously in section 3.2.3. Cell-free supernatants were collected daily by centrifugation and kept at -20 °C until subjected to antimicrobial activity screening

against MRSA DMST20651 using the agar well diffusion method, as described in section 3.2.4.

3.4.3 Secondary Antimicrobial Activity Evaluation: Minimum Inhibitory Concentration (MIC) and Minimum Bactericidal Concentration (MBC)

3.4.3.1 Minimum Inhibitory Concentration (MIC)

The MIC was determined following EUCAST guidelines (2024). A single colony of the test organism was inoculated into 5 mL of nutrient broth and incubated overnight at 37 °C, 200 rpm. The overnight culture was adjusted to an OD_{600} of 0.008 in sterile normal saline to prepare a standardized inoculum. Crude extract was initially dissolved in dimethyl sulfoxide at a stock concentration of 10 mg/mL. This stock was then diluted in Mueller–Hinton Broth (MHB) to prepare a working solution, with a maximum test concentration of 2,048 µg/mL. All solutions containing the crude extract were filter-sterile using a 0.22 µm syringe filter prior to use in the assay to ensure sterility and homogeneity. A two-fold serial dilution series was prepared in a 96-well plate. Positive control (no antibiotic), negative control (sterility) and DMSO control (to account for solvent effects) were included. Plates were incubated at 37 °C for 16–24 h. The MIC was defined as the lowest concentration at which no visible bacterial growth was observed (Kadeřábková et al., 2024).

3.4.3.2 Minimum Bactericidal Concentration (MBC)

To determine MBC, 50 µL from wells showing no visible growth in the MIC assay were spot-plated onto Mueller-Hinton Agar plates. Plates were incubated at 37 °C for 24 h. The MBC was defined as the lowest concentration resulting in no colony growth on the agar surface.

3.5 Whole Genome Sequencing, Assembly, and Visualization

3.5.1 Genomic DNA Extraction, Sequencing, and Quality Control

The strain demonstrating the highest level of adaptation, as determined by increased antimicrobial activity against multidrug-resistant (MDR) pathogens, was carefully chosen for further genomic analysis.

The genomic DNA (gDNA) of the selected strains was extracted from cells grown in ISP-2 broth at 30°C for 72 h. The salting-out method described by Kieser et al., 2000 was modified for optimized gDNA isolation (Kieser et al., 2000). Bacterial cells were collected by centrifugation at 3,000 ×g for 5 min and transferred to 50 mL centrifuge tubes. The cell pellet was washed twice and suspended in 4 mL of TE buffer (10 mM Tris-HCl and 1 mM EDTA, final pH = 8.0). 1 mL of lysozyme solution (50 mg/mL) and 125 µL of RNAse A solution (10 mg/mL) were then added, the mixture was incubated at 37°C for 60 min with occasional inversion. Subsequently, 140 µL of proteinase K solution (20 mg/mL) and 600 µL of 10% of sodium dodecyl sulfate (SDS) were added, the solution was incubated at 55°C for 30 min. To extract gDNA, 2.2 mL of 5M sodium chloride (NaCl) was added and allow to cool to room temperature before adding 5.2 mL chloroform: Isoamyl alcohol (24:1), mixed by gently inversion for 5-10 min. before being centrifuged at < 3,000 ×g for 15 min. The upper layer was carefully transferred to a new clean tube with cut P1000 pipette tip (If the solution is still opaque, additional NaCl, SDS and Chloroform: Isoamyl alcohol were added, and the extraction step was repeated). The extract was then incubated on ice for at least 2 min. before adding 2 volumes of ice-cold absolute ethanol. gDNA was precipitated as visible clumps by very gentle inversion. The gDNA was carefully spooled into a new microcentrifuge tube containing 70% ethanol using a sealed Pasteur pipette. (If the DNA clump was not intact or the amount was too small to spool, the DNA was instead collected by centrifugation at <3,000 ×g for 10 min.). The pellet was washed 2 additional times with 70% ethanol, air-dried in a biosafety cabinet and resuspended in TE buffer or nuclease-free water.

The quality of gDNA was assessed using agarose gel electrophoresis and NanoDrop™ One spectrophotometry (Thermo Scientific, USA).

This selected strain was subjected to whole genome sequencing, which will be conducted by Theragen Bio Co.,LTD., Republic of Korea, using the Illumina Novaseq 6000 sequencer (Illumina, CA, USA).

To achieve high quality reads, quality assessments, adapter trimming, and quality filtering were performed using fastp v0.23.4, with default settings (Chen, 2023; Chen et al., 2018).

3.5.2 Genome Assembly and Assessment

The quality-filtered short reads were *de novo* assembled using Unicycler v0.5.0, an assembly pipeline for bacterial genomes (Wick et al., 2017). Default parameters were applied with -conservative assemble mode. The completeness and quality of the assembled genome were assessed using two tools: (1) QUAST v5.2.0 to generate assembly statistics such as N50, total length, number of contigs, and GC content (Gurevich et al., 2013) and (2) CheckM v1.2.2 to evaluate the genome's completeness and contamination based on lineage-specific marker genes (Parks et al., 2015).

3.5.3 Genome Annotation and Visualization

Genome annotation was performed using Prokka v1.14.6, to identify coding sequences (CDS), predict encoding protein, and other genomic features (Seemann, 2014).

Proksee, which used CGView engine, was used to generate circular genome maps for all strains and also to annotate the genomes with Prokka (Grant et al., 2023).

3.6 Functional and Comparative Genomic Analysis

To characterize and compare key functional elements and genomic changes among the wild-type and evolved strains, set of tools were applied to analyze strains'

taxonomy, antibiotic resistant profile, mobile genetic element, secondary metabolites, comparative clustering, variant calling, and k-mer validation.

3.6.1 Taxonomic Comparisons

Digital DNA-DNA hybridization (dDDH) analysis and a phylogenomic tree derived from the whole genome sequences of wild-type and adapted strains with their related type strains were conducted using the Type (Strain) Genome Server (TYGS), which utilizes Genome BLAST Distance Phylogeny (GBDP) methods (Meier-Kolthoff and Göker, 2019).

The Average Nucleotide Identity (ANI) values between wild-type and evolved strains were calculated using JSpeciesWS, to quantitatively measure genomic similarity (Richter et al., 2015).

3.6.2 Antimicrobial Resistance Gene Exploration

Antimicrobial resistance (AMR) genes were identified using ResFinder (v4.7.2), a curated database and detection pipeline hosted by the Center for Genomic Epidemiology (Florensa et al., 2022), on annotated genome with default thresholds for sequence identity (> 90%) and minimum gene length.

3.6.3 Biosynthetic Gene Clusters Detection and Comparisons

The secondary metabolite biosynthetic capacity of each strain was analyzed using antiSMASH (v8.0). All assembled genomes were submitted for complete BGC detection with strict detection strictness to avoid false positives. The resulting annotations provided information on the types, locations, and predicted functions of Biosynthetic Gene Clusters (BGCs), such as Non-Ribosomal Peptide Synthetase (NRPS), Polyketide Synthase (PKS), Ribosomally synthesized and post-translationally modified peptides (RiPPs), and terpenes. These results were used for presence/absence BGC analysis (Blin et al., 2025).

3.6.4 Orthologous Gene Clustering based on Translated Amino Acid

Orthologous gene clusters were analyzed using OrthoVenn3 (Sun et al., 2023), a platform for comparative functional genomics provided a functional framework for interpreting which gene sets were gained or lost. Translated amino acid

sequences predicted by Prokka from each assembled genome were submitted for clustering using OrthoFinder algorithm, E-value and Inflation value of 10^{-2} and 1.50, respectively.

3.6.5 Structural and Point Mutational Analysis of Adapted Strains

Genomic variants between the evolved strains and the wild-type reference were analyzed using Breseq v0.38.1, a tool specifically designed for microbial genome variations detection (Deatherage and Barrick, 2014). Because the reference genome used in this study was a draft assembly composed of multiple contigs, relying solely on reference mode (-r) could lead to inaccurate or excessive detection of structural differences those might reflect incomplete or fragmented assemblies rather than true biological variation. To overcome this limitation and better distinguish between small, high-confidence mutations and possible larger-scale rearrangements or deletions, both consensus mode (-c) and reference mode (-r) were employed.

- Contigs mode (-c), a primary focused mode due to time constraints and its robustness in identifying point mutations such as single nucleotide polymorphisms (SNPs). In this mode, the reference genome was treated as an independent draft assembly, and high-confidence differences from the wild-type were reported. Only a small number of variants were detected per evolved strain, which highlighted the overall genetic similarity and stability of the core genome across conditions. The focused scope and lower susceptibility to assembly artifacts made this mode the most reliable for confident mutation calling.
- Reference mode (-r) was used to complement SNP detection and assess potential larger-scale genomic changes, such as deletions or structural losses. In this mode, reads from each evolved strain were aligned directly to the wild-type draft assembly to recapture the SNPs detected in -c, while additionally identifying numerous putative large deletions. This approach flagged the apparent loss of over 100 contigs in some strains (a result that initially seemed implausible and raised concerns

about misalignment or artifacts due to the fragmented reference). Deletion predictions from this mode were retained for downstream validation and comparative analysis.

To distinguish true genomic loss from assembly or mapping artifacts, we conducted 31-mer frequency analysis on raw FASTQ reads using Jellyfish v2.3.0 (Marçais and Kingsford, 2011). Unique 31-mers derived from each reference contig were queried against evolved strains k-mer databases (Lee et al., 2020). Contigs with zero 31-mer hits with overall high sequencing depth were classified as high-potential true deletions (Zheng et al., 2022). Those with residual 31-mers or low depth were deprioritized as likely artifacts.

3.6.6 Mobile Genetic Elements

Mobile Genetic Elements (MGEs) were annotated with MobileOG-DB through the Proksee platform. Regions of Interests were observed for integrases, transposases, conjugation machinery, or replication/recombination proteins.

3.7 Data Analysis and Visualization

Statistical analyses were performed using R (version 4.4.2). One-way ANOVA followed by Tukey's HSD post hoc test was used to assess differences between groups. A significance difference was determined by $p < 0.05$ throughout. Unless otherwise stated, all experiments were performed in triplicate (n = 3). Graphs, including box plots and line graphs, were generated using the ggplot2, reshape2 and dplyr package.

CHAPTER IV

RESULTS AND DISCUSSION

4.1 Co-Cultivation: Adaptive Laboratory Evolution

Using adaptive laboratory evolution protocol, *Streptomyces* sp. SSUT88A competed against three different pathogens. The approximately 220-day-long competition experiments yielded 4 adapted strains after the ninth (IX) cycle of adaptation-selection based on their highest antimicrobial activities across the same co-culturing condition. The strains were designated as SSUT88A$^{Ab9\text{-}5}$ (SSUT88A co-cultured with *Acinetobacter baumannii* SUTH-Isolate), SSUT88A$^{MR9\text{-}16}$ (SSUT88A co-cultured with MRSA20651), SSUT88A$^{N90PS9\text{-}32}$ (SSUT88A co-cultured with *Pseudomonas aeruginosa* SUTH-Isolate N90PS), and SSUT88A$^{3P9\text{-}1}$ (SSUT88A co-cultured with all 3 pathogens mentioned above). The adapted strains exhibited no visually different morphological character from their parental strain (Figure 4.1).

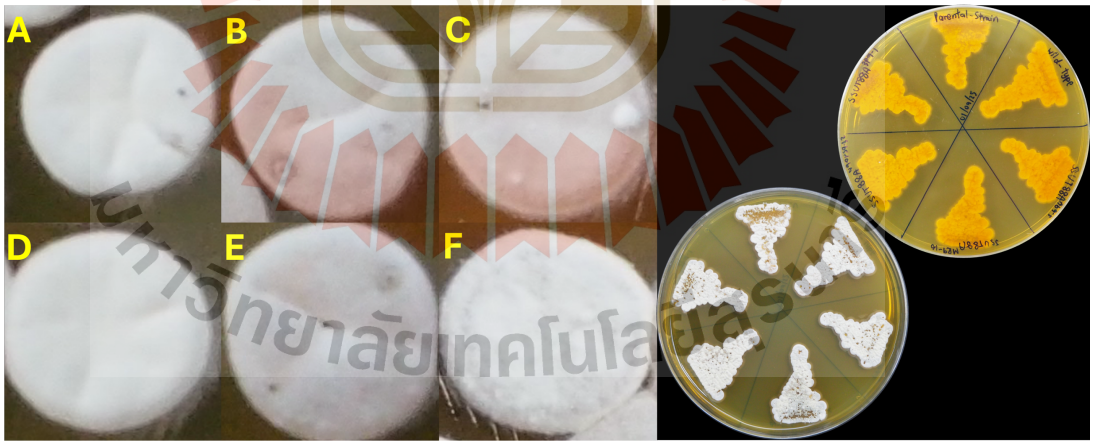

Figure 4.1 Colony morphology of *Streptomyces* sp. SSUT88A parental strain (A) and its adapted strains SSUT88A^{WT} (B), SSUT88A$^{Ab9\text{-}5}$ (C), SSUT88A$^{MR9\text{-}16}$ (D), SSUT88A$^{N90PS9\text{-}32}$ (E), SSUT88A$^{3P9\text{-}1}$ (F) grown on ISP-2 medium at 30 °C for 7 Days.

4.2 Crude Extraction of Bioactive Compounds

The cell-free supernatant after adaptation was extracted twice with ethyl acetate (1:1 v/v) by vigorously shaking in the separatory funnel and left to allow phase separation at room temperature. The ethyl acetate layer containing crude compound was evaporated to dryness. The dried crude extract was weighed to assess each strain's ability to produce crude extract. After nine cycles of adaptation, MRSA was the most potent pathogen to trigger the production of crude compound, with a 46.3% increase compared to the average wild-type (WT) crude compound production. This was followed by *A. baumannii* which induced 32.6% increase. Quadri-culture co-cultivation (3-pathogens combination) showed a lower triggering effect, increasing the crude compound production by only 5.1%, while *P. aeruginosa* led to a reduce crude compound production by 5.1% compared to the WT average. Statistical analysis was performed using one-way ANOVA followed by Tukey's HSD multiple comparison test (p-value < 0.05). Among these, only crude extract produced from MRSA and *A. baumannii* were statistically significant difference at (Figure 4.2).

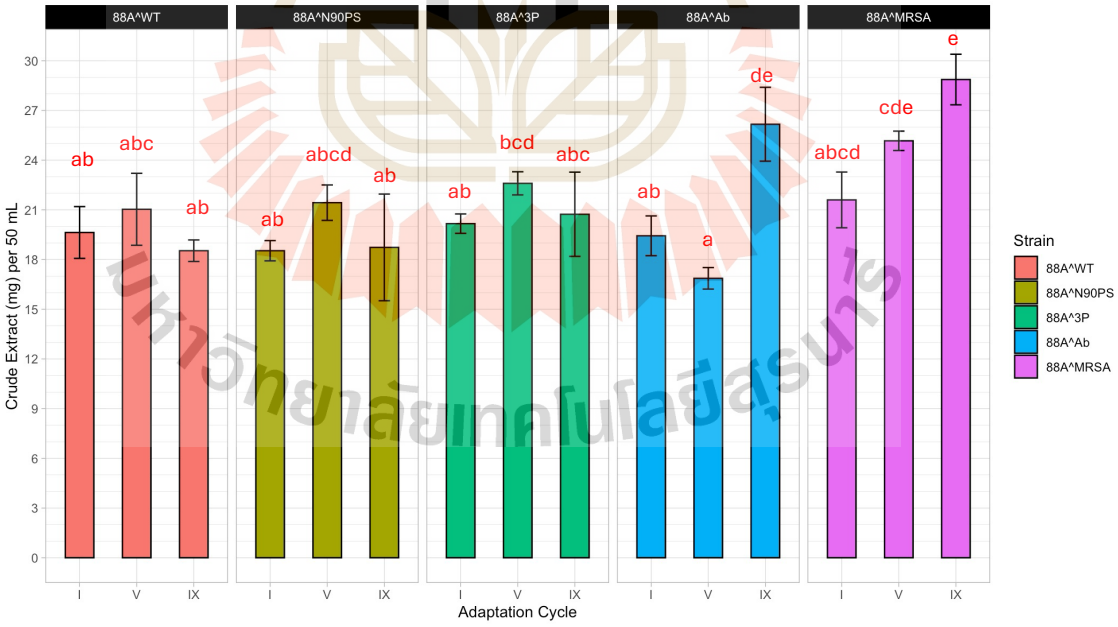

Figure 4.2 Quantity of crude extracts (mg) from each strain through adaptation cycles (n=3). 88A^WT: SSUT88A^{WT}; 88A^Ab: SSUT88A$^{Ab9\text{-}5}$; 88A^MRSA: SSUT88A$^{MR9\text{-}16}$; 88A^N90PS: SSUT88A$^{N90PS9\text{-}32}$; 88A^3P: SSUT88A$^{3P9\text{-}1}$.

The ratio of crude extract to total cell dry weight (mg/g) was used to calculate the yield, offering insight into how efficiently each strain produces its crude bioactive compounds. In the case of wild-type, a gradual decline in yield was observed along adaptation cycles, suggesting that prolonged subculturing may shift its metabolic priorities away from secondary metabolite production. For SSUT88A$^{N90PS9-32}$ and SSUT88A^{3P9-1}, yield fluctuated over the course of the adaptation without a consistent upward or downward trend, implying that co-cultivation with these pathogens may not strongly promote or suppress metabolite production but instead cause varying metabolic responses across cycles. SSUT88A^{Ab9-5} exhibited the highest overall yield, showing a 43% increase compared to the wild-type average followed by SSUT88A^{MR9-16} with a 40% increase. However, statistical analysis using one-way ANOVA followed by Tukey's HSD post hoc test showed no significant difference between these two groups ($p > 0.05$). In contrast, SSUT88A^{3P9-1} showed only a 4% increase, while SSUT88A$^{N90PS9-32}$ had a 7% decrease in yield compared to the wild-type. These differences were also not statistically significant.

The substantial increase in crude extract production observed in strain SSUT88A^{MR9-16}, co-cultured with MRSA, may be attributed to the wild-type *Streptomyces* sp. SSUT88A's prior antimicrobial activity against this pathogen. Although weaker, a similar effect was also observed against *A. baumannii*, which may partly explain the enhanced production in SSUT88A^{Ab9-5}. The presence of these pathogens likely imposed a comparatively moderate selective pressure during co-cultivation, potentially providing favorable conditions for adaptive shifts in secondary metabolism. Furthermore, the two positively adapted strains, demonstrated different crude compound production elevation profile. SSUT88A^{MR9-16} gradually and steadily increase from cycle-1 until cycle-9, while SSUT88A^{Ab9-5} seems to decrease at the earlier cycle (CI-IV) but strike back at the ninth adaptation cycle, these differences may reflect distinct adaptive strategies, where stable enhancement in biosynthetic output requires varying durations of exposure depending on the selective environment.

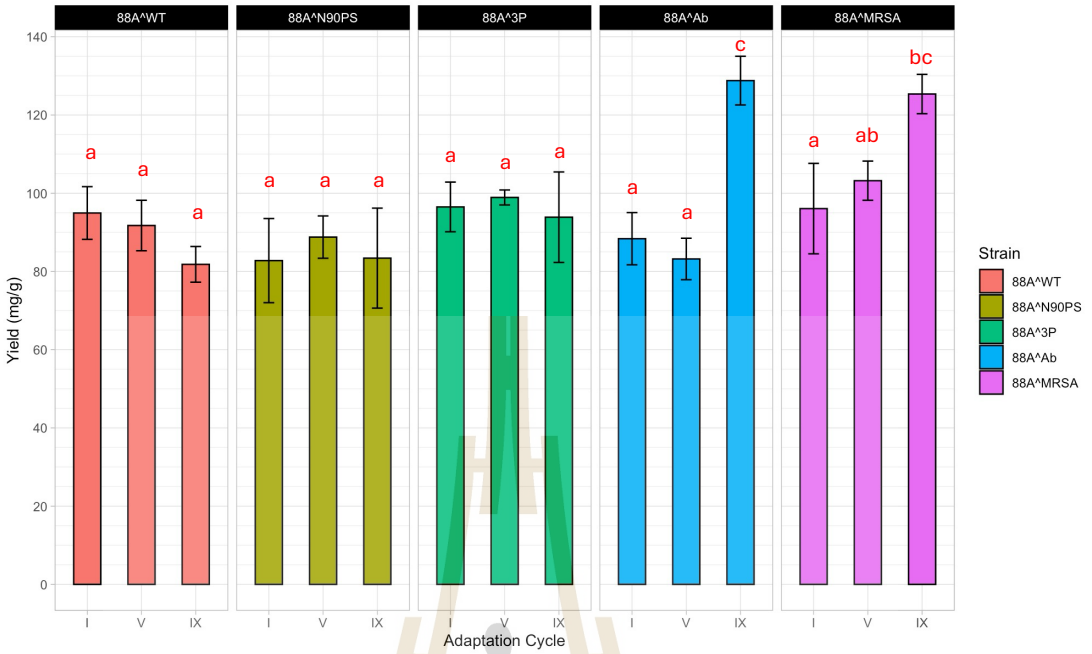

Figure 4.3 Yield of crude extracts from each strain through adaptation cycles (crude extract weight (mg)/ cell dry weight (g)). All experiments were conducted in triplicate. 88A^WT: SSUT88A^{WT}; 88A^Ab: SSUT88A$^{Ab9\text{-}5}$; 88A^MRSA: SSUT88A$^{MR9\text{-}16}$; 88A^N90PS: SSUT88A$^{N90PS9\text{-}32}$; 88A^3P: SSUT88A$^{3P9\text{-}1}$.

4.3 Antimicrobial Activity Assessment

To evaluate the bioactive potential of the adapted *Streptomyces* strains, a set of antimicrobial assays were performed to provide a comprehensive aspect of how co-cultivation influences the spectrum, strength, and timing of antimicrobial compound production in response to different selective pressures.

4.3.1 Primary Antimicrobial Activity: Agar Well Diffusion

Throughout the adaptation process, agar well diffusion assays revealed that the antimicrobial activity of crude compound produced by each strain as shown in Figure 4.4. The wild-type strain's antimicrobial activities remained relatively stable, with only minor fluctuations in inhibition zones against both Gram-positive and Gram-negative pathogens, suggesting that, in the absence of selective pressure no spontaneous upregulation or suppression was observed across cycles, the strain maintains a consistent level of bioactive compound production. Evidently, notable enhancements in antimicrobial activity were observed in strains adapted through co-

cultivation with specific suitable pathogens. Particularly, SSUT88A$^{MR9\text{-}16}$ and SSUT88A$^{Ab9\text{-}5}$ displayed significantly increased inhibition zones by cycle 9, most obvious against Gram-positive bacteria, MRSA and methicillin-resistant *Staphylococcus epidermidis* (MRSE). A moderate increase in inhibition was also noticed against Gram-negative bacteria (e.g., *A. baumannii,* MDR-*E. coli* and MDR-*P. aeruginosa*), even though the enhancement was less pronounced, the relative increase is rather similar.

On the other hand, strains SSUT88A$^{N90PS9\text{-}32}$ and SSUT88A$^{3P9\text{-}1}$ did not exhibit consistent improvements in antimicrobial activity, demonstrating variable with some slightly reduced inhibition profiles over time, implying that the respective co-cultivation conditions may not have provided a suitable selective pressures for the enhancement of bioactive compound production. Antimicrobial activity against *Klebsiella pneumoniae* 1617 SUTH-isolate was not observed in any strain, thus is not reported in this work.

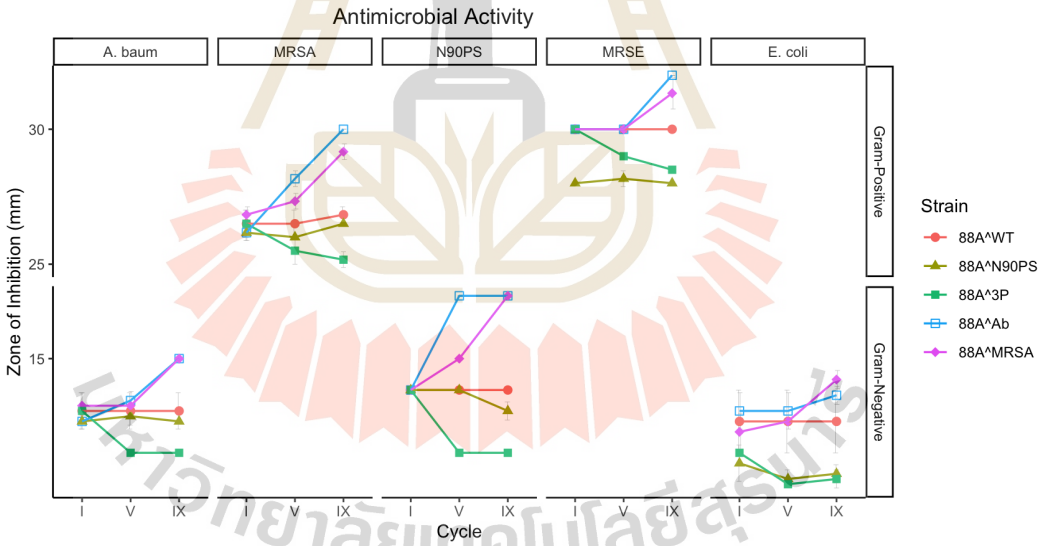

Figure 4.4 Antimicrobial activities of crude extracts from each strain across adaptation cycles 1, 5, and 9 (n=3). The pathogens are divided into Gram-positive and Gram-negative which use different Y-axis scale. Strains are denoted on the right legend, 88A^WT: SSUT88A^{WT}; 88A^Ab: SSUT88A$^{Ab9\text{-}5}$; 88A^MRSA: SSUT88A$^{MR9\text{-}16}$; 88A^N90PS: SSUT88A$^{N90PS9\text{-}32}$; 88A^3P: SSUT88A$^{3P9\text{-}1}$.

4.3.2 Time-Course Antimicrobial Activity

Throughout the adaptation process, one strain exhibiting complete loss of antimicrobial activity was isolated from the co-culture with the three-pathogen combination at the sixth adaptation cycle. This strain was designated as SSUT88A^{3P6-7} and was included as a negative adaptation effect in subsequent analyses. The strains, SSUT88A$^{N90PS9-32}$ and SSUT88A^{3P9-1}, which showed minimal difference in crude extract production, yield, and primary antimicrobial activity throughout the adaptation process, were excluded from further investigation.

Morphological observations revealed that while the wild-type strain and positively adapted strains (SSUT88A^{MR9-16} and SSUT88A^{Ab9-5}) exhibited similar colony appearance which characterized by dark orangish-yellow pigmentation and diffusible pigment, the SSUT88A^{3P6-7} strain exhibited notable morphological alterations. The characteristic yellow diffusible pigment, likely associated with antimicrobial compound production, was absent and the colony pigmentation shifted toward a more reddish hue. These morphological differences support the observed loss of bioactivity and suggest metabolic or regulatory alterations. (Figure 4.5)

Figure 4.5 Colony appearances of wild-type SSUT88A, SSUT88A^{MR9-16}, SSUT88A^{Ab9-5}, and SSUT88A^{3P6-7} (strain with activity loss).

Using MRSA DMST20651, which possess high susceptibility to bioactive compound produced from SSUT88A, as a representative pathogen for the most

sensitive model, a time-course antimicrobial assessment was conducted (Figure 4.6). Among tested isolates, SSUT88A^{Ab9-5} exhibited the earliest onset of detectable antimicrobial activity, beginning on day 2 and reaching the highest inhibition around days 5–6, while sustained the activity across experimentation period. In contrast, SSUT88A^{MR9-16} and the wild-type strain displayed similar production profiles, with inhibition zones appearing around days 3–4 and reaching maximal activity by approximately day 10. Moreover, SSUT88A^{3P6-7} failed to exhibit any observable antimicrobial activity over the entire 14-day incubation period, confirming that its loss of bioactivity is not from the compound stability over time.

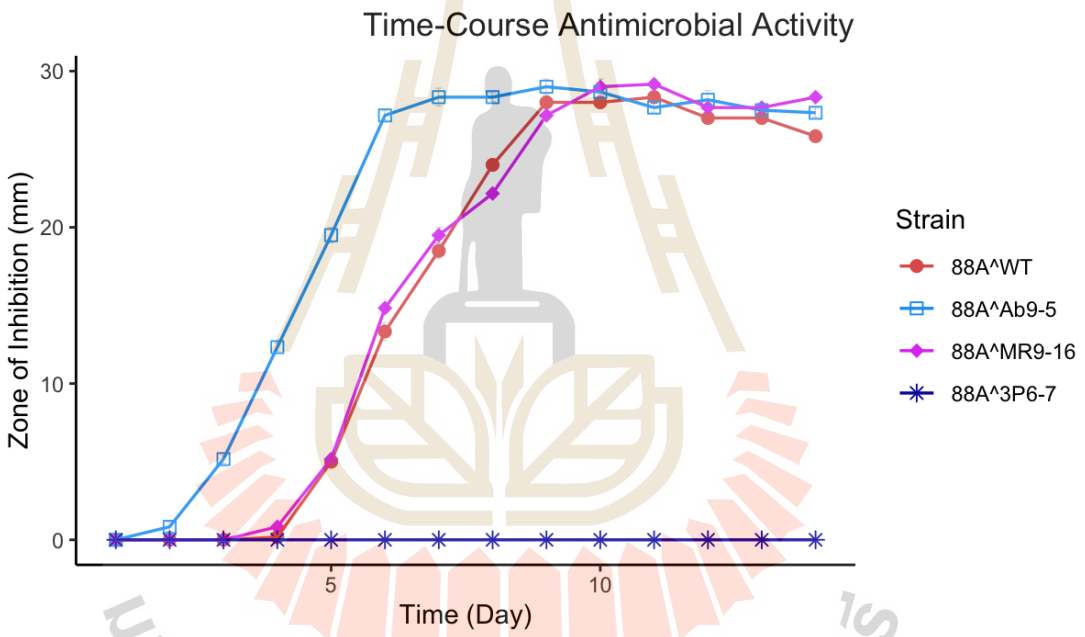

Figure 4.6 Antimicrobial activities monitoring by observing antimicrobial compound production of each strain over the course of 14 days (n=3). MRSA DMST20651 was used as the representative tested pathogens.

4.3.3 Secondary Antimicrobial Activity: MIC and MBC

MIC and MBC assays were conducted to evaluate the potency of crude extracts from selected strains against 6 drug-resistant pathogens in terms of secondary antimicrobial activity (Table 4.1). The wild-type strain displayed moderate antimicrobial activity, particularly against Gram-positive bacteria, MRSA and MRSE, with MICs of 2 µg/mL. In contrast, co-cultivation with MRSA or *A. baumannii* greatly enhanced the

antimicrobial activity of the adapted strains (SSUT88A^{MR9-16} and SSUT88A^{Ab9-5}). Both strains exhibited 4–8-fold lower MIC values against MRSA and MRSE (0.25–0.5 µg/mL) compared to the wild-type, as well as decreased MBC values (32 µg/mL), indicating stronger inhibition and bactericidal effects. Additionally, these strains also showed improvements in MIC and MBC values against *A. baumannii* and *E. coli*. On the other hand, very limited differences were observed in MIC values against *K. pneumoniae* and in MBC values against *P. aeruginosa*, while no differences were observed in MBC against *K. pneumoniae* or MIC against *P. aeruginosa* across all strains. Regardless, all strains required very high concentrations of crude extract to inhibit or kill these pathogens. On the other hand, SSUT88A^{3P6-7}, adapted through co-culture with all three pathogens, completely lost measurable antimicrobial activity across all tested organisms (MIC and MBC >2,048 µg/mL), aligning with earlier time-course and inhibition zone findings.

Table 4.1 Minimum inhibitory concentration (MIC) and minimum bactericidal concentration (MBC) values (µg/mL) of crude extracts from selected *Streptomyces* sp. SSUT88A strains. All experiments were conducted in triplicate.

Drug-Resistant Pathogen	2nd Antimicrobial Activity (MIC/MBC in µg/mL)			
	Wild-type	SSUT88A^{MR9-16}	SSUT88A^{Ab9-5}	SSUT88A^{3P6-7}
MRSA	2/64	0.25/32	0.5/32	>2,048/>2,048
A. baumannii	1,024/1,024	512/512	512/512	>2,048/>2,048
P. aeruginosa	1,024/>2,048	1,024/2,048	1,024/>2,048	>2,048/>2,048
MRSE	2/64	0.25/32	0.5/32	>2,048/>2,048
E. coli	2,048/2,048	1,024/1,024	1,024/1,024	>2,048/>2,048
K. pneumoniae	2,048/>2,048	1,024/>2,048	1,024/>2,048	>2,048/>2,048

Pathogens Used: MRSA – DMST20651; *A. baumannii* – MDR, SUTH-Isolate; *P. aeruginosa* – N90PS, MDR, SUTH-Isolate; MRSE – methicillin-resistant, SUTH-Isolate; *E. coli* – 2026, MDR, SUTH-Isolate; *K. pneumoniae* – 1617, MDR, SUTH-Isolate.

These results demonstrate the potential of adaptive laboratory evolution using co-cultivation to enhance antimicrobial compounds that were already present in the wild-type strain, either by accelerating their production, as seen in the

precocious activity of SSUT88A^{Ab9-5}, or by increasing their potency, as demonstrated by SSUT88A^{MR9-16}. This enhancement could help reduce antibiotics production costs by shortening fermentation time and improving yield efficiency. Moreover, these findings reflect the dynamic nature of microbial adaptation under ecological pressure, which can be strategically harnessed to fine-tune secondary metabolite expression. Further studies to isolate and characterize the upregulated compounds may shed light on their mechanisms of action and reveal novel paths for antimicrobial development.

4.4 Whole Genome Sequencing, Assembly, and Visualization

4.4.1 Genomic DNA Extraction, Sequencing, and Quality Control

Among all adapted strains, three representative strains were selected for whole genome sequencing and comparative analysis, including SSUT88A^{Ab9-5} and SSUT88A^{MR9-16}, which showed most prominent enhancement in antimicrobial activity after adaptive co-culture, and SSUT88A^{3P6-7}, a strain isolated from the cycle-VI of adaptation with a three-pathogen combination that exhibited a complete loss of bioactivity. The genomic DNA was successfully extracted from all strains, and subsequent Illumina sequencing yielded high-quality paired-end reads. The raw reads were processed using fastp v0.23.4, which conducted adapter trimming, quality filtering, and per-read quality control. Final Q30 scores >96% and average GC content around 69-71%, consistent with Streptomyces high GC content description (Ramasamy and Sudalaimuthu, 2022).

4.4.2 Genome Assembly and Assessment

Unicycler v0.5.0 with the conservative mode was used to assemble the high-quality reads into draft genomic sequences. The resulting assemblies were evaluated using QUAST and CheckM to determine structural metrics and completeness. All assembled genomes exhibited characteristics consistent with typical *Streptomyces* species, with large genome sizes ranging from 10.2 to 11.1 Mbp and GC content averaging around 72% relating to fastP data before assembly. The number of contigs varied strains (241–548). CheckM analysis, detected Streptomycetaceae family accurately and used as marker, further confirmed high assembly completeness, with all strains showing >99% completeness and <2% contamination.

The genome assembly of the wild-type strain was approximately 1 Mbp larger than that of the adapted strains. This difference is likely caused by the higher sequencing depth and different sequencing provider used for the wild-type, potentially capturing more low-abundance or repetitive regions. Despite this variation, the assembly quality (e.g., N50, completeness) was high across all samples (Table 4.2), supporting the use of the wild-type genome as a suitable reference for downstream comparative analyses. Variant analysis and k-mer-based deletion screening were used to further examine the potential for biological significant differences in the adapted strains (Section 3.2.7.4).

Table 4.2 Summary of genome assembly statistics generated by QUAST and CheckM for wild-type and adapted Streptomyces strains. All genomes show high completeness and low contamination, supporting assembly quality.

Variable	SSUT88A^{WT}	SSUT88A^{MR9-16}	SSUT88A^{Ab9-5}	SSUT88A^{3P6-7}
Total Length (bp)	11,128,670	10,220,793	10,220,825	10,310,976
GC-Content (%)	71.55	71.66	71.66	71.69
Contigs	548	242	248	241
Largest Contigs	186,269	345,593	427,242	375,625
N50	46,449	112,456	102,227	112,652
N90	11,786	26,695	26,277	28,351
L50	80	26	28	26
L90	287	92	99	92
Completeness* (%)	99.94	99.94	99.94	99.94
Contamination* (%)	1.29	1.07	1.07	1.07

* Genome completeness and contamination is assessed by CheckM v1.2.2

4.4.3 Genome Annotation and Visualization

Genome annotation using Prokka predicted 9,530; 9,011; 9,008; and 8,965 coding sequences for SSUT88A^{WT}; SSUT88A^{MR9-16}; SSUT88A^{Ab9-5}; and SSUT88A^{3P6-7}, genome respectively. The number and types of annotated features were

largely consistent across wild-type and adapted strains, showing the overall genomic conservation.

Circular genome maps generated by Proksee provided an overview of the genomic architecture. The illustrated features are locations of CDSs, tRNAs, tmRNAs, GC-content and GC-skewness. The annotated regions were distributed throughout the chromosomes (Figure 4.7, A-D). Detailed comparative analyses of genome structure and feature distribution, including mobile genetic elements and putative transferred regions, are further discussed in Section 3.2.7.4.

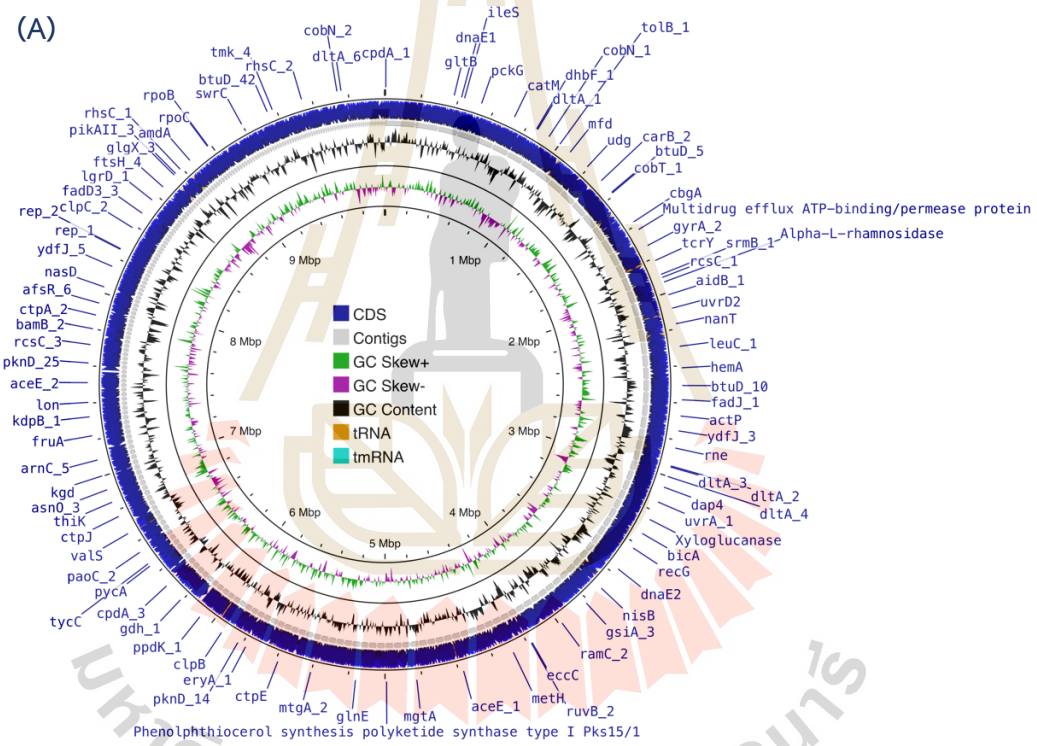

Figure 4.7 Draft genome maps of *Streptomyces* sp. SSUT88A strains generated by Proksee. CDSs are marked in dark blue, Contigs are represented in grey arrows. The green and purple illustrate GC skew+ and GC skew-, respectively, and the black represent GC content. (A) SSUT88A^{WT}; (B) SSUT88A$^{MR9\text{-}16}$; (C) SSUT88A$^{Ab9\text{-}5}$; and (D) SSUT88A$^{3P6\text{-}7}$.

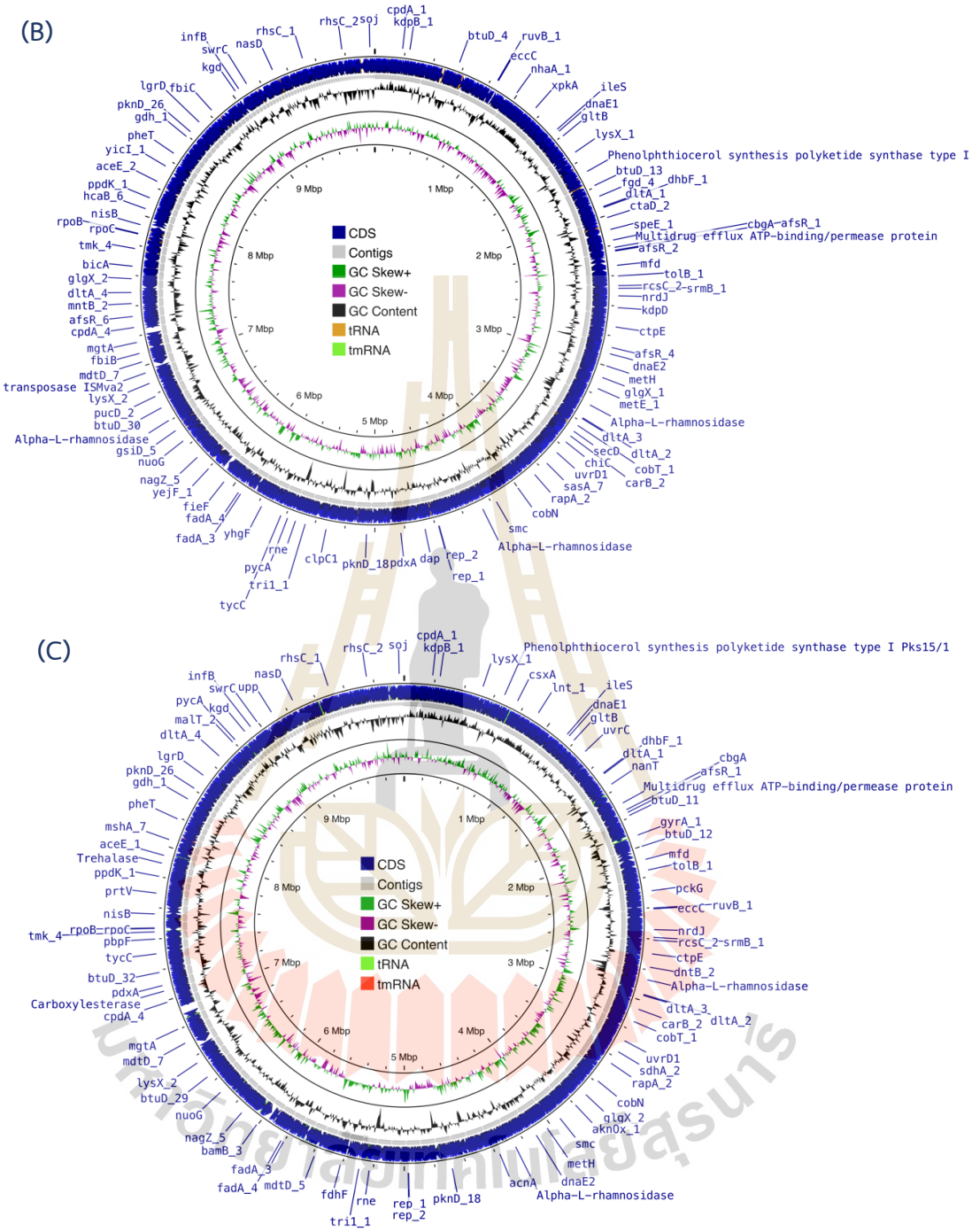

Figure 4.7 (Continued) Draft genome maps of *Streptomyces* sp. SSUT88A strains generated by Proksee. CDSs are marked in dark blue, Contigs are represented in grey arrows. The green and purple illustrate GC skew+ and GC skew-, respectively, and the black represent GC content. (A) SSUT88A^{WT}; (B) SSUT88A$^{MR9\text{-}16}$; (C) SSUT88A$^{Ab9\text{-}5}$; and (D) SSUT88A$^{3P6\text{-}7}$.

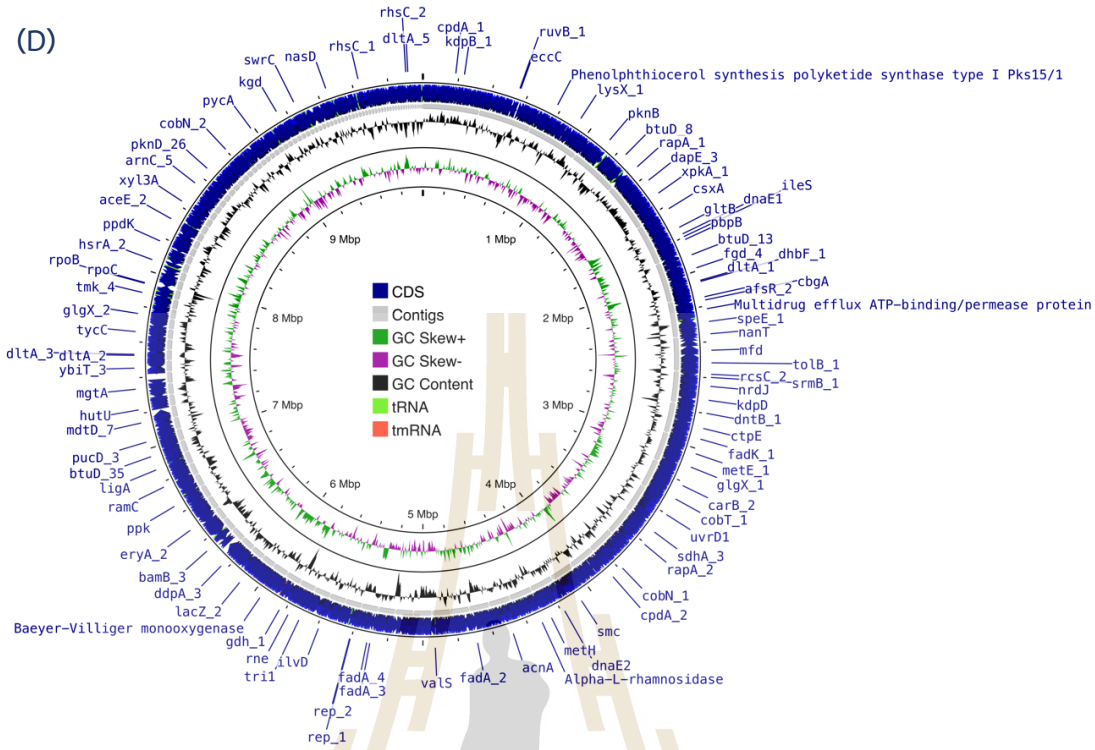

Figure 4.7 (Continued) Draft genome maps of *Streptomyces* sp. SSUT88A strains generated by Proksee. CDSs are marked in dark blue, Contigs are represented in grey arrows. The green and purple illustrate GC skew+ and GC skew-, respectively, and the black represent GC content. (A) SSUT88A^{WT}; (B) SSUT88A$^{MR9\text{-}16}$; (C) SSUT88A$^{Ab9\text{-}5}$; and (D) SSUT88A$^{3P6\text{-}7}$.

4.5 Functional and Comparative Genomic Analysis

4.5.1 Taxonomic Comparisons

Comparative taxonomic analyses confirmed that the wild-type and the adapted strains belong to the same species, therefore excluding the possibility of any contamination during the adaptation or sequencing processes. dDDH values exceeded 99.5%, and ANI values calculated based on both Blast+ (ANIb) and MUMmer (ANIm) were consistently above 99.5%, well above the commonly accepted species-level thresholds. Pairwise Tetra-Correlation analysis also supported species identity, with all pairwise comparisons correlation coefficients above 0.999 cut-off. Moreover, Phylogenomic tree based on whole-genome sequences showed tight clustering of all strains (Figure 4.8).

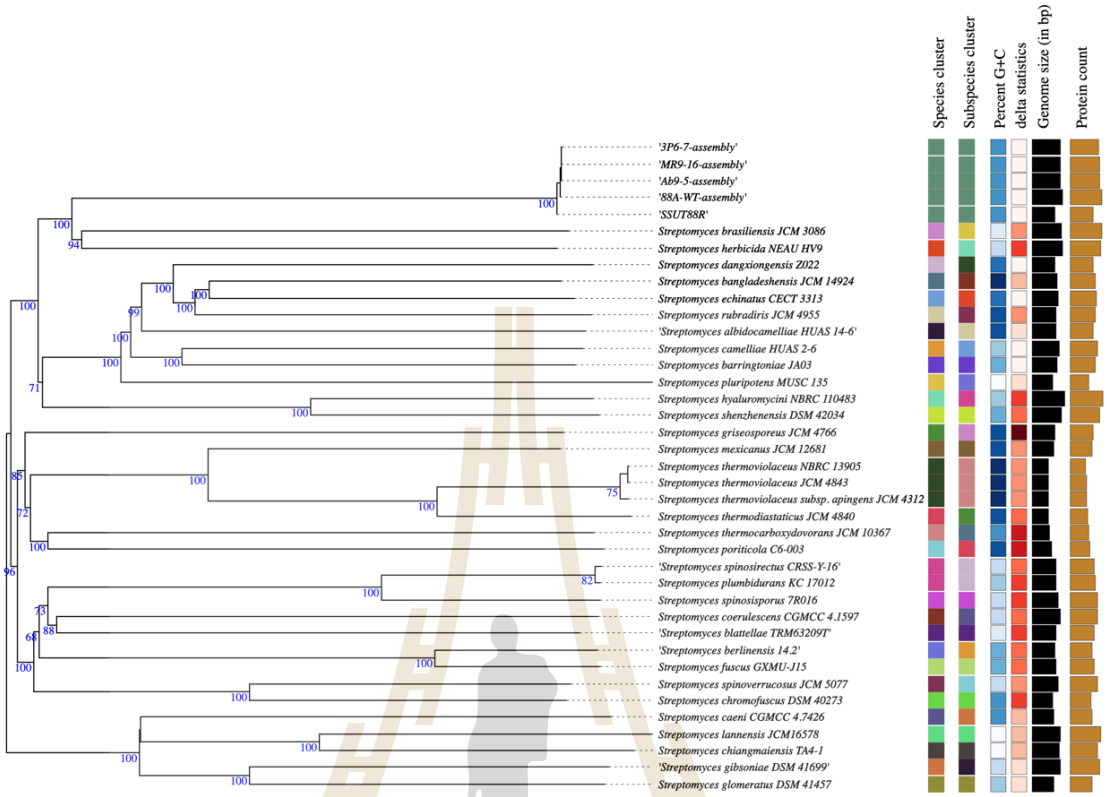

Figure 4.8 Phylogenomic tree of wild-type and evolved *Streptomyces* sp. SSUT88A strains using assembled whole-genome sequence along with their closely related type strain on the TYGS platform.

4.5.2 Antimicrobial Resistance Genes

Based on ResFinder v4.7.2 with default thresholds (>90% identity and minimum length coverage) the wild-type strain does not contain any AMR genes. No acquired AMR genes were detected in any of the evolved strains harbored even after repetitively exposed to drug-resistant pathogens.

4.5.3 Secondary Metabolite Biosynthetic Gene Clusters

Presence/absence analysis of BGCs, predicted by antiSMASH, revealed variation between the wild-type and evolved strains. While several BGCs in the wild-type retain in all evolved strains, others were found exclusively in antibiotics producing strains (wild-type, SSUT88A$^{MR9\text{-}16}$ and SSUT88A$^{Ab9\text{-}5}$), one or more of the high-producing strains (SSUT88A$^{MR9\text{-}16}$ and SSUT88A$^{Ab9\text{-}5}$) or uniquely retained in the wild-type and non-producer (SSUT88A$^{3P6\text{-}7}$). All conserved clusters across all strains are summarized in

Appendix A for reference. The strain-specific and differentially distributed clusters focusing on potential biological relevance are presented in Table 4.3.

The antibiotic producer strains (wild-type, SSUT88A^{MR9-16} and SSUT88A^{Ab9-5}) shared six clusters which are absent in the non-producing SSUT88A^{3P6-7}, suggesting the contribution to core secondary metabolism linked to antibiotic activity. By product type, the clusters found are predicted to synthesize:

- Lanthipeptide-Class-III / NAPAA Hybrid Cluster: A shared cluster among wild-type, SSUT88A^{MR9-16} and SSUT88A^{Ab9-}shows biosynthetic features consistent with both lanthipeptide-class-III and Non-alpha poly-amino acids like e-Polylysin (NAPAA) core biosynthetic genes. This prediction suggests the cluster may encode for either or both compound types.
- Terpene: one terpene BGCs (~21,607 bp) was found, this cluster does not correspond to known terpene pathways, hopene or geosmin, which were present in all four strains, suggesting it may encode an uncharacterized compound. Since terpenoid compounds and their derivatives are extremely diverse and have been demonstrated to have antimicrobial, antifungal, anti-inflammatory, antiviral, immunomodulatory, antioxidant or antitumor activities (Duttaroy, 2021), this BGC exclusive presence in the antibiotic-producing group may take functional role in antimicrobial activity, though further experiment would be needed to determine its product and its activity.
- Nucleoside: A nitrogen-containing heterocyclic nitrogenous base and a pentose sugar (Huang et al., 2014), even though mostly related to fundamental building block of DNA and RNA, nucleosides and their derivatives are found to exhibit wide biological activities including antimicrobial (Zhang et al., 2022), with no exceptions to most categories of antibiotics, nucleoside antibiotics are also found to be produced by *Streptomyces* sp. In this analysis, nucleoside BGC was exclusively found in the antibiotic-producers. Although no known compound could be confidently assigned to this cluster, its conserved presence in the active

strains implies a possible association with the antibiotic-producing phenotype.

- Benzoxazole (Most similar know cluster showed Mycemycin C/A/B with medium confidence): Mycemycins are benzoxazole antibiotics, more specifically dibenzoxazepinone group, known for weak a HIV-1 reverse transcriptase inhibitory effect (Liu et al., 2015). While the similarity confidence failed to certainly confirm mycemycin clusters, the prediction suggests the potential for production of closely related molecules. The fact that they were only detected in antibiotic-producing strain strengthen the possible involvement in the observed antimicrobial activity.
- Aryl polyenes: known to be membrane-associated yellow pigments produced by various bacteria (Schöner et al., 2016). They are structurally similar to carotenoids and functionally act as antioxidants, protecting cells from oxidative stress caused by reactive oxygen species (ROS). Present in these strains with antimicrobial activity and visually yellow colored, this BGC may contribute or at least take part in their antibiotics production, yellow pigmentation and increased fitness. Although further experimental validation would be required to confirm this role, some compound like spinamycin has been demonstrated to have antifungal activities and produced from *Streptomyces* (Kawai et al., 2023).

The positively adapted strains defined by increased antimicrobial activity (SSUT88A$^{MR9\text{-}16}$ and SSUT88A$^{Ab9\text{-}5}$) shared two types of clusters which are NRPS and Type I Polyketide Synthase (T1PKS).

Two NRPS clusters were uniquely shared between them, one of these clusters was annotated with low-confidence similarity to actinomycin D, spanning part of one core biosynthetic genes and some additional genes. Actinomycin D is a well-characterized antibiotic produced by *Streptomyces* sp. and is known for its antimicrobial against Gram-positive bacteria (Xia et al., 2022; Zimowska et al., 2024).

Although the annotation confidence was low, the presence of this cluster exclusively in the two strains exhibiting enhanced antimicrobial activity suggests it may contribute to this phenomenon.

In addition, one T1PKS cluster was also identified exclusively between them. T1PKSs are large modular enzymes responsible for the synthesis of various polyketide antibiotics in *Streptomyces* (Wang et al., 2020). Although no strong match to known compounds was found for this cluster, its presence only in the enhanced bioactivity strains makes it a candidate of interest. It is possible that this cluster encodes a novel or modified polyketide compound with antimicrobial activity, potentially contributing to the elevated activity observed in these strains.

Although the annotation confidence was low, the exclusive presence of this cluster in the two strains with enhanced antimicrobial activity opens the possibility that it encodes a novel or modified compound contributing to the observed phenotype.

Lastly, a group of BGCs was identified as being present only in the wild-type and the non-producing SSUT88A^{3P6-7} strain, but absent in antibiotic-enhanced strains. These include a lanthipeptide-class-III, redox-cofactor, T1PKS cluster predicted to produce butyrolactol A, a type III polyketide synthase (T3PKS) cluster associated with germicidin biosynthesis, and an aminopolycarboxylic acid cluster linked to ethylenediaminesuccinic acid hydroxyarginine (EDHA) production.

Lanthipeptides are often associated with morphogenetic (Kodani et al., 2005; Takano et al., 2017; Wang and van der Donk, 2012) and antimicrobial activity (Völler et al., 2012). The redox-cofactor component may play a supportive metabolic role and some was proposed to be essential for antimicrobial production (Wang et al., 2013). Butyrolactol A is primarily reported as an antifungal compound, while it demonstrates potent antifungal activity, it's antibacterial aspects remain unclear (Chen et al., 2025). Germicidin is involved in auto-inhibition of spore germination in *Streptomyces*, helping regulate the initiation of growth under unfavorable conditions (Aoki et al., 2011), and the function of EDHA in this context remains unclear. None of these compounds are primarily linked to antibacterial activity, which supports the idea

that these clusters may not be relevant to the enhanced antimicrobial traits observed in other two strains.

Table 4.3 Shared biosynthetic gene clusters presence or absence correlates with each strain. "WT" = wild-type; "3P" = SSUT88A^{3P6-7}; "Ab" = SSUT88A^{Ab9-5}; "MR" = SSUT88AMR$^{9-16}$. The presence of each cluster is indicated with highlighted cell.

Type	Average Size (bp)	Most Similar Known Cluster	Present in Strain			
			WT	MR	Ab	3P
Shared Among Antibiotic-Producers						
Terpene	21,607					
Nucleoside	20,704					
Lanthipeptide-class-iii,NAPAA	42,199					
Benzoxazole	32,650	Mycemycin#				
Arylpolyene	23,960					
Shared Among Increased-Antibiotic-Producing Strains						
NRPS	24,574	Actinomycin D*				
NRPS	8,379					
T1PKS	5,486					
Shared Between wild-type and loss-activity strain						
Lanthipeptide-class-iii	22,567					
Redox-cofactor	21,333					
T1PKS	38,892	Butyrolactol A+				
T3PKS	41,184	Germicide+				
Aminopolycarboxylic-acid	13,457	Ethylenediaminesuccinic acid hydroxyarginine+				

* low, # medium, + high similarity confidence

Overall, the varying patterns of BGC retention and loss across the strains suggest a dynamic genomic response during the adaptation process. One possibility is that genome rearrangements may have contributed to the observed differences in

antimicrobial activity by selectively retaining or eliminating specific biosynthetic clusters. Given the well-known plasticity of *Streptomyces* genomes (Um et al., 2021), particularly in regions associated with secondary metabolism (Bentley et al., 2002), the rearrangements could reflect adaptations favoring more relevant or efficient pathways. However, further experimental validation would be necessary to confirm the functional consequences of these genomic changes.

4.5.4 Orthologous Gene Clustering based on Translated Amino Acid

To investigate differences in functional gene content across strains, orthologous clustering of amino acid sequences annotated by Prokka was performed using OrthoVenn3. A total of 36,812 protein sequences from four *Streptomyces* strains were analyzed, yielding 9,113 orthologous clusters. Of these, 7,714 clusters were conserved across all strains, with 7,230 identified as single-copy orthologs. Only 138 clusters were singletons, representing unique, non-clustered proteins. The clustering also revealed clusters uniquely present or absent in strains with differential antibiotic production, offering information on strain-specific gene retention or loss potentially associated with adaptive evolution (Figure 4.9).

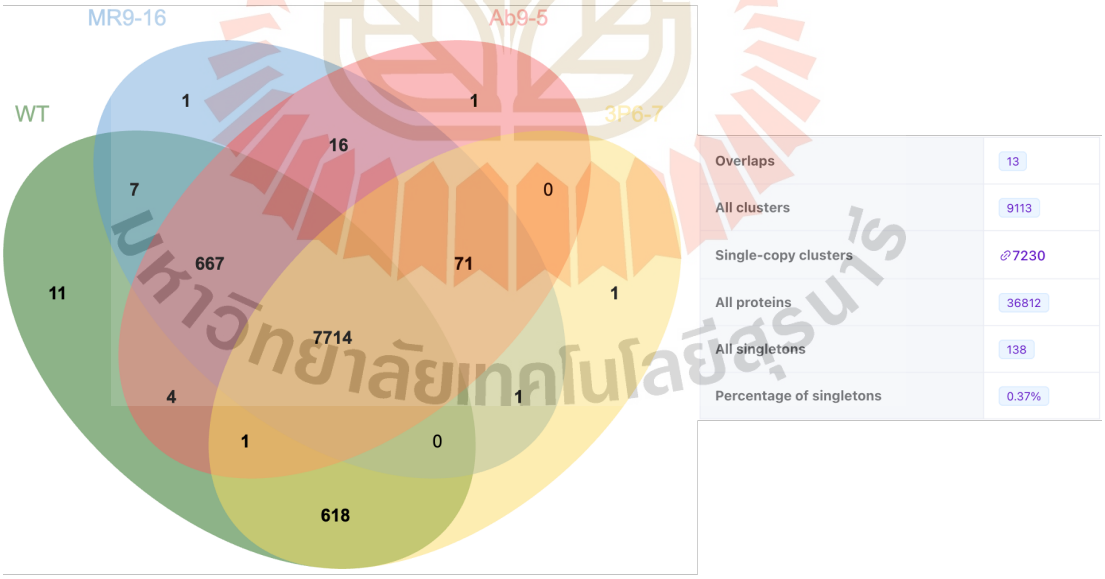

Figure 4.9 Venn diagram of comparative homologous protein clustering and result statics of SSUT88A^{WT} (WT), SSUT88A^{MR9-16} (MR9-16), SSUT88A^{Ab9-5} (Ab9-5), and SSUT88A^{3P6-7} (3P6-7). Generated by Orthovenn3.

Of particular interest, 16 clusters were uniquely shared between the two high antibiotic-producing strains (SSUT88A^{MR9-16} and SSUT88A^{Ab9-5}). Among these were genes associated with RNA secondary structure unwinding and trehalose catabolic processes, while the remainder lacked functional annotations. In contrast, 667 clusters were shared among all three antibiotic-producing strains (wild-type, SSUT88A^{MR9-16} and SSUT88A^{Ab9-5}), representing conserved functions potentially include some those are necessary for bioactivity.

The wild-type shared 618 clusters exclusively with the non-producer strain SSUT88A^{3P6-7}, which may represent gene content that is unnecessary for the enhanced antimicrobial activity. One unique cluster was identified in each of the evolved strains, though none showed known annotated functions.

The wild-type also contained 11 unique clusters, but only one (a transmembrane transporter) had an identifiable function. Additionally, 71 clusters were found to be shared among all evolved strains but absent in WT, which could be derived from co-culture pressure. These two groups were deprioritized as potential natural mutation or background genomic variation independently on selective pressure.

Figure 4.10 demonstrates a phylogenetic tree constructed from the orthologous clusters showed that WT diverged earliest, with SSUT88A^{3P6-7} forming a separate branch prior to the clustering of SSUT88A^{MR9-16} and SSUT88A^{Ab9-5}. While branch lengths were very minimal the topology supports the idea that SSUT88A^{MR9-16} and SSUT88A^{Ab9-5} followed a more similar adaptive path, potentially linked to their enhanced antimicrobial activity.

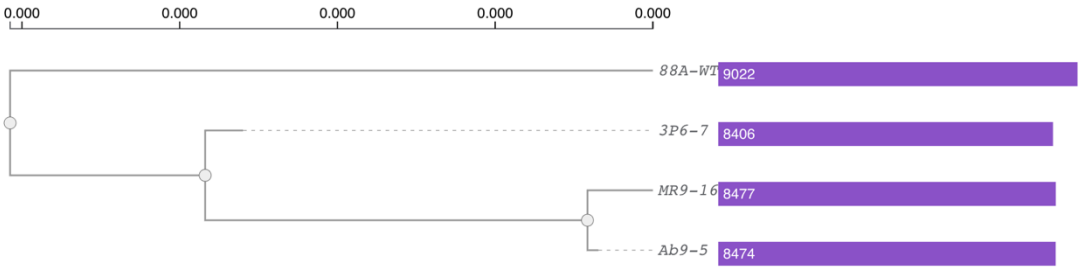

Figure 4.10 Phylogenetic tree based on OrthoVenn-derived orthologous clusters among strains using maximum likelihood method.

While OrthoVenn operates at the amino acid level and clusters genes based on amino acid annotated, antiSMASH provides genes-based predictions specifically for secondary metabolism. Integrating output from both tools allows for a more comprehensive understanding of how gene content and biosynthetic potential have shifted across strains. Therefore, key BGCs identified by antiSMASH were cross-referenced with OrthoVenn clusters to explore whether changes in orthologous content may relate to the observed phenotypic differences. Only the core biosynthetic genes, responsible for the main enzymatic steps in secondary metabolite biosynthesis, of each predicted region were selected for correlation. Due to the complexity and volume of data, representative examples are presented from each comparison group, including cases of both complete and partial correlations. Additional clusters are provided in Appendix B.

For the group of BGCs shared among all antibiotic-producing strains, two representative clusters were examined:

- Mycemycin-like BGC: This complex region includes four core biosynthetic genes. In OrthoVenn, three of these cores formed shared orthologous clusters present in wild-type, SSUT88A^{MR9-16} and SSUT88A^{Ab9-5}. However, one of the clusters also included a homolog from SSUT88A^{3P6-7}, which antiSMASH did not predict to possess this BGC. In this case, SSUT88A^{3P6-7} contributed only one node to the cluster, whereas the antibiotic-producing strains contributed two nodes each. This pattern suggests partial homology in SSUT88A^{3P6-7} at the amino acid

level, potentially reflecting an incomplete biosynthesis process. This suggests that while one of the core genes may still be present in SSUT88A[3P6-7], the other core genes are missing. As a result, antiSMASH likely dropped this region from a complete biosynthetic gene cluster (Figure 4.11A).

- Nucleoside BGC: This cluster, containing a single core biosynthetic gene, showed complete correlation across all three strains in OrthoVenn, comprising one protein from each strain, reflecting strong conservation at the amino acid level and supporting its shared functionality (Figure 4.11B).

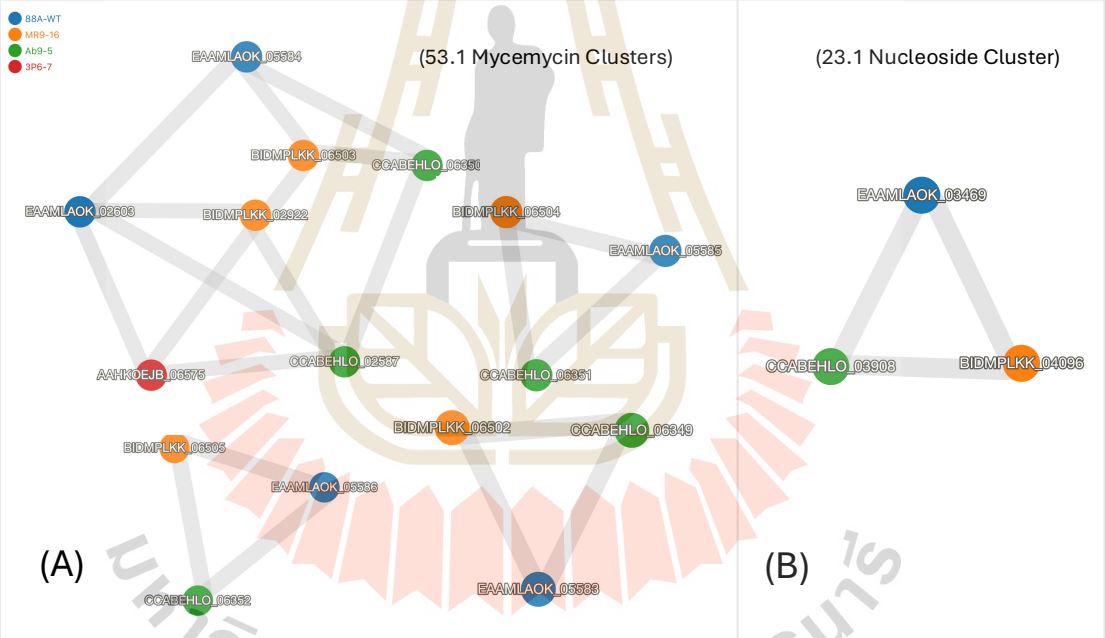

Figure 4.11 Representative OrthoVenn orthologous clustering of core biosynthetic genes from BGCs shared among all antibiotic-producing strains. (A) Mycemycin BGC clusters; (B) Nucleoside cluster.

Among the biosynthetic gene clusters uniquely shared between the two high-antimicrobial-producing strains, the actinomycin D cluster was selected as a representative example (Figure 4.12). Notably, this cluster was identified by antiSMASH with low similarity confidence to known BGCs (see Section 4.5.3). The cluster includes one core biosynthetic gene, which was successfully traced back to its orthologous cluster in OrthoVenn. This correlation supports the functional relevance of this cluster in the enhanced antimicrobial phenotype.

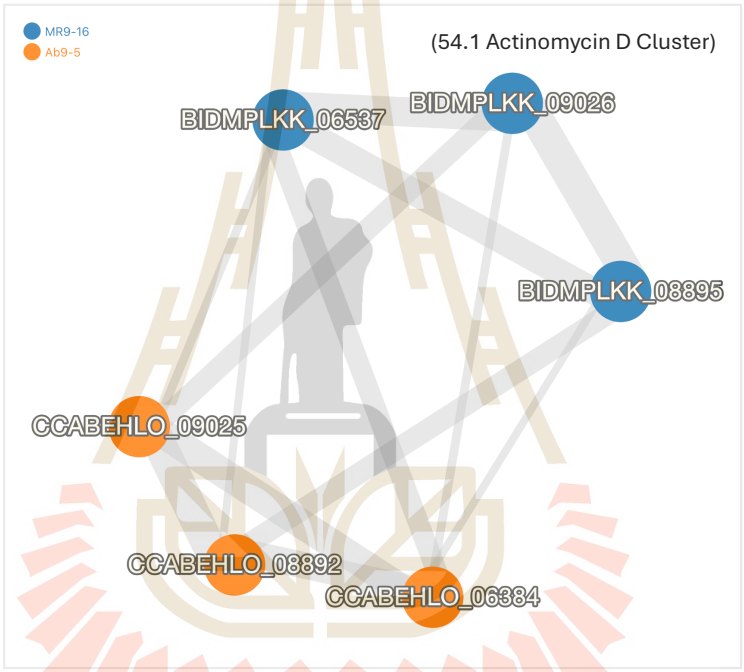

Figure 4.12 Orthologous cluster visualization of core actinomycin D-like biosynthetic genes uniquely shared between high-antimicrobial-producing strains.

Among the biosynthetic clusters shared exclusively between the wild-type the strain lacking antimicrobial activity (SSUT88A^{3P6-7}), two representative clusters were examined: the EDHA-like cluster and a redox cofactor biosynthesis cluster.

- The redox cofactor–associated cluster presented a complex pattern. It contained four core biosynthetic genes, of which three could be correlated in OrthoVenn. Interestingly, the other one orthologous cluster included three nodes from SSUT88A^{3P6-7} and two nodes each from the antibiotic-producing strains. This suggests that some

homologous genes remain in the bioactive strains, but this strain may retain additional or diverged copies. It is possible that this redundancy reflects supplementary functions not directly related to antimicrobial biosynthesis (Figure 4.13A).

- The EDHA cluster, predicted by antiSMASH to encode an aminopolycarboxylic acid-type compound, contained three core biosynthetic genes. All three were found within the same orthologous cluster in OrthoVenn and were exclusive to wild-type and SSUT88A$^{3P6\text{-}7}$ (Figure 4.13B). This strong correlation suggests that these genes are well-conserved at the amino acid level between the two strains, but absent from the evolved bioactive strains. Given that EDHA compounds are not clearly linked to antimicrobial activity, their presence may reflect functions unrelated to the enhanced bioactivity phenotype.

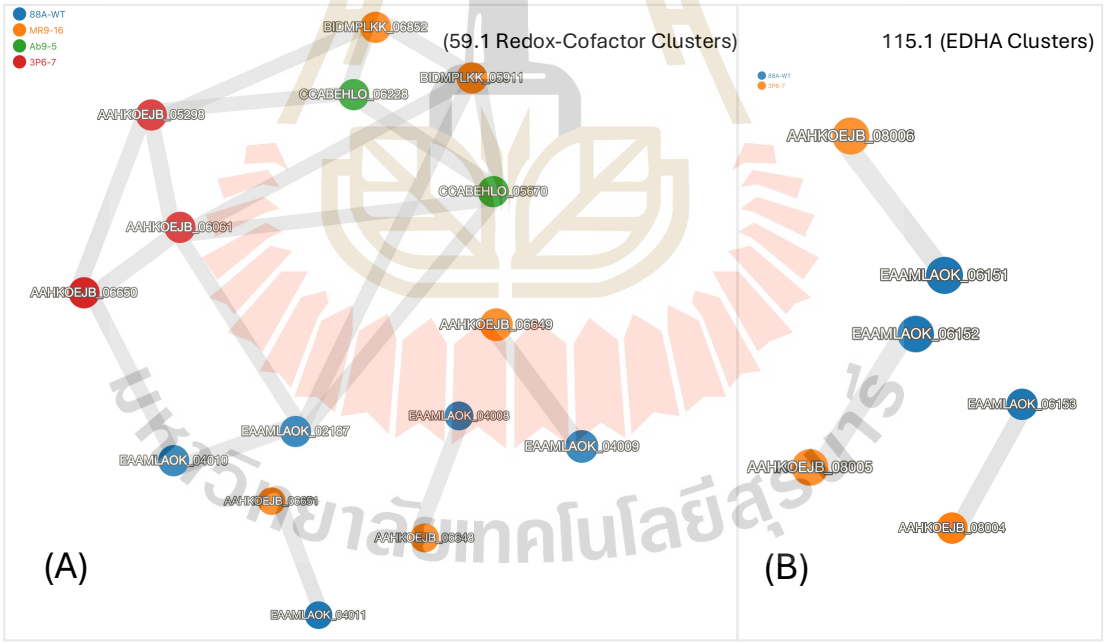

Figure 4.13 Orthologous cluster visualization of biosynthetic gene clusters shared between wild-type and non-producing strain (SSUT88A$^{3P6\text{-}7}$). (A) Redox-cofactor clusters and (B) EDHA cluster.

Taken together, the comparative analysis between antiSMASH-predicted core biosynthetic genes and OrthoVenn orthologous clusters highlights that most core biosynthetic genes identified by antiSMASH could be reliably traced to corresponding orthologous clusters, affirming that functional biosynthetic capacity often aligns with conserved amino acid sequences. However, in some cases, partial clustering or unique node distributions revealed limitations in genome context–based prediction tools.

4.5.5 Structural and Point Mutational Analysis of Adapted Strains

To investigate the genetic basis of phenotypic changes observed in the adapted *Streptomyces* strains, whole-genome resequencing data were analyzed using Breseq, a tool designed to identify mutations relative to a reference genome. Two complementary Breseq modes were used: reference mode (-r) to identify large-scale structural variations, including deletions, duplications, by mapping raw reads against the wild-type reference assembly. And consensus mode (-c) was used to detect small-scale mutations such as single nucleotide polymorphisms (SNPs), short insertions/deletions (indels), and potential frameshift-causing events.

Breseq's reference mode (-r) was used to explore structural changes in the evolved strains by aligning short reads from each evolved genome to the fragmented wild-type draft assembly as an assumed complete reference. The results initially flagged 154 contigs as deleted across at least one evolved genome. However, due to the fragmented nature of the wild-type assembly and the potential for mapping artifacts, these candidates were subjected to additional filtering and validation.

In order to select putative high-possibility true deletions, a multi-step pipeline was employed. First, we re-mapped raw sequencing reads using both Breseq and BWA to ensure consistency across alignment tools. Second, a 31-mer presence/absence analysis using Jellyfish was conducted, querying unique 31-mers from wild-type contigs against the evolved strains' k-mer libraries generated by raw reads. Contigs that showed zero read alignment in both Breseq and BWA, as well as no 31-mer presence, were considered high-confidence deletions. We further visualized

candidate regions using IGV to confirm clean coverage gaps across the contigs. Only deletions supported by all three methods were retained for downstream analysis.

Out of 154 Breseq-flagged deletions, only nine were classified as biologically irrelevant, indicating that the majority of the deletions have high possibility to be true biological events potentially structural genome reduction.

Due to the volume of flagged deletions, every contig analysis was impractical. Instead, representative contigs were selected based on biological relevance, mapping clarity, the curation criteria were demonstrated in Appendix C (Figure S2 – S5).

While the primary interest was in deletions directly impacting secondary metabolism, a subset of biologically relevant deletions that did not directly affect BGCs was also analyzed. These were chosen not as random contrasts, but as informative examples that illustrate the broader view of genome reduction during adaptation.

The goal was to highlight that although not all deletions can be confidently said that they were tied to antimicrobial production, many still reflected meaningful structural or regulatory changes. We grouped the selected deletions into two categories:

(A) Deletions not contributing to BGCs were selected based on high relative read depth in the wild-type and retained genome, with the absence across mapping/31-mer validation. To ensure the selected cases were biologically informative, we chose representatives that exemplified the range of observed deletion patterns including:

- Contig 112, which was deleted in high-activity stains SSUT88A^{MR9-16} and SSUT88A^{Ab9-5} with no detected MGE (Figure 4.14). Breseq and BWA mapping show complete loss of read alignment in the evolved strains relative to SSUT88A^{3P6-7}. k-mer analysis confirms absence of contig-specific 31-mers. Annotations reveal no MGEs, suggesting a dispensable region was purged during adaptive evolution.

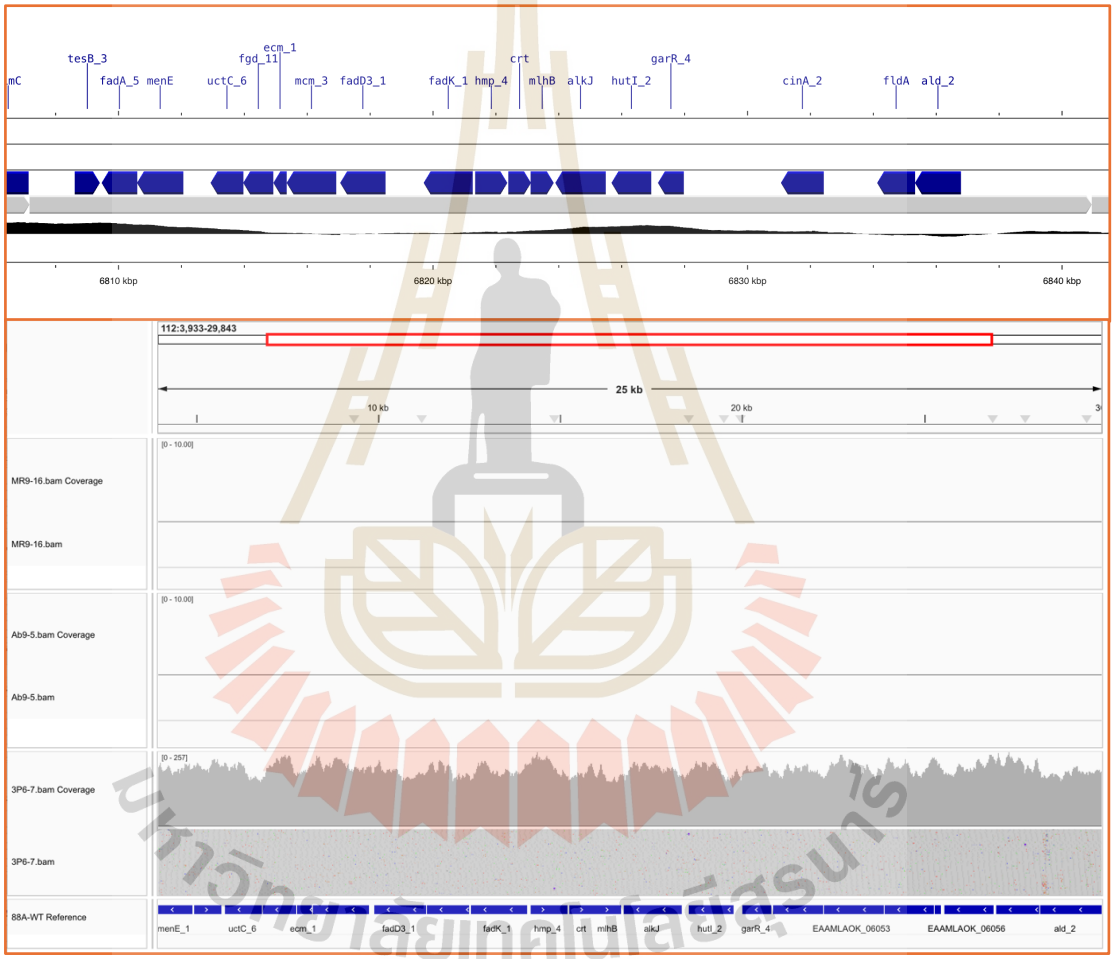

Figure 4.14 Deletion of contig 112 in SSUT88A^{MR9-16} and SSUT88A^{Ab9-5} without MGE signatures.

- Contig 108, which was deleted in the stains SSUT88A^{MR9-16} and SSUT88A^{Ab9-5}. This contig encoded *OppF*, a transporter typically associated with MGE contexts, potentially related to mechanisms during laboratory adaptation evolution. Read mapping and k-mer absence validate loss of the contig in both high-activity strains. Annotation identifies *oppF*, a component of an oligopeptide permease system often found in mobile or horizontally transferred regions (Figure 4.15).

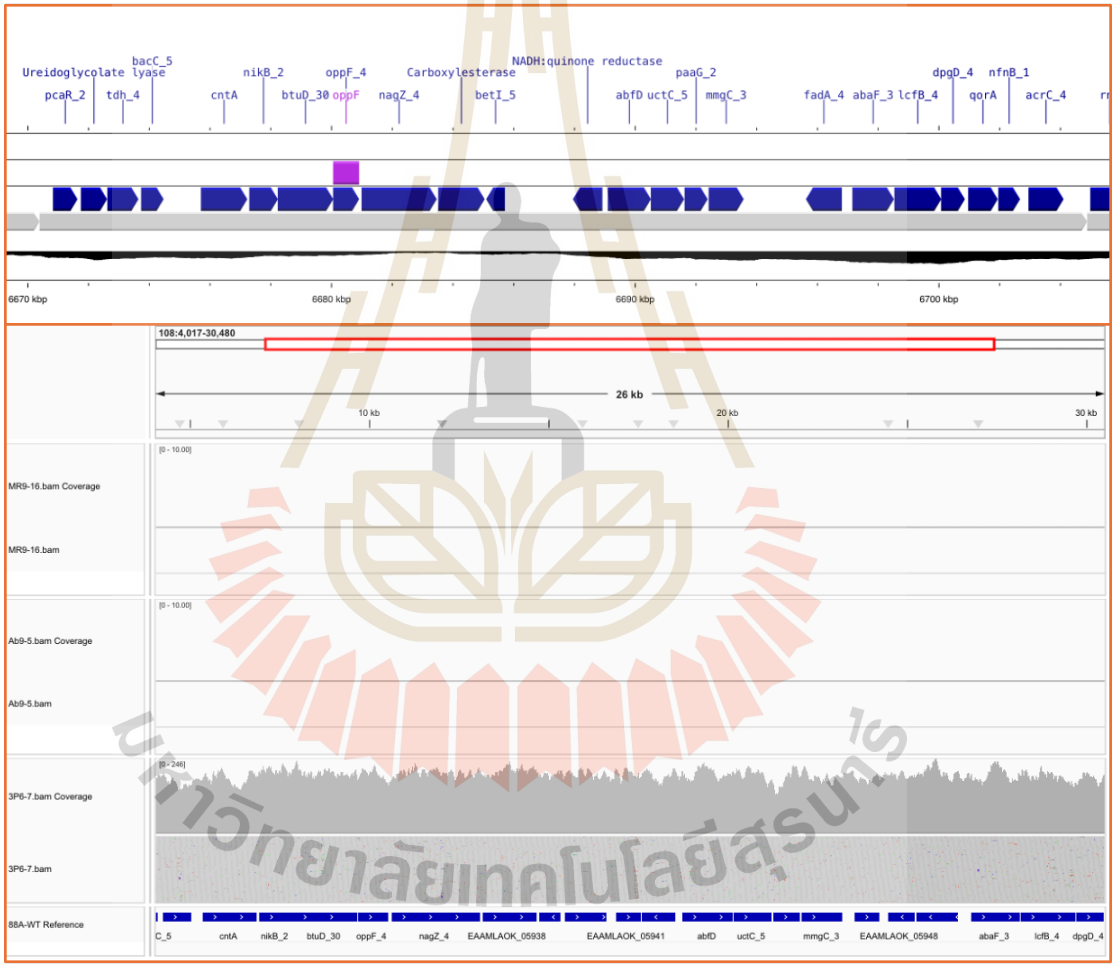

Figure 4.15 Deletion of contig 108 in SSUT88A^{MR9-16} and SSUT88A^{Ab9-5} with putative MGE-associated transporter gene *oppF*.

- Contig 141, a SSUT88A^{3P6-7} deleted contig without MGE annotated (Figure 4.16). Absence of read coverage and k-mer matches confirm a SSUT88A^{3P6-7}-specific deletion. Functional annotation shows no MGE-related domains, consistent with a non-mobile but nonessential region being deleted in the low-activity strain.

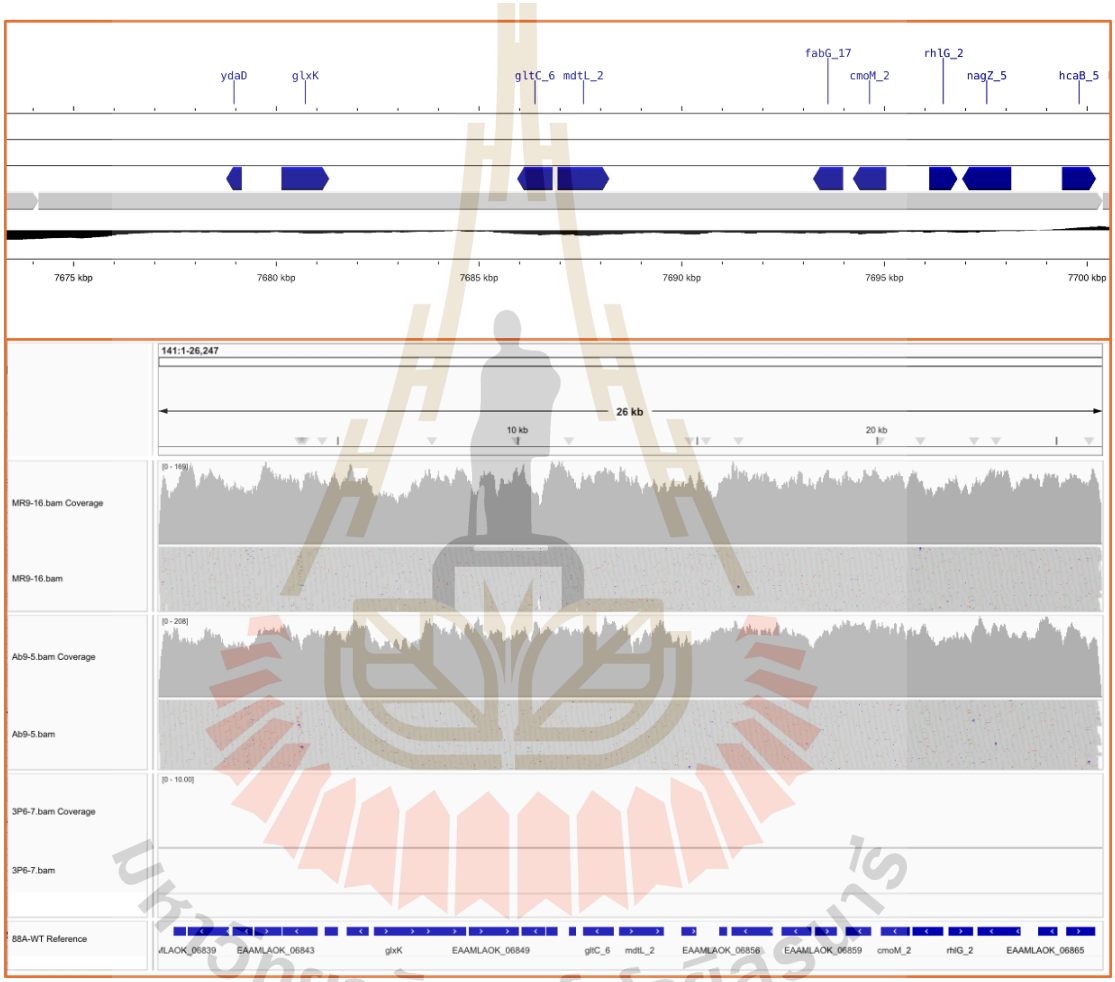

Figure 4.16 Loss of contig 141 in SSUT88A^{3P6-7}, with no detected mobile genetic elements.

- Contig 136, loss contig from non-activity producing strain SSUT88A^{3P6-7} with five integration/excision MGEs. The absence in the strain across all validation criteria. Annotation reveals five genes associated with integration and excision functions, including transposases (*tpase*) and hypothetical integrases (R00164). This could indicate that mobile genetic elements contributed to genome instability and were selectively removed (Figure 4.17).

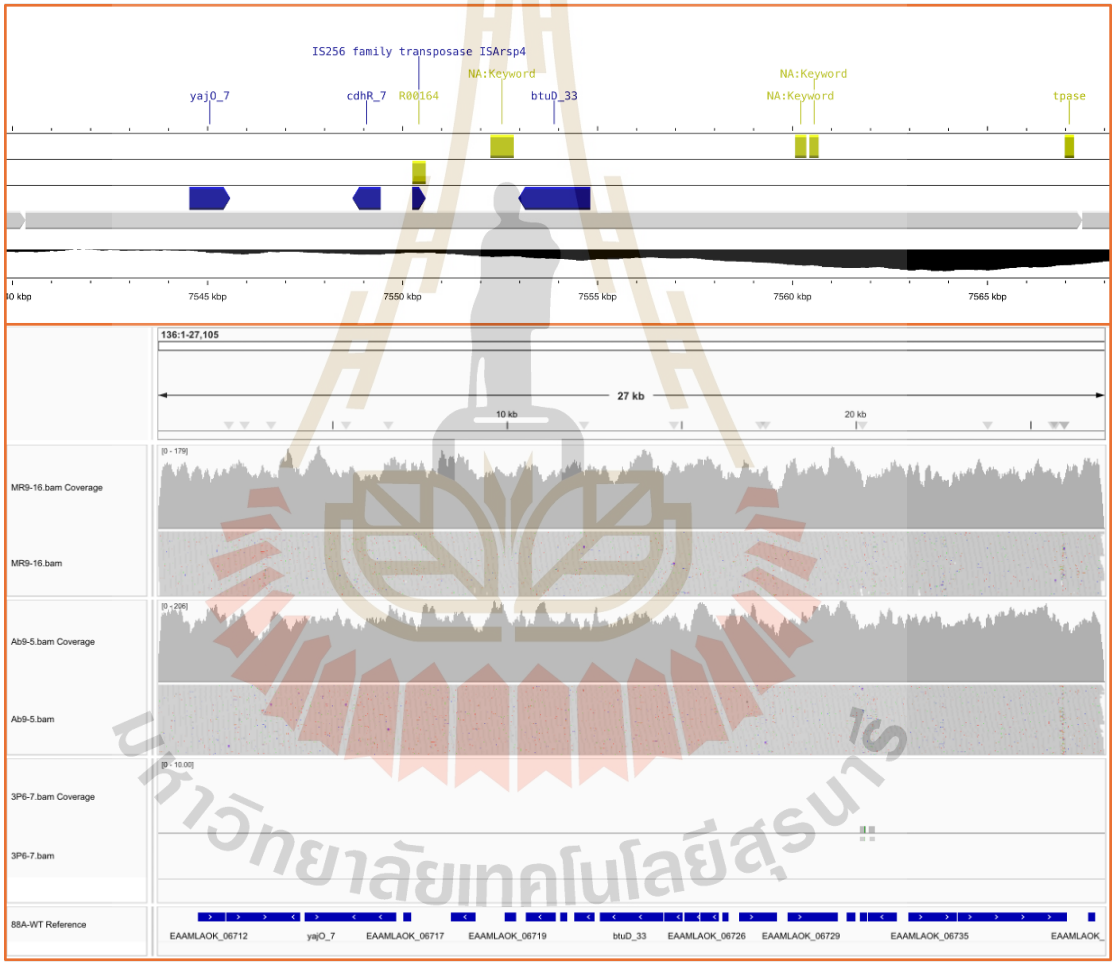

Figure 4.17 Loss of contig 136 in SSUT88A^{3P6-7}, containing multiple mobile element-related genes.

(B) Deletions Correlated with Secondary Metabolism and Ortholog Clusters contributing to BGCs

- Contig 48 (lost in SSUT88A^{3P6-7}) corresponded to a nucleoside cluster found in wild-type, SSUT88A^{MR9-16} and SSUT88A^{Ab9-5} by both OrthoVenn and antiSMASH, but absent in SSUT88A^{3P6-7}. No MGE signatures were found, supporting selective deletion (Figure 4.18). Based on both OrthoVenn and antiSMASH predictions. Its deletion was confirmed by mapping and k-mer analysis. No MGE domains were identified, suggesting this was a stable but metabolically costly region lost under disadvantageous selective pressure.

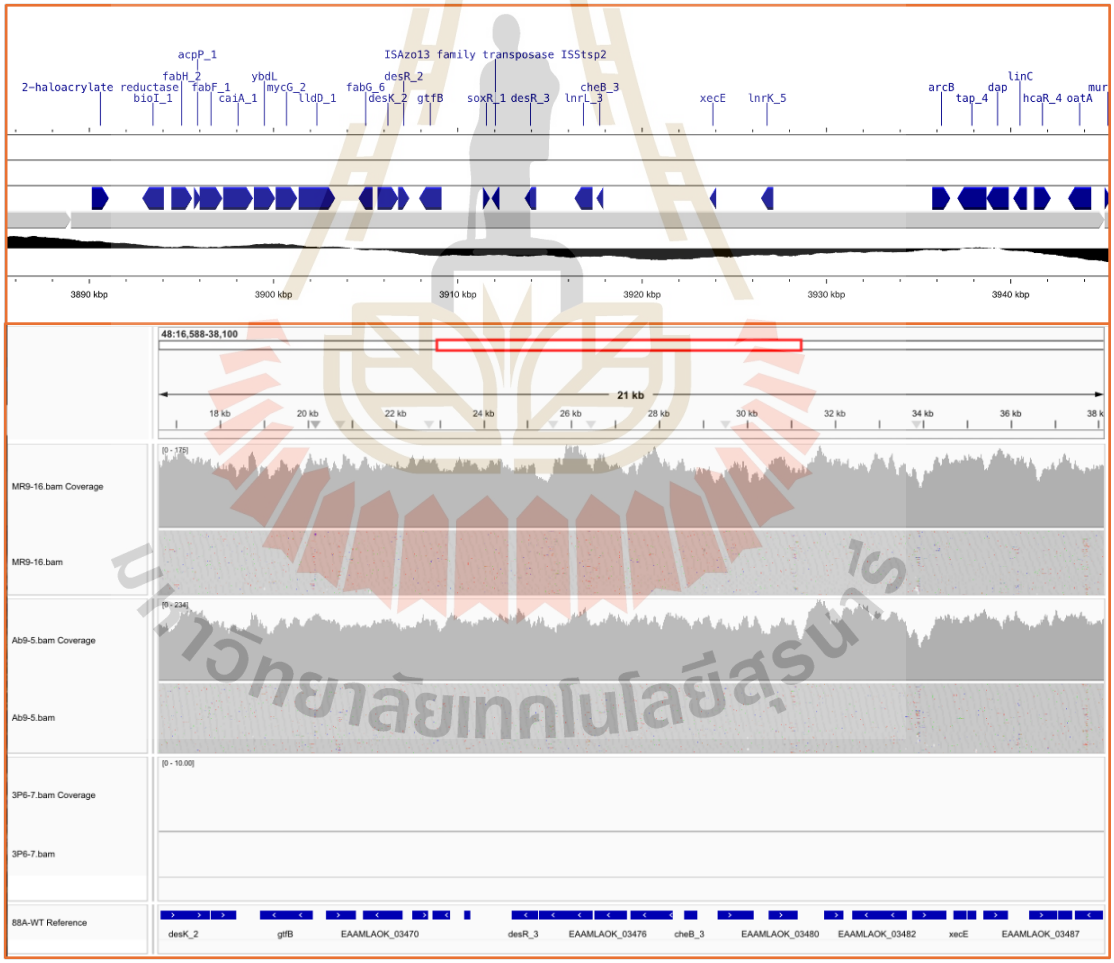

Figure 4.18 Deletion of contig 48 in SSUT88A^{3P6-7} associated with a nucleoside biosynthetic cluster.

- Contig 97 (also lost in SSUT88A^{3P6-7}) encoded the Mycemycin BGC, flagged by antiSMASH and linked to multiple ortholog clusters. One integration/excision-associated MGE was annotated, but the broader cluster loss suggests functional deletion (Figure 4.19). The contig was fully deleted in SSUT88A^{3P6-7}. Annotation detected one integration/excision-associated gene of unknown annotation.

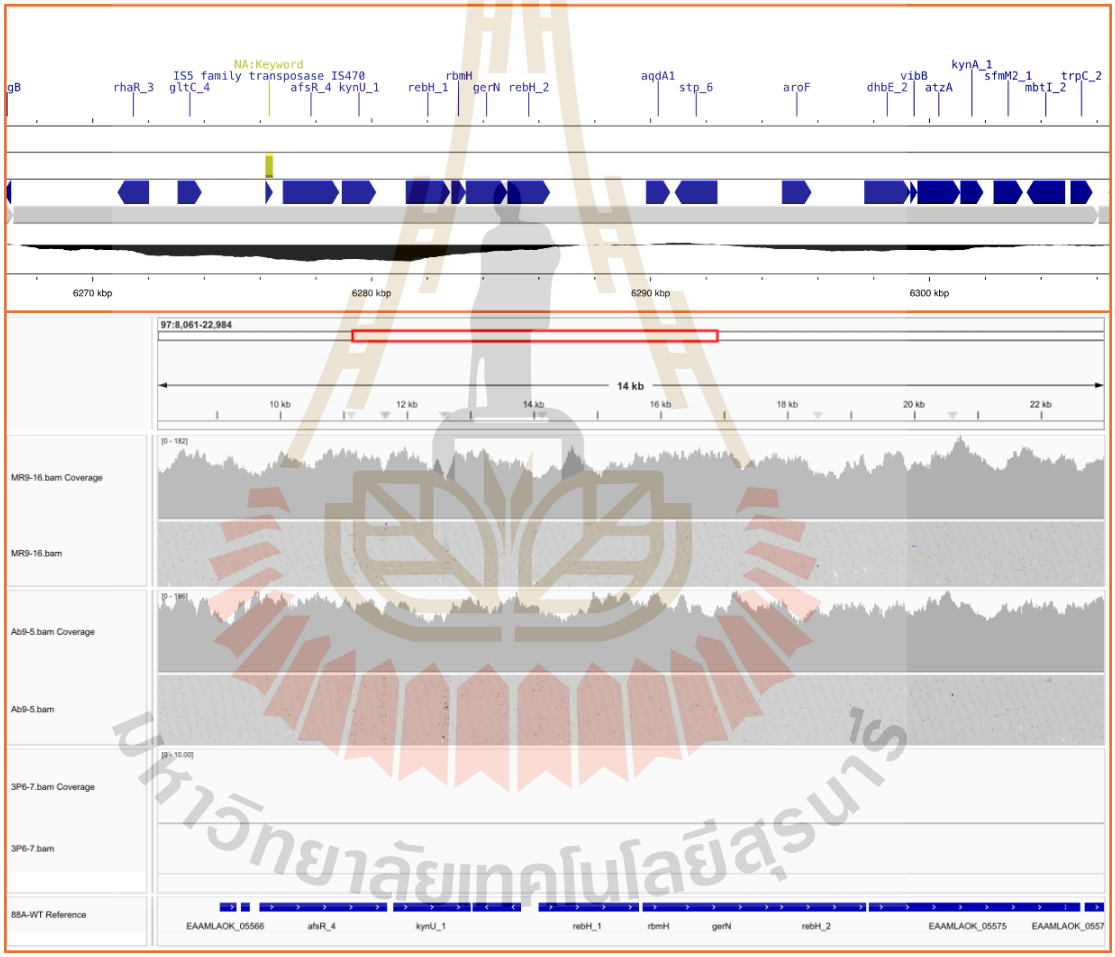

Figure 4.19 Loss of contig 97 in SSUT88A^{3P6-7}, encoding the Mycemycin BGC with partial MGE involvement.

- Contig 59 (lost in SSUT88A^{MR9-16} and SSUT88A^{Ab9-5}) was linked was linked to multiple OrthoVenn clusters and biosynthetic genes predicted to contribute to redox cofactor pathways. Its complete deletion, without MGE signatures (Figure 4.20), supports the notion of functional gene loss driven by adaptive metabolic evolution.

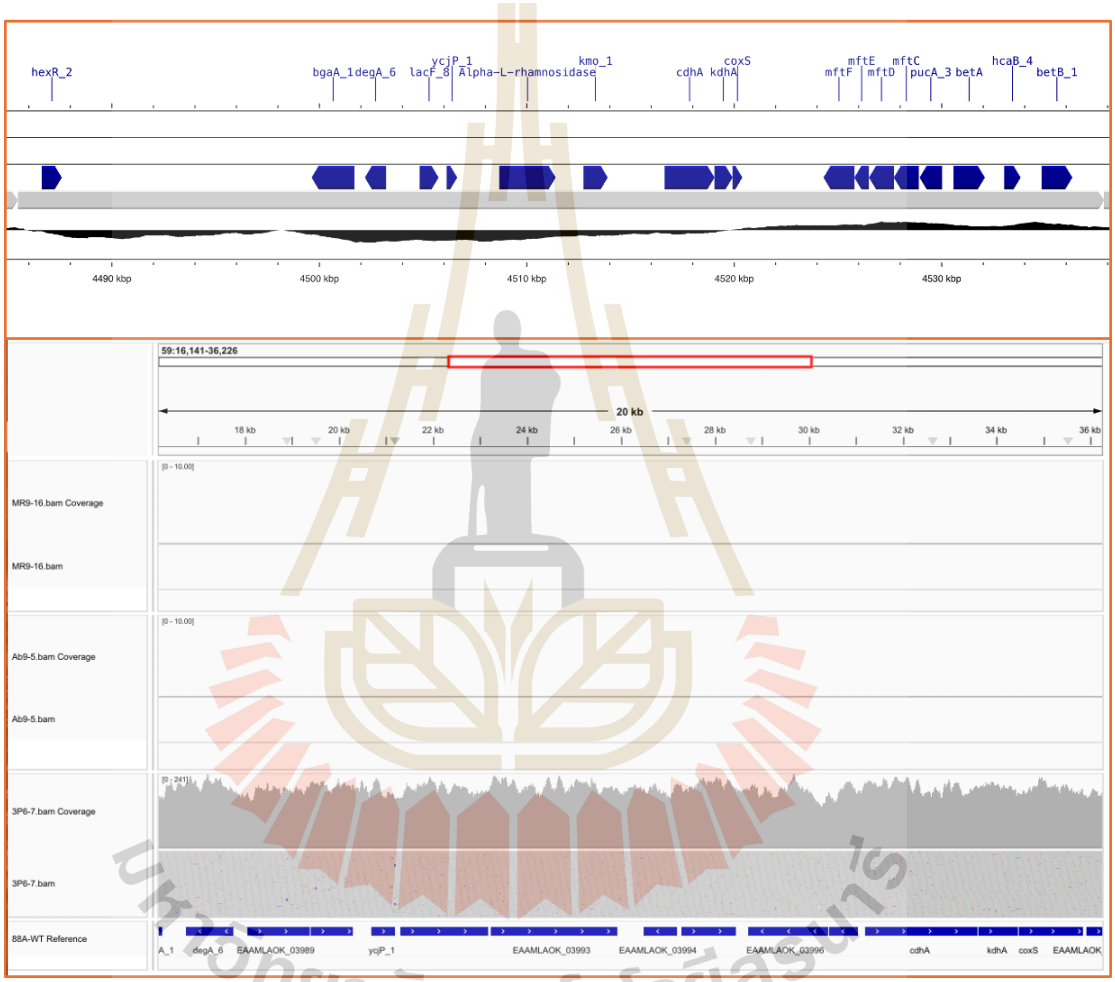

Figure 4.20 Deletion of contig 59 in SSUT88A^{MR9-16} and SSUT88A^{Ab9-5}associated with redox cofactor biosynthesis.

- Contig 115 (also lost in SSUT88A^{MR9-16} and SSUT88A^{Ab9-5}) encoded genes related to EDHA biosynthesis, overlapping with four ortholog clusters, but showed no MGE domains (Figure 4.21). This contig overlaps with four OrthoVenn clusters and harbors EDHA-related genes, as identified in antiSMASH outputs. Despite its biosynthetic relevance, no mobile genetic elements were detected, indicating that deletion was not mediated by MGEs.

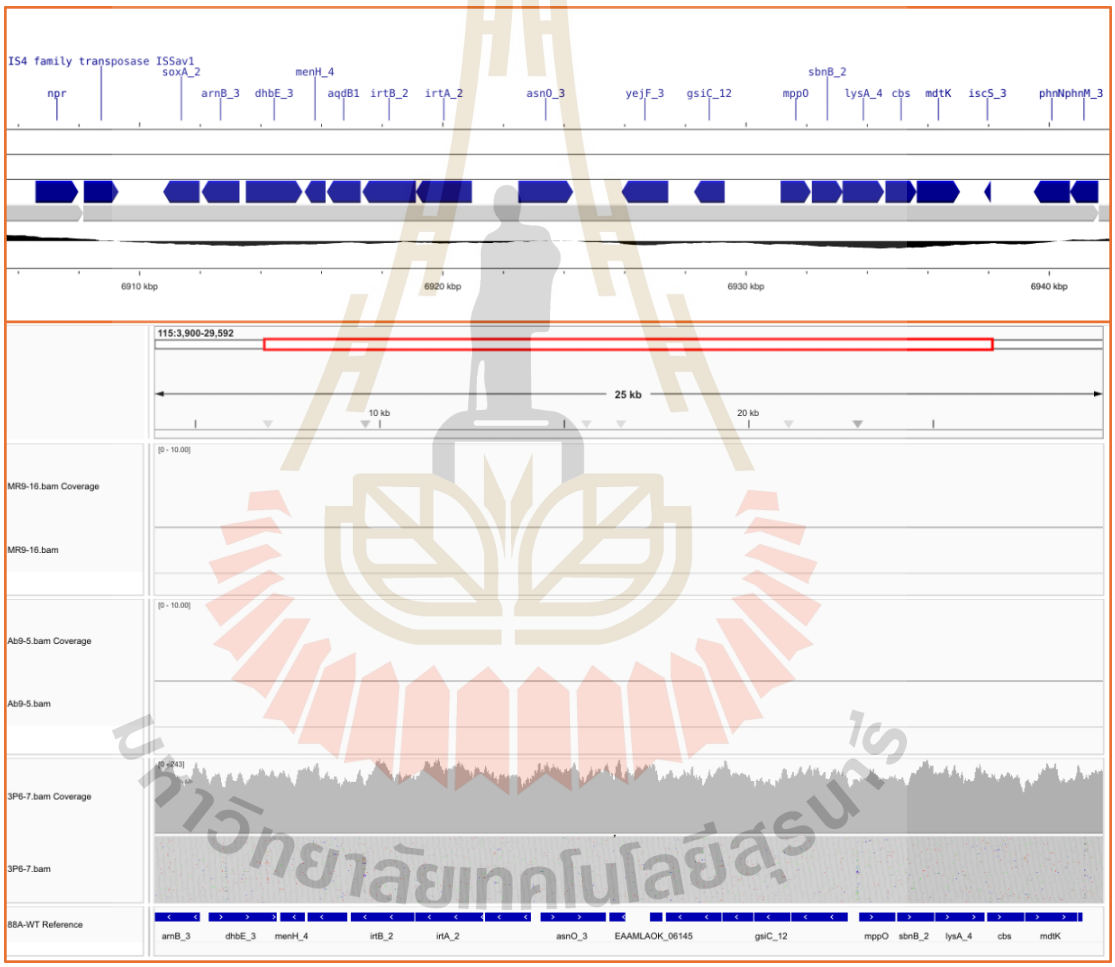

Figure 4.21 Loss of contig 115 in SSUT88A^{MR9-16} and SSUT88A^{Ab9-5}, associated with EDHA biosynthesis.

While we cannot rule out all technical sources of contig absence, we believe that some deletions observed in this study could be true biological losses. Illumina sequencing libraries were prepared using random fragmentation, ensuring

broad genomic coverage (CD-Genomics, 2025). If random dropout or assembly gaps were responsible, we would expect inconsistent patterns across strains or partial mapping within contigs. Instead, we observed clean, strain-specific deletions, which were highly biologically correlated. These were independently confirmed with Breseq, BWA, k-mer analysis, and IGV visualization. Moreover, only 9 out of 154 Breseq-flagged deletions failed to meet our validation criteria, suggesting that the majority were not due to technical noise.

To identify small-scale genomic variants potentially responsible for adaptive phenotypes in evolved strains, the short-read data from SSUT88A^{MR9-16}, SSUT88A^{Ab9-5}, and SSUT88A^{3P6-7} were analyzed using Breseq v0.38.1 in consensus mode (-c). This method does not rely on alignment to a fragmented reference genome but instead reconstructs each sample as an independent contig. It enables the detection of point mutations, particularly SNPs, with reduced susceptibility to reference-related artifacts. Consensus mode was used in addition to reference mode for its improved sensitivity of small-scale detections.

The Initial outputs yielded a large number of candidate SNPs across the evolved strains. However, a stringent manual curation workflow was applied to refine the dataset. Candidate mutations were assessed for sequencing depth, mutation quality scores, alignment confidence in surrounding bases, and potential biological relevance. Through this conservative filtering, only three high-confidence SNPs were retained.

- Shared SNP in High-Antibiotic-Producing Strains (SSUT88A^{MR9-16} and SSUT88A^{Ab9-5}): A single nucleotide polymorphism was identified in the intergenic region between *valS* (valyl-tRNA synthetase) and *murE_2* (UDP-N-acetylmuramoylalanine–D-glutamate ligase), located 37 base pairs upstream of *murE_2*. While the exact promoter boundaries are unconfirmed, this position falls near where a -35 motif of a **σ**^70 promoter would be expected, raising the possibility of regulatory impact. *murE_2* is involved in peptidoglycan biosynthesis via the addition of diamino acid (*meso*-diamino-pimelate or *L*-lysine) to UDP-N-acetylmuramoyl-L-alanyl-D-glutamate (UMAG) (Mol et al., 2003), and

the mutation's consistent presence in both high-producing strains suggests it may contribute to peptidoglycan alteration or adaptive evolution under co-culture selective stress, though further functional validation would be needed (Figure 4.22).

- Unique SNP in the SSUT88A$^{Ab9\text{-}5}$ (Precocious Antibiotic-Producing Strain): This mutation lies in the intergenic region between EAAMLAOK_05902 and EAAMLAOK_05903 (Prokka annotation ID), positioned 14 base pairs upstream of EAAMLAOK_05903. While both genes were annotated as hypothetical proteins, BLASTP analysis revealed that EAAMLAOK_05903 encodes a conserved protein with a DUF2637 (*SpdA*-like) domain, widely distributed in *Streptomyces* species. Although its exact function is unclear, the SNP's proximity to the presumed promoter region, potentially within striking distance of a -10 motif of **σ** factor, makes a regulatory role plausible, therefore speculative. This mutation could fine-tune expression of a yet-uncharacterized regulator, possibly contributing to the early or enhanced secondary metabolism observed in this strain (Figure 4.23).
- Unique SNP in the Pigment-Deficient, Activity-Loss Strain (SSUT88A$^{3P6\text{-}7}$): A silent coding mutation was detected within a gene annotated as Prokka-Annotated hypothetical protein ID, EAAMLAOK_05879, where the codon CGG (arginine) was changed to AGG (another synonymous arginine codon). Notably, this mutation occurs at the first base of the codon, meaning it is not a case of typical third-base redundancy, which is observed more frequently. While the protein sequence remains unchanged, studies have found that synonymous mutations can still influence biological function through various effects on mRNA secondary structure, translational efficiency, or codon usage bias (Plotkin and Kudla, 2011). In addition, consequences of synonymous mutations' functionality and non-neutrality for numerous analyses and conclusions relevant to genetics, evolution, conservation, and illness, have been proposed (Zhang and Qian, 2025). Some studies even stated

that “synonymous mutations in representative yeast genes are mostly strongly non-neutral” (Shen et al., 2022). Given its exclusive presence in the SSUT88A$^{3P6\text{-}7}$ strain, which exhibits both pigment loss and diminished antimicrobial activity, this mutation may subtly disrupt regulatory dynamics at the RNA level or interfere with precise protein expression control (Figure 4.24).

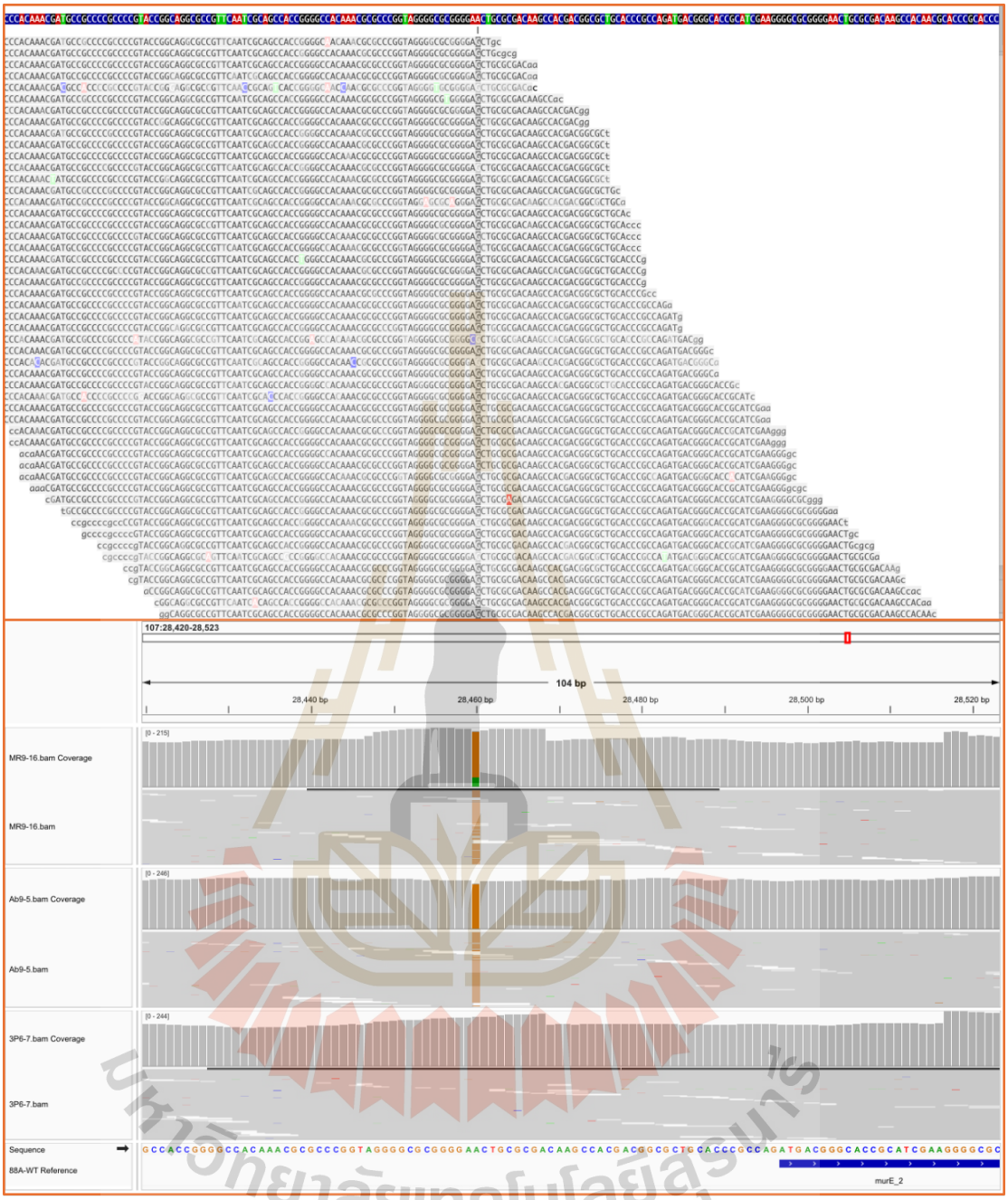

Figure 4.22 Shared SNP in High-Antibiotic-Producing Strains.

Breseq and IGV visualizations of a shared intergenic SNP located −37 bp upstream of *murE_2* (UDP-N-acetylmuramoylalanine–D-glutamate ligase), between *valS* and *murE_2*. The mutation is present in both SSUT88A$^{MR9\text{-}16}$ and SSUT88A$^{Ab9\text{-}5}$, but absent in the wild-type and SSUT88A$^{3P6\text{-}7}$. The mutation site is proximal to the theoretical -35 promoter region of *murE_2*, potentially impacting transcriptional regulation and contributing to enhanced antibiotic production.

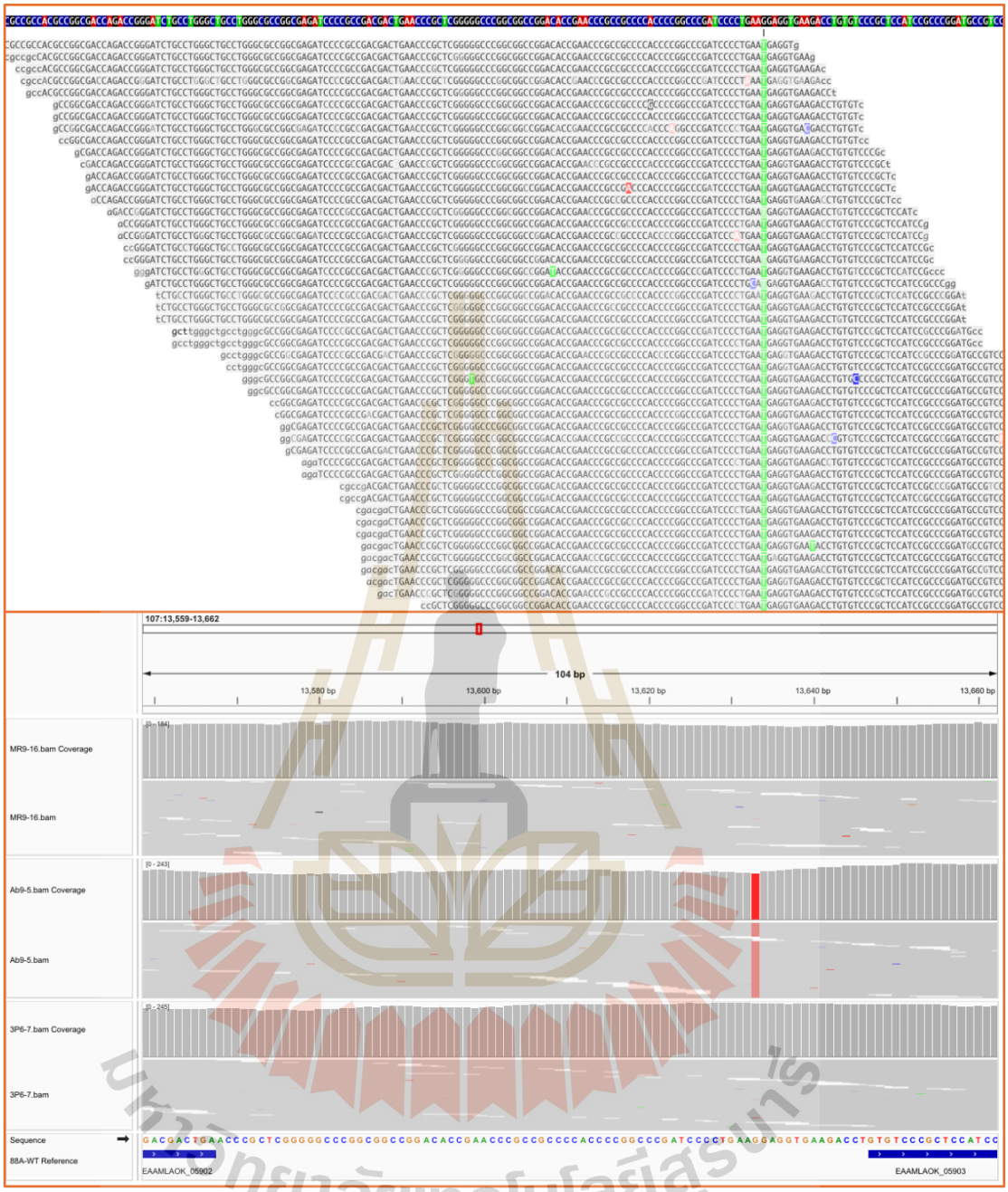

Figure 4.23 Unique SNP in the SSUT88A$^{Ab9\text{-}5}$ (Precocious Antibiotic-Producing Strain). Breseq and IGV snapshots highlighting a unique intergenic SNP in SSUT88A$^{Ab9\text{-}5}$, located −14 bp upstream of EAAMLAOK_05903. The mutation is absent in other strains. Its location is immediately upstream of a gene later identified (via BLASTP) as encoding a DUF2637 (*SpdA*-like) domain-containing protein. The mutation lies close to the presumed -10 region of the promoter, potentially influencing early or enhanced antibiotic production via regulatory alteration.

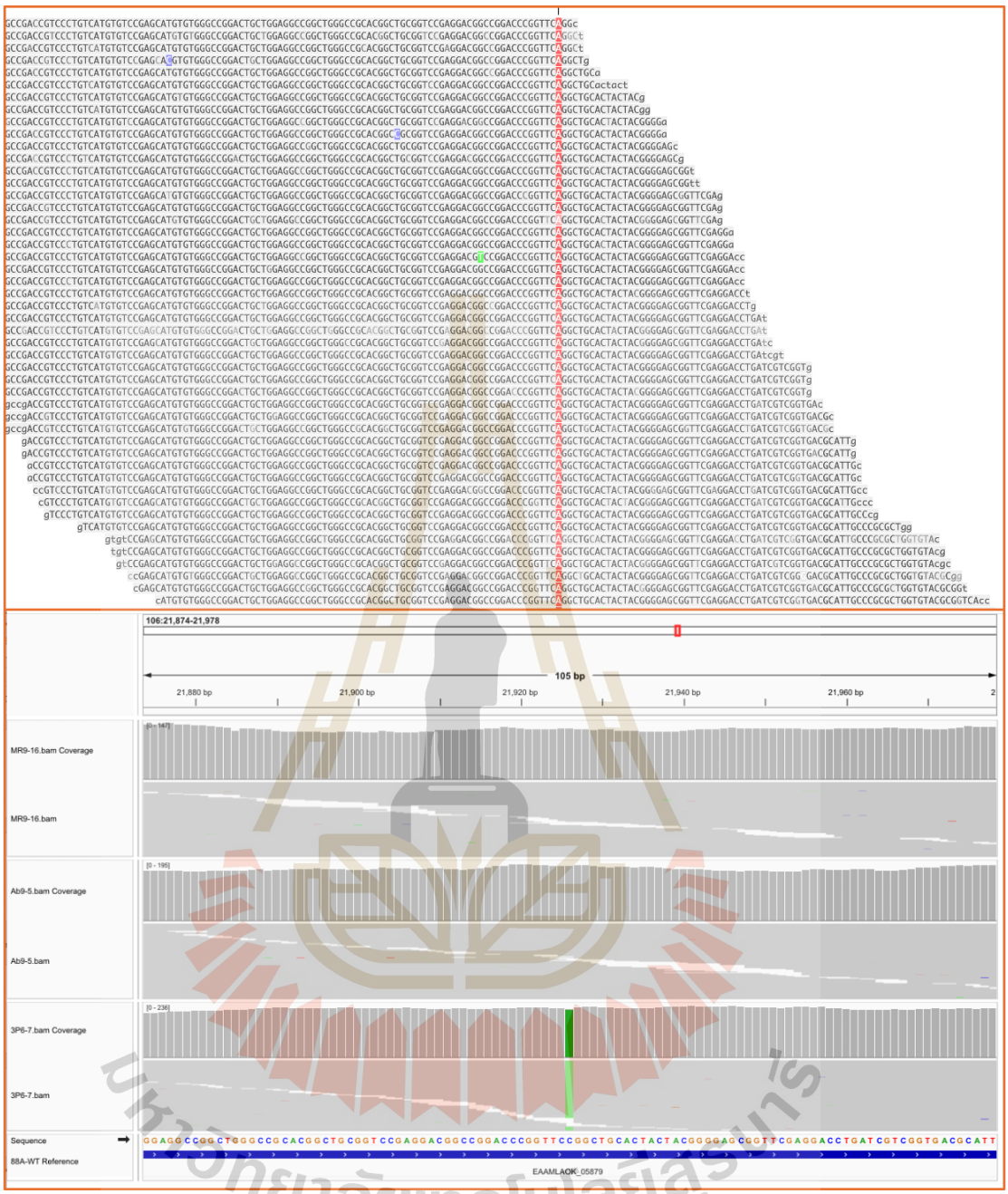

Figure 4.24 Unique SNP in the Pigment-Deficient, Activity-Loss Strain (SSUT88A^{3P6-7}). Breseq and IGV views of a unique silent mutation (CGG ⟶ AGG; Arg⟶Arg) found exclusively in SSUT88A^{3P6-7} within EAAMLAOK_05879, a gene annotated as a hypothetical protein. Though the protein sequence remains unchanged, possible functional effects include altered mRNA structure, codon usage bias, or translational efficiency, which may relate to the observed loss of pigmentation and antimicrobial activity.

Together, the Breseq -r and -c mode analyses provided complementary insights into the genomic basis of phenotypic divergence among evolved strains. Reference alignment mode (-r) enabled detection of large-scale structural changes such as deletions, many of which were validated by k-mer analysis, MGE annotation, and orthology-based context. These structural changes helped explain varied phenotypic traits through the potential loss of biosynthetic gene clusters. On the other hand, consensus mode (-c) revealed a small set of high-confidence SNPs.

The combined functional genomics approach across antiSMASH, OrthoVenn, and Breseq analyses reveals a complex and layered picture of adaptive evolution in the strains subjected to co-culture pressure. Each method contributed a unique resolution. Together, these analyses show that increased or diminished antimicrobial activity correlates with multiple layers of genomic change. High-producing strains retained and shared a core of biosynthetic clusters and unique orthologs, while simultaneously acquiring targeted deletions and a shared regulatory SNP. Conversely, the loss-of-function SSUT88A$^{3P6\text{-}7}$ strain exhibited deletions of key clusters (e.g., mycemycin), pigment-associated regions, and unique SNPs potentially affecting translation or regulation. Additionally, Mobile genetic elements were unevenly associated with deletions, suggesting that some genomic remodeling occurred via excision-mediated mechanisms, while others may reflect selective pressures acting on non-mobile but functionally important loci.

CHAPTER V
CONCLUSION

In this study, adaptive laboratory evolution through strategic co-cultivation with drug-resistant pathogens effectively regulate secondary metabolism in *Streptomyces* sp. SSUT88A. Phenotypic assessments revealed that while most evolved strains retained wild-type-like morphology, one lineage (SSUT88A^{3P6-7}) isolated after the sixth cycle of three-pathogen co-culture, exhibited dramatic morphological changes, losing its characteristic yellow diffusible pigment and shifting to a red colony phenotype. This pigment loss coincided with a complete loss of antimicrobial activity, supporting the link between morphological traits and secondary metabolite production.

Pathogen-specific adaptation drove markedly different outcomes in bioactive compound yields: MRSA was the strongest pathogen, enhancing crude extract production by 46.3%, followed by *A. baumannii* with a 32.6% increase, whereas *P. aeruginosa* decreased output and the three-pathogen combination showed only a modest effect. Among adapted strains, SSUT88A^{Ab9-5} produced the highest yield (43% increase), followed closely by SSUT88A^{MR9-16} (40%). Antimicrobial activity assays further corroborated these findings: SSUT88A^{Ab9-5} and SSUT88A^{MR9-16} showed significant improvements in inhibition zones, particularly against Gram-positive pathogens. A time-course assay using MRSA confirmed that SSUT88A^{Ab9-5} initiated bioactivity as early as day 2 (faster than the wild-type and SSUT88A^{MR9-16}) and maintained potent inhibition, while the SSUT88A^{3P6-7} strain demonstrated a complete loss of bioactivity. MIC and MBC assays showed 4–8-fold improved potency in the adapted strains compared to the wild-type, especially against MRSA and MRSE, while SSUT88A^{3P6-7} exhibited no detectable antimicrobial activity.

All genome assemblies exhibited high completeness (99.94% as assessed by CheckM), ensuring the reliability of downstream comparative analyses. Taxonomic validation through digital DNA–DNA hybridization, average nucleotide identity, and phylogenomic tree analysis confirmed that all adapted strains remained taxonomically

identical to the wild-type, ruling out contamination during adaptive laboratory evolution or sequencing. Furthermore, antimicrobial resistance profiling via ResFinder revealed that the wild-type strain contains no AMR genes, and none were detected in any of the evolved strains despite prolonged exposure to multiple drug-resistant pathogens.

Comparative analysis of biosynthetic gene clusters predicted by antiSMASH revealed dynamic structural shifts that likely underlie the observed phenotypic divergence in antimicrobial activity across strains. While several BGCs were conserved across all strains, others were found to be differentially retained, either exclusively in the enhanced antibiotic-producing strains (SSUT88A$^{MR9\text{-}16}$ and SSUT88A$^{Ab9\text{-}5}$) or uniquely preserved in the wild-type and the non-producing SSUT88A$^{3P6\text{-}7}$. These patterns suggest adaptive genomic remodeling favoring the retention of clusters with greater bioactive potential. Six clusters were consistently shared among the antibiotic-producing strains but absent in the non-producing strain., each of these BGCs encodes compound classes with known or potential antimicrobial properties, implying a functional role in the enhanced bioactivity observed. In particular, the aryl polyene cluster may also contribute to the pigment-associated phenotype, reinforcing the link between metabolite production and strain-specific coloration. Further distinguishing the high-producing strains, SSUT88A$^{MR9\text{-}16}$ and SSUT88A$^{Ab9\text{-}5}$ harbored two unique clusters: a NRPS cluster with low-confidence similarity to actinomycin D, and a T1PKS cluster with no clear homolog but strong candidate potential for novel antimicrobial activity. Although functional confirmation remains unclear, the restriction of these clusters to strains with elevated antimicrobial activity strengthens the hypothesis that they play a direct role in the observed phenotype. Conversely, a group of clusters was detected only in the wild-type and non-producer. These clusters, while potentially biologically active, are not commonly associated with antibacterial potency and may represent less relevant, their absence in the enhanced strains may reflect selective loss during adaptive evolution. Altogether, the antiSMASH-based comparative BGC analysis suggests that adaptive laboratory evolution leading to the emergence or enrichment of specific biosynthetic pathways.

Orthologous clustering of amino acid sequences across all four strains using OrthoVenn3 revealed broad conservation alongside key differences in gene content likely shaped by adaptive pressures. The relatively small number of unique clusters further supports the high degree of overall genomic conservation. However, among the remaining variable clusters, several were strain-specific or shared only among phenotypically similar groups, highlighting regions of potential relevance to adaptive divergence, particularly with respect to antimicrobial activity. Importantly, 667 clusters were shared among all three antibiotic-producing strains, potentially representing a functional core underpinning antibiotic biosynthesis. In contrast, 16 clusters were uniquely shared between the two evolved strains exhibiting enhanced antibiotic production. Among these were clusters associated with RNA secondary structure unwinding and trehalose catabolic processes, both of which may play roles in transcriptional regulation or stress response during co-culture adaptation. On the other hand, 618 clusters were uniquely shared between the wild-type and the non-producer strain, suggesting the retention of gene content unrelated to increased antimicrobial production. Phylogenetic tree reconstruction based on shared orthologous clusters supported a branching pattern consistent with observed phenotypes: the wild-type diverged first, followed by the loss-of-function strain, while enhached production strain clustered most closely, suggesting parallel evolutionary route.

To integrate functional and biosynthetic insights, antiSMASH-predicted BGCs were cross-referenced with OrthoVenn orthologous clusters based on core biosynthetic genes. Cross-comparison revealed that many key core biosynthetic genes predicted by antiSMASH could be reliably mapped to orthologous clusters, strengthening the connection between genotype and bioactive phenotype.

Lastly, genome-wide analysis using Breseq provided critical insight into both structural and fine-scale sequence changes that accompanied adaptation. Large-scale deletions identified in evolved strains helped explain some of the observed phenotypic differences, where deleted contigs corresponded to antiSMASH-predicted biosynthetic and Orthologous gene clusters.

In parallel, SNP analysis revealed surprisingly few high-confidence point mutations across evolved genomes. However, only three high-confidence SNPs were

ultimately retained after strict manual curation for read depth, quality, alignment confidence, and contextual biological plausibility. Of these, two occurred exclusively in the high-antibiotic-producing strains.

The first was located 37 bp upstream of *murE*_2, a gene involved in peptidoglycan biosynthesis, in the intergenic region between *valS* and *murE*_2. This SNP is positioned near the expected location of a -35-promoter motif, raising the possibility of transcriptional modulation. Since *murE*_2 plays a role in cell wall precursor assembly, this mutation may reflect adaptation evolution to co-culture-induced cell wall alteration.

The second SNP was unique to the precocious producer SSUT88AAb9-5 and lies 14 bp upstream of a gene encoding a DUF2637-domain (*SpdA*-like) protein. Although the function of this gene remains uncharacterized, its conservation across *Streptomyces* species and the SNP's proximity to a likely -10 promoter region suggest a potential regulatory impact on the function.

The third SNP was found only in the pigment-deficient, non-producing strain SSUT88A3P6-7. This was a synonymous mutation within a gene annotated as a hypothetical protein (EAAMLAOK_05879), altering the codon CGG to AGG (both coding for arginine). Despite being silent at the protein level, this mutation affects the first codon position and may influence translation efficiency, mRNA structure, or codon usage factors increasingly recognized as functionally significant in gene regulation. Given its exclusive occurrence in the strain with complete loss of pigment and bioactivity, a subtle post-transcriptional or translational effect cannot be ruled out.

None of the mutations mapped to core biosynthetic genes identified by antiSMASH, implying that phenotypic divergence among strains was not driven by coding sequence changes within BGCs but altering the regulatory regions, alongside structural changes such as BGC loss. Taken together, Breseq results complement the functional and comparative genomic analyses by highlighting two major evolutionary trends: targeted gene loss in the non-producing strain and subtle, potentially regulatory sequence changes in the bioactive strains.

These findings underscore that enhanced antimicrobial phenotypes emerged not through directly modification of biosynthetic gene content, but through a

combination of selective gene retention, gene loss, and modest but impactful genomic refinements.

These results demonstrate that adaptive laboratory evolution through co-cultivation drives meaningful genomic changes, as revealed by whole-genome sequencing. Structural deletions and regulatory-region mutations were linked to observable phenotypic improvements, such as precocious bioactive compound production in SSUT88A$^{Ab9\text{-}5}$ and enhanced antimicrobial potency in SSUT88A$^{MR9\text{-}16}$. These evolved traits can potentially reduce production time and improve yields, making this approach a valuable strategy for generating industrially improved *Streptomyces* strains for antibiotic production.

REFERENCES

REFERENCES

Abirami, M., and Kannabiran, K. (2016). *Streptomyces ghanaensis* VITHM1 mediated green synthesis of silver nanoparticles: Mechanism and biological applications. *Frontiers of Chemical Science and Engineering*, *10*(4), 542-551. https://doi.org/10.1007/s11705-016-1599-6

Adedeji, W. A. (2016). The Treaure Called Antibiotics. *Annals of Ibadan postgraduate medicine*, *14*(2), 56-57. https://www.ncbi.nlm.nih.gov/pmc/articles/PMC5354621/

Ahsan, T., Chen, J., Zhao, X., Irfan, M., and Wu, Y. (2017). Extraction and identification of bioactive compounds (eicosane and dibutyl phthalate) produced by *Streptomyces* strain KX852460 for the biological control of *Rhizoctonia solani* AG-3 strain KX852461 to control target spot disease in tobacco leaf. *AMB Express*, *7*(1), 54. https://doi.org/10.1186/s13568-017-0351-z

Aoki, Y., Matsumoto, D., Kawaide, H., and Natsume, M. (2011). Physiological role of germicidins in spore germination and hyphal elongation in *Streptomyces coelicolor* A3(2). *The Journal of antibiotics*, *64*(9), 607-611. https://doi.org/10.1038/ja.2011.59

Appelbaum, P. C. (2006). The emergence of vancomycin-intermediate and vancomycin-resistant *Staphylococcus aureus*. *Clinical Microbiology and Infection*, *12*(s1), 16-23. https://doi.org/10.1111/j.1469-0691.2006.01344.x

Bentley, S. D., Chater, K. F., Cerdeño-Tárraga, A. M., Challis, G. L., Thomson, N. R., James, K. D., Harris, D. E., Quail, M. A., Kieser, H., Harper, D., Bateman, A., Brown, S., Chandra, G., Chen, C. W., Collins, M., Cronin, A., Fraser, A., Goble, A., Hidalgo, J., . . . Hopwood, D. A. (2002). Complete genome sequence of the model actinomycete *Streptomyces coelicolor* A3(2). *Nature*, *417*(6885), 141-147. https://doi.org/10.1038/417141a

Bhat, M. P., and Nayaka, S. (2023). Cave Soil *Streptomyces* sp. strain YC69 Antagonistic to Chilli Fungal Pathogens Exhibits In Vitro Anticancer Activity Against Human

Cervical Cancer Cells. *Applied Biochemistry and Biotechnology*. https://doi.org/10.1007/s12010-023-04388-y

Blin, K., Shaw, S., Vader, L., Szenei, J., Reitz, Zachary L., Augustijn, Hannah E., Cediel-Becerra, José D. D., de Crécy-Lagard, V., Koetsier, Robert A., Williams, Sam E., Cruz-Morales, P., Wongwas, S., Segurado Luchsinger, Alejandro E., Biermann, F., Korenskaia, A., Zdouc, Mitja M., Meijer, D., Terlouw, Barbara R., van der Hooft, Justin J. J., . . . Weber, T. (2025). antiSMASH 8.0: extended gene cluster detection capabilities and analyses of chemistry, enzymology, and regulation. *Nucleic Acids Research*. https://doi.org/10.1093/nar/gkaf334

Boruta, T. (2021). A bioprocess perspective on the production of secondary metabolites by *Streptomyces* in submerged co-cultures. *World Journal of Microbiology and Biotechnology*, *37*(10), 171. https://doi.org/10.1007/s11274-021-03141-z

CD-Genomics. (2025). *Illumina Library Preparation*. https://www.cd-genomics.com/resource-illumina-library-preparation.html

Challis, G. L., and Hopwood, D. A. (2003). Synergy and contingency as driving forces for the evolution of multiple secondary metabolite production by *Streptomyces* species. *Proceedings of the National Academy of Sciences*, *100*(suppl_2), 14555-14561. https://doi.org/10.1073/pnas.1934677100

Charusanti, P., Fong, N. L., Nagarajan, H., Pereira, A. R., Li, H. J., Abate, E. A., Su, Y., Gerwick, W. H., and Palsson, B. O. (2012). Exploiting Adaptive Laboratory Evolution of *Streptomyces clavuligerus* for Antibiotic Discovery and Overproduction. *PLOS ONE*, *7*(3), e33727. https://doi.org/10.1371/journal.pone.0033727

Chen, S. (2023). Ultrafast one-pass FASTQ data preprocessing, quality control, and deduplication using fastp. *iMeta*, *2*(2), e107. https://doi.org/https://doi.org/10.1002/imt2.107

Chen, S., Zhou, Y., Chen, Y., and Gu, J. (2018). *fastp*: an ultra-fast all-in-one FASTQ preprocessor. *Bioinformatics*, *34*(17), i884-i890. https://doi.org/10.1093/bioinformatics/bty560

Chen, X., Duan, H. D., Hoy, M. J., Koteva, K., Spitzer, M., Guitor, A. K., Puumala, E., Hu, G., Yiu, B., Chou, S., Bian, Z., Guo, A. B. Y., Sun, S., Robbins, N., Cook, M. A., Truant, R., MacNeil, L. T., Brown, E. D., Kronstad, J. W., . . . Wright, G. D. (2025). Butyrolactol A is a phospholipid flippase inhibitor that potentiates the bioactivity of caspofungin against resistant fungi. *bioRxiv*, 2025.2001.2006.630955. https://doi.org/10.1101/2025.01.06.630955

Conrad, T., Joyce, A., and Kenyon Applebee, M. (2009). Whole-genome resequencing of *Escherichia coli* K-12 MG1655 undergoing short-term laboratory evolution in lactate minimal media reveals flexible selection of adaptive mutations. *Genome biology*, *10*, R118.

de Lima Procópio, R. E., da Silva, I. R., Martins, M. K., de Azevedo, J. L., and de Araújo, J. M. (2012). Antibiotics produced by *Streptomyces*. *The Brazilian Journal of Infectious Diseases*, *16*(5), 466-471. https://doi.org/10.1016/j.bjid.2012.08.014

De Roy, K., Marzorati, M., Van den Abbeele, P., Van de Wiele, T., and Boon, N. (2014). Synthetic microbial ecosystems: an exciting tool to understand and apply microbial communities. *Environmental Microbiology*, *16*(6), 1472-1481. https://doi.org/10.1111/1462-2920.12343

Deatherage, D. E., and Barrick, J. E. (2014). Identification of Mutations in Laboratory-Evolved Microbes from Next-Generation Sequencing Data Using breseq. In L. Sun and W. Shou (Eds.), *Engineering and Analyzing Multicellular Systems: Methods and Protocols* (pp. 165-188). Springer New York. https://doi.org/10.1007/978-1-4939-0554-6_12

Demain, A. L., and Elander, R. P. (1999). The β-lactam antibiotics: past, present, and future. *Antonie van Leeuwenhoek*, *75*(1), 5-19. https://doi.org/10.1023/A:1001738823146

Dettman, J. R., Rodrigue, N., Melnyk, A. H., Wong, A., Bailey, S. F., and Kassen, R. (2012). Evolutionary insight from whole-genome sequencing of experimentally evolved microbes. *Molecular Ecology*, *21*(9), 2058-2077. https://doi.org/10.1111/j.1365-294X.2012.05484.x

Duttaroy, A. K. (2021). Chapter 28 - Health effects of terpenoids. In A. K. Duttaroy (Ed.), *Evidence-Based Nutrition and Clinical Evidence of Bioactive Foods in Human*

Health and Disease (pp. 413-424). Academic Press. https://doi.org/https://doi.org/10.1016/B978-0-12-822405-2.00017-7

Fleming, A. (1929). On the Antibacterial Action of Cultures of a *Penicillium*, with Special Reference to their Use in the Isolation of *B. influenzæ*. *British journal of experimental pathology*, *10*(3), 226-236. https://www.ncbi.nlm.nih.gov/pmc/articles/PMC2048009/

Florensa, A. F., Kaas, R. S., Clausen, P. T. L. C., Aytan-Aktug, D., and Aarestrup, F. M. (2022). ResFinder – an open online resource for identification of antimicrobial resistance genes in next-generation sequencing data and prediction of phenotypes from genotypes. *Microbial Genomics*, *8*(1). https://doi.org/https://doi.org/10.1099/mgen.0.000748

Grant, J. R., Enns, E., Marinier, E., Mandal, A., Herman, E. K., Chen, C.-y., Graham, M., Van Domselaar, G., and Stothard, P. (2023). Proksee: in-depth characterization and visualization of bacterial genomes. *Nucleic Acids Research*, *51*(W1), W484-W492. https://doi.org/10.1093/nar/gkad326

Gurevich, A., Saveliev, V., Vyahhi, N., and Tesler, G. (2013). QUAST: quality assessment tool for genome assemblies. *Bioinformatics*, *29*(8), 1072-1075. https://doi.org/10.1093/bioinformatics/btt086

Harwani, D., Begani, J., Barupal, S., and Lakhani, J. (2022). Adaptive laboratory evolution triggers pathogen-dependent broad-spectrum antimicrobial potency in *Streptomyces*. *Journal, genetic engineering and biotechnology*, *20*(1), 1-1. https://doi.org/10.1186/s43141-021-00283-3

Harwani, D., Begani, J., and Lakhani, J. (2018). Co-cultivation Strategies to Induce De Novo Synthesis of Novel Chemical Scaffolds from Cryptic Secondary Metabolite Gene Clusters. In (pp. 617-631). https://doi.org/10.1007/978-981-13-0393-7_33

Herring, C. D., Raghunathan, A., Honisch, C., Patel, T., Applebee, M. K., Joyce, A. R., Albert, T. J., Blattner, F. R., van den Boom, D., Cantor, C. R., and Palsson, B. Ø. (2006). Comparative genome sequencing of *Escherichia coli* allows observation of bacterial evolution on a laboratory timescale. *Nature Genetics*, *38*(12), 1406-1412. https://doi.org/10.1038/ng1906

Herron, J. C., and Freeman, S. (2013). *Evolutionary Analysis*. Pearson Education.

Huang, R.-M., Chen, Y.-N., Zeng, Z., Gao, C.-H., Su, X., and Peng, Y. (2014). Marine Nucleosides: Structure, Bioactivity, Synthesis and Biosynthesis. *Marine Drugs*, *12*(12), 5817-5838. https://www.mdpi.com/1660-3397/12/12/5817

Hutchings, M. I., Truman, A. W., and Wilkinson, B. (2019). Antibiotics: past, present and future. *Current Opinion in Microbiology*, *51*, 72-80. https://doi.org/10.1016/j.mib.2019.10.008

Kadeřábková, N., Mahmood, A. J. S., and Mavridou, D. A. I. (2024). Antibiotic susceptibility testing using minimum inhibitory concentration (MIC) assays. *npj Antimicrobials and Resistance*, *2*(1), 37. https://doi.org/10.1038/s44259-024-00051-6

Katz, L., and Baltz, R. H. (2016). Natural product discovery: past, present, and future. *Journal of Industrial Microbiology and Biotechnology*, *43*(2-3), 155-176. https://doi.org/10.1007/s10295-015-1723-5

Kawai, S., Yamada, A., Du, D., Sugai, Y., Katsuyama, Y., and Ohnishi, Y. (2023). Identification and Analysis of the Biosynthetic Gene Cluster for the Hydrazide-Containing Aryl Polyene Spinamycin. *ACS Chemical Biology*, *18*(8), 1821-1828. https://doi.org/10.1021/acschembio.3c00248

Khan, S. T., Komaki, H., Motohashi, K., Kozone, I., Mukai, A., Takagi, M., and Shin-ya, K. (2011). *Streptomyces* associated with a marine sponge *Haliclona* sp.; biosynthetic genes for secondary metabolites and products. *Environmental Microbiology*, *13*(2), 391-403. https://doi.org/10.1111/j.1462-2920.2010.02337.x

Khanna, M., and Solanki, R. (2012). *Streptomyces antibioticalis*, a Novel Species from a Sanitary Landfill Soil. *Indian J Microbiol*, *52*(4), 605-611. https://doi.org/10.1007/s12088-012-0309-4

Kieser, T., Bibb, M. J., Buttner, M. J., Chater, K. F., and Hopwood, D. A. (2000). Practical *Streptomyces* Genetic Guide. *Genetics*, *59*.

Klevens, R. M., Morrison, M. A., Nadle, J., Petit, S., Gershman, K., Ray, S., Harrison, L. H., Lynfield, R., Dumyati, G., Townes, J. M., Craig, A. S., Zell, E. R., Fosheim, G. E., McDougal, L. K., Carey, R. B., Fridkin, S. K., and Active Bacterial Core surveillance MRSA Investigators, f. t. (2007). Invasive Methicillin-Resistant

Staphylococcus aureus Infections in the United States. *JAMA*, *298*(15), 1763-1771. https://doi.org/10.1001/jama.298.15.1763

Kodani, S., Lodato, M. A., Durrant, M. C., Picart, F., and Willey, J. M. (2005). SapT, a lanthionine-containing peptide involved in aerial hyphae formation in the streptomycetes. *Molecular Microbiology*, *58*(5), 1368-1380. https://doi.org/https://doi.org/10.1111/j.1365-2958.2005.04921.x

Kourtis, A. P., Hatfield, K., Baggs, J., Mu, Y., See, I., Epson, E., Nadle, J., Kainer, M. A., Dumyati, G., and Petit, S. (2019). Vital signs: epidemiology and recent trends in methicillin-resistant and in methicillin-susceptible *Staphylococcus aureus* bloodstream infections—United States. *Morbidity and Mortality Weekly Report*, *68*(9), 214.

Kurosawa, K., Ghiviriga, I., Sambandan, T. G., Lessard, P. A., Barbara, J. E., Rha, C., and Sinskey, A. J. (2008). Rhodostreptomycins, Antibiotics Biosynthesized Following Horizontal Gene Transfer from *Streptomyces padanus* to *Rhodococcus fascians*. *Journal of the American Chemical Society*, *130*(4), 1126-1127. https://doi.org/10.1021/ja077821p

Law, J., Pusparajah, P., Ab Mutalib, N.-S., Wong, S., Goh, B. H., and Lee, L. H. (2019). A Review on Mangrove Actinobacterial Diversity: The Roles of *Streptomyces* and Novel Species Discovery. *Progress In Microbes and Molecular Biology*, *2*. https://doi.org/10.36877/pmmb.a0000024

Lee, H., Shuaibi, A., Bell, J. M., Pavlichin, D. S., and Ji, H. P. (2020). Unique k-mer sequences for validating cancer-related substitution, insertion and deletion mutations. *NAR Cancer*, *2*(4). https://doi.org/10.1093/narcan/zcaa034

Liu, N., Song, F., Shang, F., and Huang, Y. (2015). Mycemycins A–E, New Dibenzoxazepinones Isolated from Two Different Streptomycetes. *Marine Drugs*, *13*(10), 6247-6258. https://www.mdpi.com/1660-3397/13/10/6247

Liu, Y., Tong, Z., Shi, J., Li, R., Upton, M., and Wang, Z. (2021). Drug repurposing for next-generation combination therapies against multidrug-resistant bacteria. *Theranostics*, *11*(10), 4910-4928. https://doi.org/10.7150/thno.56205

Marçais, G., and Kingsford, C. (2011). A fast, lock-free approach for efficient parallel counting of occurrences of k-mers. *Bioinformatics*, *27*(6), 764-770. https://doi.org/10.1093/bioinformatics/btr011

Meier-Kolthoff, J. P., and Göker, M. (2019). TYGS is an automated high-throughput platform for state-of-the-art genome-based taxonomy. *Nature Communications*, *10*(1), 2182. https://doi.org/10.1038/s41467-019-10210-3

Mol, C. D., Brooun, A., Dougan, D. R., Hilgers, M. T., Tari, L. W., Wijnands, R. A., Knuth, M. W., McRee, D. E., and Swanson, R. V. (2003). Crystal Structures of Active Fully Assembled Substrate- and Product-Bound Complexes of UDP-*N*-Acetylmuramic Acid:L-alanine ligase (MurC) from *Haemophilus influenzae*. *Journal of Bacteriology*, *185*(14), 4152-4162. https://doi.org/doi:10.1128/jb.185.14.4152-4162.2003

Neil, J. (2016). *Report on Antimicrobial Resistance* [Interview].

Nelson, M. L., and Levy, S. B. (2011). The history of the tetracyclines. *Annals of the New York Academy of Sciences*, *1241*(1), 17-32. https://doi.org/10.1111/j.1749-6632.2011.06354.x

Oh, D.-C., Kauffman, C. A., Jensen, P. R., and Fenical, W. (2007). Induced Production of Emericellamides A and B from the Marine-Derived Fungus *Emericella* sp. in Competing Co-culture. *Journal of Natural Products*, *70*(4), 515-520. https://doi.org/10.1021/np060381f

Ohnishi, Y., Ishikawa, J., Hara, H., Suzuki, H., Ikenoya, M., Ikeda, H., Yamashita, A., Hattori, M., and Horinouchi, S. (2008). Genome Sequence of the Streptomycin-Producing Microorganism *Streptomyces griseus* IFO 13350. *Journal of Bacteriology*, *190*(11), 4050-4060. https://doi.org/10.1128/JB.00204-08

Ōmura, S., Ikeda, H., Ishikawa, J., Hanamoto, A., Takahashi, C., Shinose, M., Takahashi, Y., Horikawa, H., Nakazawa, H., Osonoe, T., Kikuchi, H., Shiba, T., Sakaki, Y., and Hattori, M. (2001). Genome sequence of an industrial microorganism *Streptomyces avermitilis*: Deducing the ability of producing secondary metabolites. *Proceedings of the National Academy of Sciences*, *98*(21), 12215-12220. https://doi.org/10.1073/pnas.211433198

Papagianni, M. (2012). Recent advances in engineering the central carbon metabolism of industrially important bacteria. *Microbial Cell Factories*, *11*(1), 50. https://doi.org/10.1186/1475-2859-11-50

Parks, D. H., Imelfort, M., Skennerton, C. T., Hugenholtz, P., and Tyson, G. W. (2015). CheckM: assessing the quality of microbial genomes recovered from isolates, single cells, and metagenomes. *Genome Research*, *25*(7), 1043-1055. https://doi.org/10.1101/gr.186072.114

Phodha, T., Riewpaiboon, A., Malathum, K., and Coyte, P. C. (2019). Excess annual economic burdens from nosocomial infections caused by multi-drug resistant bacteria in Thailand. *Expert Review of Pharmacoeconomics and Outcomes Research*, *19*(3), 305-312. https://doi.org/10.1080/14737167.2019.1537123

Phumart, P., Phodha, P., Thamlikitkul, V., Riewpaiboon, A., Prakongsai, P., and Limwattananon, S. (2012). Health and economic impacts of antimicrobial resistant infections in Thailand: a preliminary study. *J Health Syst Res*, *6*(3), 352-360.

Plotkin, J. B., and Kudla, G. (2011). Synonymous but not the same: the causes and consequences of codon bias. *Nature Reviews Genetics*, *12*(1), 32-42. https://doi.org/10.1038/nrg2899

Polly, M., de Almeida, B. L., Lennon, R. P., Cortês, M. F., Costa, S. F., and Guimarães, T. (2022). Impact of the COVID-19 pandemic on the incidence of multidrug-resistant bacterial infections in an acute care hospital in Brazil. *American Journal of Infection Control*, *50*(1), 32-38. https://doi.org/10.1016/j.ajic.2021.09.018

Prescott, J. F. (2014). The resistance tsunami, antimicrobial stewardship, and the golden age of microbiology. *Veterinary Microbiology*, *171*(3), 273-278. https://doi.org/10.1016/j.vetmic.2014.02.035

Ramasamy, V., and Sudalaimuthu, R. S. S. (2022). Chemotaxonomical Characterization of Actinobacteria. In D. Dharumadurai (Ed.), *Methods in Actinobacteriology* (pp. 181-186). Springer US. https://doi.org/10.1007/978-1-0716-1728-1_26

Richter, M., Rosselló-Móra, R., Oliver Glöckner, F., and Peplies, J. (2015). JSpeciesWS: a web server for prokaryotic species circumscription based on pairwise genome

comparison. *Bioinformatics*, *32*(6), 929-931. https://doi.org/10.1093/bioinformatics/btv681

Rosyidah, A., Nantapong, N., Chudapongse, N., Weeranantanapan, O., and Limphirat, W. (2021). Optimization of silver nanoparticles synthesis by the green method using *Streptomyces* sp. SSUT88A and their antimicrobial activity against *Pseudomonas aeruginosa*. *IOP Conference Series: Earth and Environmental Science*, *948*(1), 012085. https://doi.org/10.1088/1755-1315/948/1/012085

Rosyidah, A. l., Weeranantanapan, O., Chudapongse, N., Limphirat, W., and Nantapong, N. (2022). *Streptomyces chiangmaiensis* SSUT88A mediated green synthesis of silver nanoparticles: characterization and evaluation of antibacterial action against clinical drug-resistant strains. *RSC advances*, *12*(7), 4336-4345. https://doi.org/10.1039/d1ra08238h

Rütten, A., Kirchner, T., and Musiol-Kroll, E. M. (2022). Overview on Strategies and Assays for Antibiotic Discovery. *Pharmaceuticals*, *15*(10), 1302. https://www.mdpi.com/1424-8247/15/10/1302

Schöner, T. A., Gassel, S., Osawa, A., Tobias, N. J., Okuno, Y., Sakakibara, Y., Shindo, K., Sandmann, G., and Bode, H. B. (2016). Aryl Polyenes, a Highly Abundant Class of Bacterial Natural Products, Are Functionally Related to Antioxidative Carotenoids. *ChemBioChem*, *17*(3), 247-253. https://doi.org/https://doi.org/10.1002/cbic.201500474

Seemann, T. (2014). Prokka: rapid prokaryotic genome annotation. *Bioinformatics*, *30*(14), 2068-2069. https://doi.org/10.1093/bioinformatics/btu153

Shen, X., Song, S., Li, C., and Zhang, J. (2022). Synonymous mutations in representative yeast genes are mostly strongly non-neutral. *Nature*, *606*(7915), 725-731. https://doi.org/10.1038/s41586-022-04823-w

Shi, A., Fan, F., and Broach, J. R. (2021). Microbial adaptive evolution. *Journal of Industrial Microbiology and Biotechnology*, *49*(2). https://doi.org/10.1093/jimb/kuab076

Slattery, M., Rajbhandari, I., and Wesson, K. (2001). Competition-mediated antibiotic induction in the marine bacterium *Streptomyces tenjimariensis*. *Microbial Ecology*, *41*(2), 90-96. https://doi.org/10.1007/s002480000084

Spellberg, B., Blaser, M., Guidos, R. J., Boucher, H. W., Bradley, J. S., Eisenstein, B. I., Gerding, D., Lynfield, R., Reller, L. B., Rex, J., Schwartz, D., Septimus, E., Tenover, F. C., and Gilbert, D. N. (2011). Combating antimicrobial resistance: policy recommendations to save lives. *Clinical infectious diseases : an official publication of the Infectious Diseases Society of America*, *52 Suppl 5*(Suppl 5), S397-S428. https://doi.org/10.1093/cid/cir153

Stoebel, D. M., Hokamp, K., Last, M. S., and Dorman, C. J. (2009). Compensatory Evolution of Gene Regulation in Response to Stress by *Escherichia coli* Lacking RpoS. *PLOS Genetics*, *5*(10), e1000671. https://doi.org/10.1371/journal.pgen.1000671

Sun, J., Lu, F., Luo, Y., Bie, L., Xu, L., and Wang, Y. (2023). OrthoVenn3: an integrated platform for exploring and visualizing orthologous data across genomes. *Nucleic Acids Research*, *51*(W1), W397-W403. https://doi.org/10.1093/nar/gkad313

Takano, H., Yuhei, M., Junpei, N., Masahiro, F., Naoto, K., Takafumi, K., Isamu, M., Shoichi, A., Hatsumi, S.-T., Mamoru, K., Haruo, I., and and Ueda, K. (2017). High production of a class III lantipeptide AmfS in Streptomyces griseus. *Bioscience, Biotechnology, and Biochemistry*, *81*(1), 153-164. https://doi.org/10.1080/09168451.2016.1238297

Thompson, C., Fink, D., and Nguyen, L. (2002). Principles of microbial alchemy: Insights from the *Streptomyces coelicolor* genome sequence. *Genome biology*, *3*, REVIEWS1020. https://doi.org/10.1186/gb-2002-3-7-reviews1020

Ueda, K., Kawai, S., Ogawa, H.-o., Kiyama, A., Kubota, T., Kawanobe, H., and Beppu, T. (2000). Wide distribution of interspecific stimulatory events on antibiotic production and sporulation among *Streptomyces* species. *The Journal of antibiotics*, *53*(9), 979-982.

Um, S., Guo, H., Thiengmag, S., Benndorf, R., Murphy, R., Rischer, M., Braga, D., Poulsen, M., de Beer, Z. W., Lackner, G., and Beemelmanns, C. (2021). Comparative Genomic and Metabolic Analysis of Streptomyces sp. RB110 Morphotypes Illuminates Genomic Rearrangements and Formation of a New 46-Membered

Antimicrobial Macrolide. *ACS Chemical Biology*, *16*(8), 1482-1492. https://doi.org/10.1021/acschembio.1c00357

van Duin, D., and Paterson, D. L. (2016). Multidrug-Resistant Bacteria in the Community: Trends and Lessons Learned. *Infectious Disease Clinics of North America*, *30*(2), 377-390. https://doi.org/10.1016/j.idc.2016.02.004

Völler, G. H., Krawczyk, J. M., Pesic, A., Krawczyk, B., Nachtigall, J., and Süssmuth, R. D. (2012). Characterization of New Class III Lantibiotics—Erythreapeptin, Avermipeptin and Griseopeptin from Saccharopolyspora erythraea, Streptomyces avermitilis and Streptomyces griseus Demonstrates Stepwise N-Terminal Leader Processing. *ChemBioChem*, *13*(8), 1174-1183. https://doi.org/https://doi.org/10.1002/cbic.201200118

Waksman, S. A. (1947). What is an Antibiotic or an Antibiotic Substance? *Mycologia*, *39*(5), 565-569. https://doi.org/10.1080/00275514.1947.12017635

Wang, B., Guo, F., Huang, C., and Zhao, H. (2020). Unraveling the iterative type I polyketide synthases hidden in *Streptomyces*. *Proceedings of the National Academy of Sciences*, *117*(15), 8449-8454. https://doi.org/doi:10.1073/pnas.1917664117

Wang, H., and van der Donk, W. A. (2012). Biosynthesis of the Class III Lantipeptide Catenulipeptin. *ACS Chemical Biology*, *7*(9), 1529-1535. https://doi.org/10.1021/cb3002446

Wang, P., Bashiri, G., Gao, X., Sawaya, M. R., and Tang, Y. (2013). Uncovering the Enzymes that Catalyze the Final Steps in Oxytetracycline Biosynthesis. *Journal of the American Chemical Society*, *135*(19), 7138-7141. https://doi.org/10.1021/ja403516u

Wang, Y., Manow, R., Finan, C., Wang, J., Garza, E., and Zhou, S. (2011). Adaptive evolution of nontransgenic *Escherichia coli* KC01 for improved ethanol tolerance and homoethanol fermentation from xylose. *Journal of Industrial Microbiology and Biotechnology*, *38*(9), 1371-1377. https://doi.org/10.1007/s10295-010-0920-5

White Jr, J. F., and Torres, M. S. (2009). *Defensive mutualism in microbial symbiosis*. CRC Press.

Wick, R. R., Judd, L. M., Gorrie, C. L., and Holt, K. E. (2017). Unicycler: Resolving bacterial genome assemblies from short and long sequencing reads. *PLOS Computational Biology*, *13*(6), e1005595. https://doi.org/10.1371/journal.pcbi.1005595

World Health Organization. Regional Office for South-East, A. (2011). *Step-by-step approach for development and implementation of hospital and antibiotic policy and standard treatment guidelines*. WHO Regional Office for South-East Asia. https://apps.who.int/iris/handle/10665/205912

Wu, C., Zacchetti, B., Ram, A. F. J., van Wezel, G. P., Claessen, D., and Hae Choi, Y. (2015). Expanding the chemical space for natural products by *Aspergillus-Streptomyces* co-cultivation and biotransformation. *Scientific Reports*, *5*(1), 10868. https://doi.org/10.1038/srep10868

Wu, X.-C., Miao, K.-P., and Qian, K.-X. (2005). Advances of genome and secondary metabolism in *Streptomyces*. *Yi chuan xue bao = Acta genetica Sinica*, *32*(11), 1221-1226. http://europepmc.org/abstract/MED/16318289

Xia, X., Liu, J., Huang, L., Zhang, X., Deng, Y., Li, F., Liu, Z., and Huang, R. (2022). Molecular Details of Actinomycin D-Treated MRSA Revealed via High-Dimensional Data. *Marine Drugs*, *20*(2), 114. https://www.mdpi.com/1660-3397/20/2/114

Zhang, J., and Qian, W. (2025). Functional synonymous mutations and their evolutionary consequences. *Nature Reviews Genetics*. https://doi.org/10.1038/s41576-025-00850-1

Zhang, M., Kong, L., Gong, R., Iorio, M., Donadio, S., Deng, Z., Sosio, M., and Chen, W. (2022). Biosynthesis of C-nucleoside antibiotics in actinobacteria: recent advances and future developments. *Microbial Cell Factories*, *21*(1), 2. https://doi.org/10.1186/s12934-021-01722-z

Zheng, Y., Shi, J., Chen, Q., Deng, C., Yang, F., and Wang, Y. (2022). Identifying individual-specific microbial DNA fingerprints from skin microbiomes [Original Research]. *Frontiers in Microbiology, Volume 13 - 2022*. https://doi.org/10.3389/fmicb.2022.960043

Zimowska, K., Filipovic, V., Nikodinovic-Runic, J., Simic, J., Ilic-Tomic, T., Zimowska, M., Gurgul, J., and Ponjavic, M. (2024). Modulating the Release Kinetics of Natural Product Actinomycin from Bacterial Nanocellulose Films and Their Antimicrobial Activity. *Bioengineering*, *11*(8), 847. https://www.mdpi.com/2306-5354/11/8/847

APPENDICES

APPENDIX A

SHARED BIOSYNTHETIC GENE CLUSTERS PRESENCE IN ALL STRAINS

Table S1 BGCs annotated from antiSMASH found in wild-type and all evolved strains.

Type	Average Size	Most similar known cluster
NI-siderophore	31,146	
NRPS	43,980	detoxin S1*
ectoine	10,404	ectoine^{+}
NI-siderophore	25,270	desferrioxamin B/desferrioxamine E^{+}
NI-siderophore	29,799	
terpene	21,031	
terpene	18,379	hopene$^{\#}$
T3PKS	35,833	flaviolin/1,3,6,8-tetrahydroxynaphthalene^{+}
NRP-metallophore,NRPS	63,409	coelibactin^{+}
lanthipeptide-class-i	24,786	
hglE-KS,T1PKS	32,896	
T1PKS,lanthipeptide-class-v	53,706	cacaoidin*
T1PKS,butyrolactone	31,815	4-hexadecanoyl-3-hydroxy-2-(hydroxymethyl)-2H-furan-5-one$^{\#}$
T2PKS,azole-containing-RiPP	50,802	cinerubin B^{+}
lassopeptide	15,874	
NRPS,NAPAA	34,095	
T2PKS	15,603	spore pigment$^{\#}$
NI-siderophore	25,572	
terpene	6,492	geosmin^{+}

* low, $^{\#}$ medium, $^{+}$ high similarity confidence

APPENDIX B

ADDITIONAL BGC-RELATED ORTHOLOG CLUSTERS

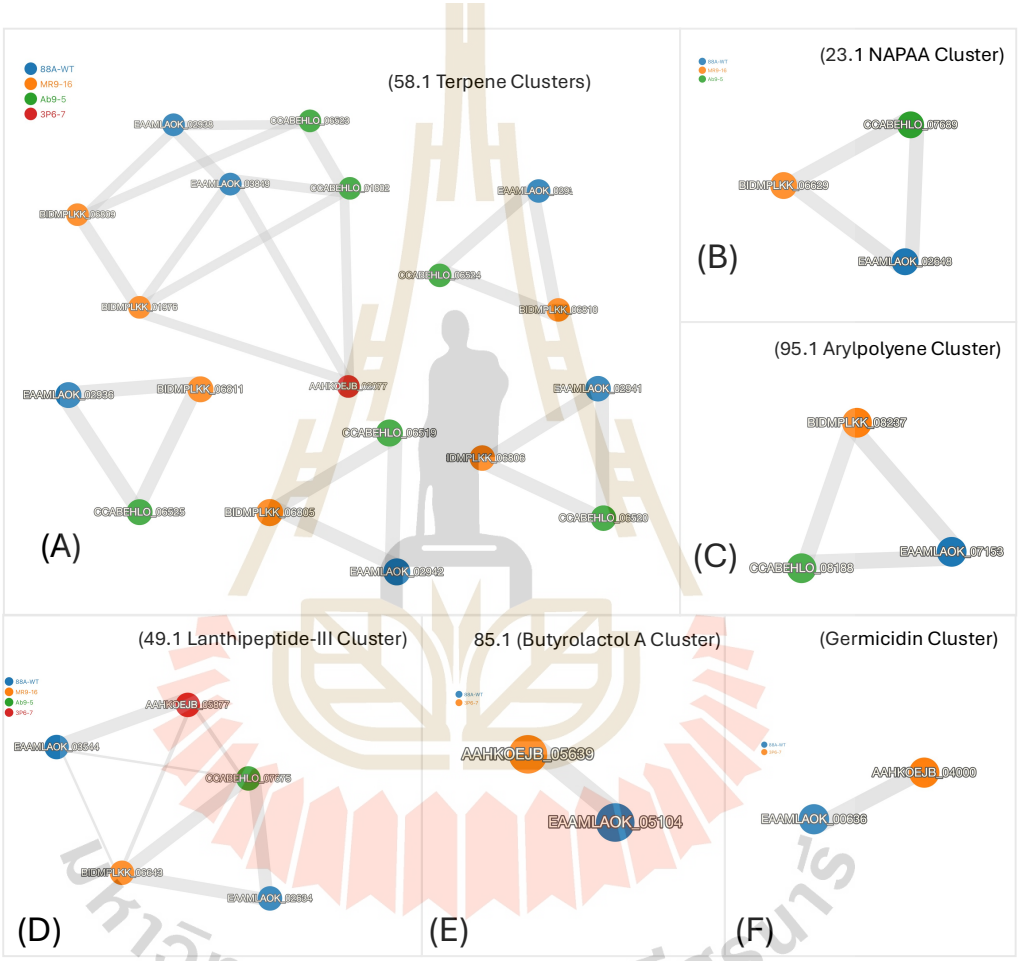

Figure S1 Orthologous cluster visualization of biosynthetic gene clusters.

(A, B, and C) shared between wild-type and non-producing strain (SSUT88A^{3P6-7}). (A) Terpene clusters, (B) Non-alpha poly-amino acids like e-Polylysin cluster, and (C) Aryl polyene cluster.

(D, E, and F) shared between wild-type and non-producing strain (SSUT88A^{3P6-7}). (D) Lanthipeptide class III cluster and (E) Butyrolactol A cluster, and (F) Germicidin cluster.

APPENDIX C

CRITERIA FOR HIGH-CONFIDENCE MUTATION SELECTION

To filter biologically meaningful deletions from initial Breseq predictions, multiple exclusion criteria were applied. The following figures illustrate common reasons for excluding contigs from downstream interpretation. These examples collectively informed the final selection of representative deletions used in the main analysis.

seq id	position	mutation	Ab9-5	MR9-16	3P6-7	annotation	gene	description
101	25,213	C→T	100%	100%	100%	intergenic (+131/-427)	*EAAMLAOK_05724* → / → *fdhA_2*	hypothetical protein/Glutathione-independent formaldehyde dehydrogenase
101	27,013	C→A	100%	100%	100%	intergenic (+171/+33)	*fdhA_2* → / ← *EAAMLAOK_05726*	Glutathione-independent formaldehyde dehydrogenase/hypothetical protein
104	18,168	G→T	100%	100%	100%	intergenic (+55/-206)	*EAAMLAOK_05810* → / → *hcnC_1*	hypothetical protein/Hydrogen cyanide synthase subunit HcnC

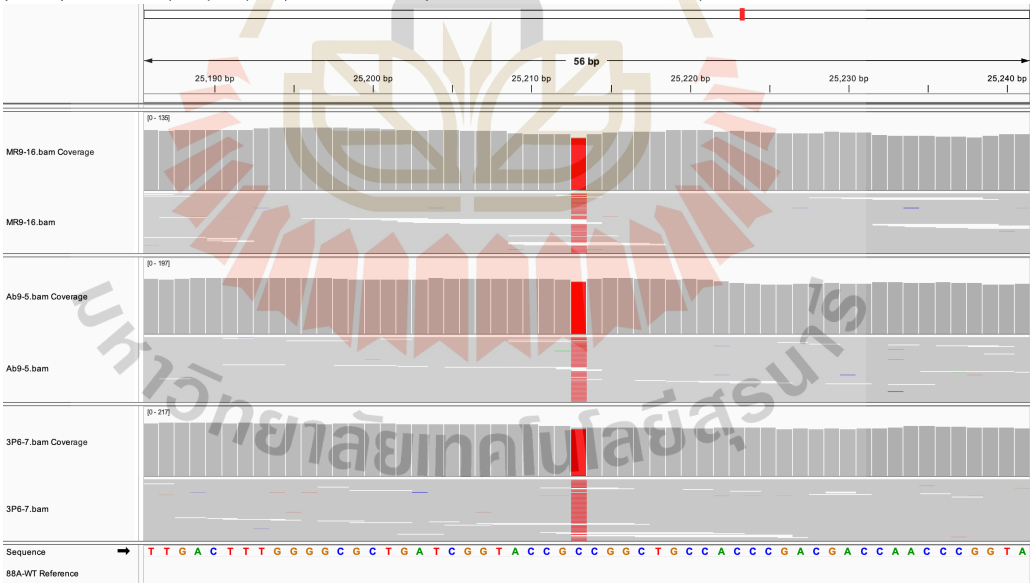

Figure S2 Breseq-predicted mutations with no biological relevancy, which were deprioritized from analysis. In this case, mutations at contigs 101, position 25,213 that cause base substitution from C to T were present in all strains and were categorized as biologically irrelevant.

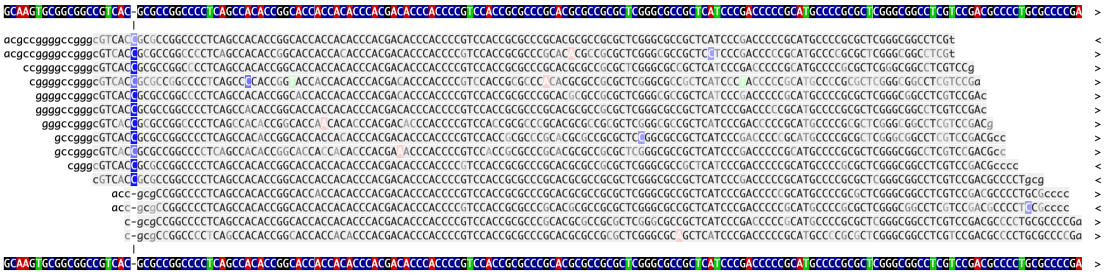

Figure S3 Low read depth across the contig (<40 reads). This example shows inadequate mapped read coverage. Due to insufficient data, reliable confirmation of mutation status was not possible.

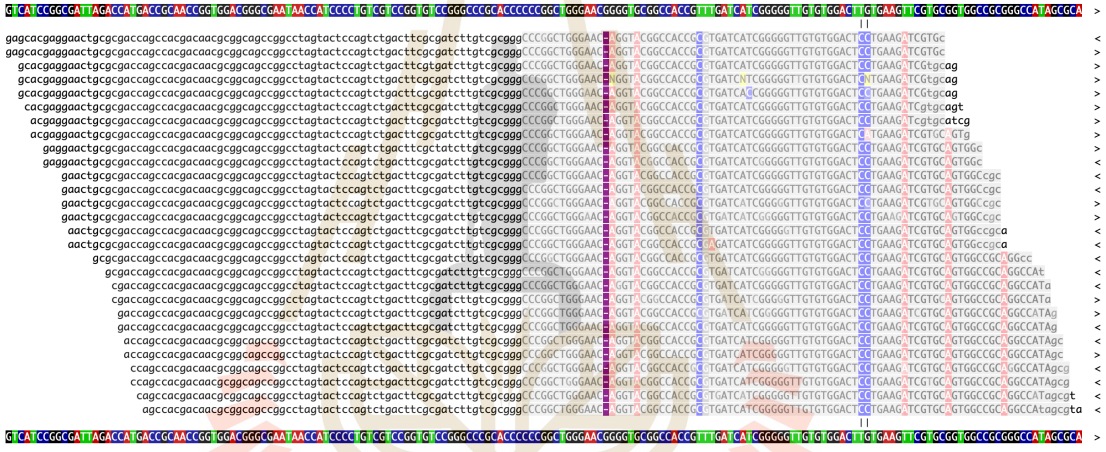

Figure S4 Low base quality from Breseq mutation calls. Although flagged as variations, this contig exhibits poor base quality scores in the wild-type assembly, which can result in false positive deletion calls during alignment.

seq id	position	mutation	Ab9-5	MR9-16	3P6-7	annotation	gene	description
RA	491	323	T→C	C104C (TGT→TGC)		*EAAMLAOK_09890* →		hypothetical protein
RA	491	327	G→A	D106K (GAC→AAG)		*EAAMLAOK_09890* →		hypothetical protein
RA	491	329	C→G	D106K (GAC→AAG)		*EAAMLAOK_09890* →		hypothetical protein

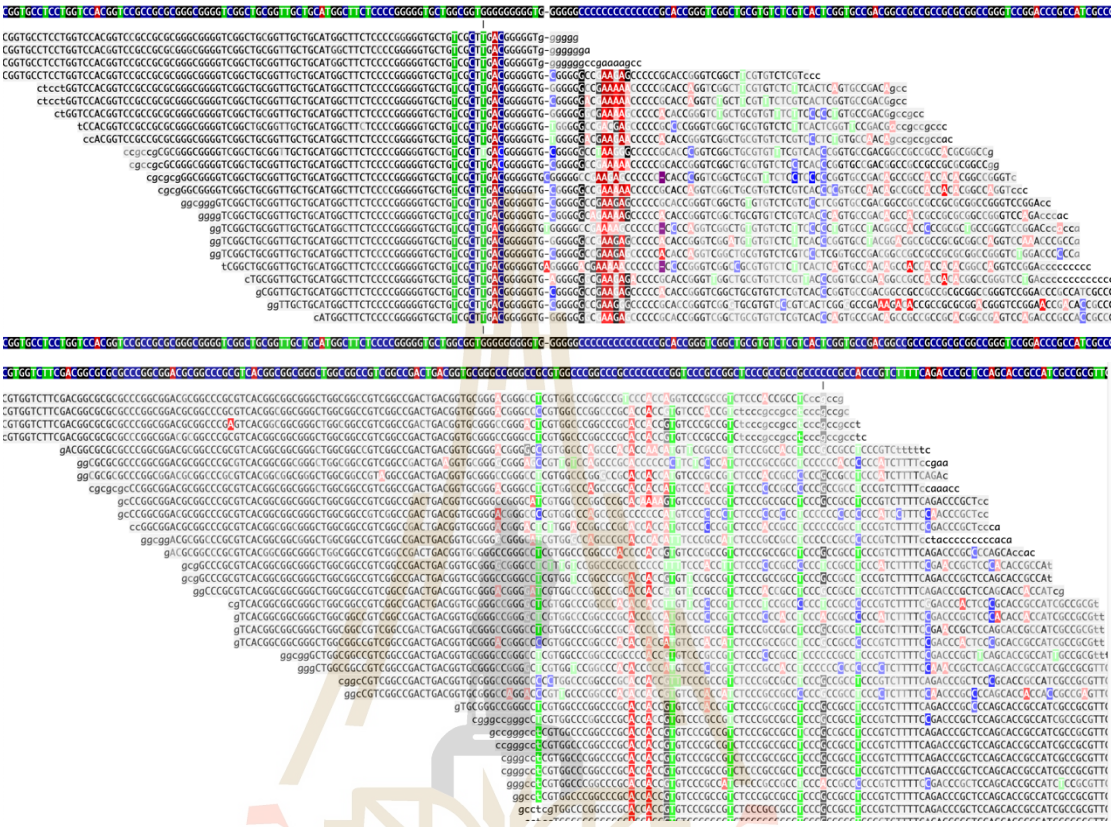

Figure S4 Example of poor overall mapping clarity. These contigs exhibit inconsistent read alignment, with frequent mismatches. Such noisy mapping profiles reduce confidence in structural variant calls and make it difficult to distinguish true deletions from artifacts. Contigs with this alignment pattern were excluded from downstream interpretation.

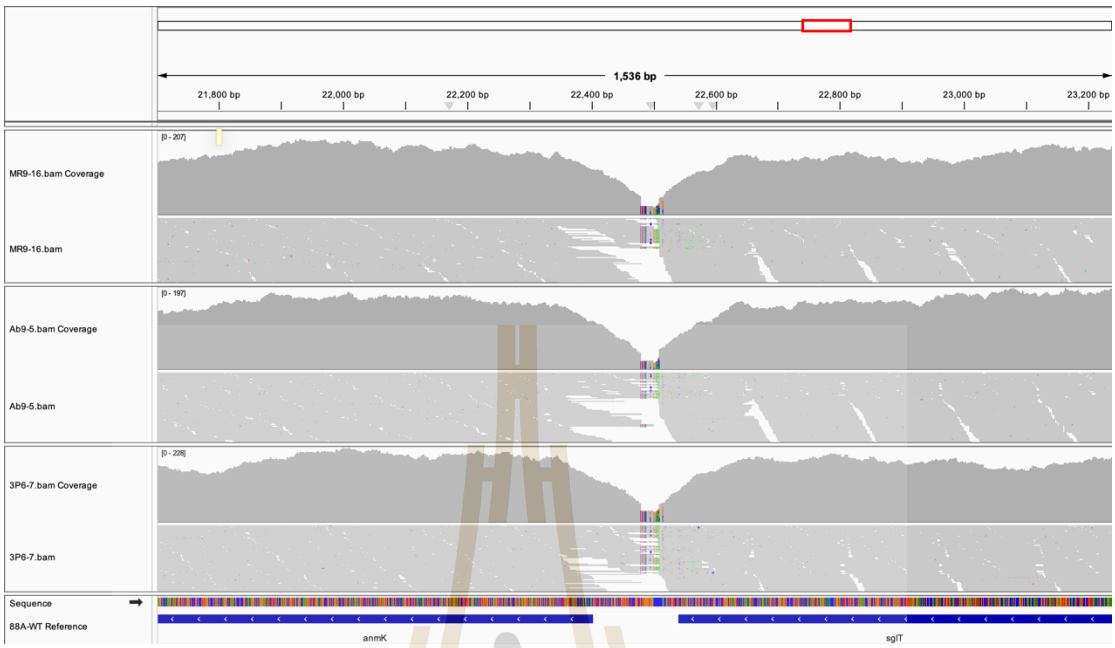

Figure S5 Outlying coverage drops restricted only to the mutation site. Unlike expected clean dropouts across the full contig, this pattern may represent mapping artifacts or sequencing bias rather than true biological deletion.

CURRICULUM VITAE

Name: Wissarut Srisakvarangkool

Date of Birth: August 12th, 2000 at Nakhon Ratchasima, Thailand

Education:

2022 - present	M.Sc. in Microbiology, Suranaree University of Technology, Thailand (GPAX : 4.00, expected 2025).
2018 - 2021	B.Sc. in Biology, Suranaree University of Technology, Thailand. (First-class honors)

Internship:

- Visiting scholar at Texas A&M University, Texas, USA for 5 months, under the supervision of Dr. Jeffrey D. Cirillo.
- Visiting at Archaea Lab, Chulabhorn Graduate Institute, Thailand, for 1 month, under the supervision of Asst. Prof. Dr. Montri Yasawong.

Scholarships:

- Development and Promotion of Science and Technology Talents project (DSPT), supported by the Thai government (2021 – present).
- Scholarships in honor of His Majesty the King's 84th birthday (2018-2021).

Conferences and presentations:

- 2025 Microbiology Society Conference
- Science Postgrad Annual Research Conference 2023 (SPARC 2023)
- DSPT Conference Science and Technology 2022.
- 19th Young Scientist Online Seminar organized by Yamaguchi University
- The 48th International Congress on Science, Technology and Technology-based Innovation (48th STT)

Awards:

- Best Oral Presentation Award of The 48th International Congress on Science, Technology and Technology-based Innovation (48th STT)